

## Technical Report Documentation Page

**1. REPORT No.**

FHWA/CA/NT-2001/10

**2. GOVERNMENT ACCESSION No.****3. RECIPIENT'S CATALOG No.****4. TITLE AND SUBTITLE**

Pavement Evaluation Using Integrated Data from High-speed Sensors

**5. REPORT DATE**

May 2001

**6. PERFORMING ORGANIZATION****7. AUTHOR(S)**

Dr. Samer Madanat (UC Berkeley)  
Dr. Kenneth Maser (INFRASENSE, Inc.)

**8. PERFORMING ORGANIZATION REPORT No.****9. PERFORMING ORGANIZATION NAME AND ADDRESS**

University of California at Berkeley  
Institute of Transportation Studies  
Berkeley, CA 94720

**10. WORK UNIT No.****11. CONTRACT OR GRANT No.**

65A0048

**12. SPONSORING AGENCY NAME AND ADDRESS**

California Department of Transportation  
Sacramento, California 95814

**13. TYPE OF REPORT & PERIOD COVERED**

Final Report

**14. SPONSORING AGENCY CODE****15. SUPPLEMENTARY NOTES**

In cooperation with the U.S. Department of Transportation, Federal Highway Administration

**16. ABSTRACT**

This report describes the development of a methodology for the evaluation of pavement properties from data collected by high-speed sensors, and the development of pavement performance models that form the basis of the methodology. These include a pavement rutting progression model, a pavement cracking initiation and prediction model system.

The report also describes the development of an analytical procedure for inferring pavement resistance by using measurements obtained from high-speed sensors. The procedure is based on Bayesian updating principles, and combines the predictions from the relevant pavement performance model and the measurements obtained from the sensors.

The methodology was tested on two different types of field data: a data set obtained from the Mn/Road site, a set of specially built pavement sections, and condition survey data obtained from various sites in the U.S.

The results of the tests indicated that the use of the measurements obtained from high-speed sensors in the analytical procedure jointly with the performance prediction models helped improve the precision of pavement rutting progression.

The report includes complete documentation of the software that includes the methodology developed in this research, as well as hardware specifications for its future implementation.

**17. KEYWORDS**

Pavement Condition Assessment, Pavement Performance Prediction, High-Speed Sensors, Statistical Modeling, Pavement Management, Structural Number, Pavement Rutting, Pavement Cracking

**18. No. OF PAGES:**

130

**19. DRI WEBSITE LINK**

<http://www.dot.ca.gov/hq/research/researchreports/1997-2001/pavementeval.pdf>

**20. FILE NAME**

pavementeval.pdf

University of California at Berkeley  
Institute of Transportation Studies

**PAVEMENT EVALUATION  
USING INTEGRATED DATA  
FROM HIGH-SPEED SENSORS**

Samer Madanat (U.C. Berkeley)  
Kenneth Maser (INFRASENSE)

ITS Research Report

Final Report of Contract

65A0048

August 31, 2001

This work was supported by the California Department of Transportation, Division of  
New Technology and Research

## **DISCLAIMER STATEMENT**

The contents of this report reflect the views of the author(s) who is (are) responsible for the facts and the accuracy of the data presented herein. The contents do not necessarily reflect the official views or policies of the STATE OF CALIFORNIA or the FEDERAL HIGHWAY ADMINISTRATION and the UNIVERSITY OF CALIFORNIA. The report does not constitute a standard, specification, or regulation.

## **DISCLOSURE STATEMENT**

"This research has been funded by the Division of New Technology and Research of the State of California Department of Transportation and the Federal Highway Administration, under contract 65A0048. Total funding for the contract, with amendments, for the period of July 1, 1999 to March 31, 2001 was \$178,773. Included in this total amount is one sub-contract for \$100,012 with INFRASENSE, Inc. for supporting work."

1. Report No. FHWA/CA/NT-2001/10	2. Government Accession No.	3. Recipient's Catalog No.	
4. Title and Subtitle Pavement Evaluation Using Integrated Data from High-speed Sensors		5. Report Date May 2001	
		6. Performing Organization Code	
7. Author(s) Dr. Samer Madanat (UC Berkeley) Dr. Kenneth Maser (INFRASENSE, Inc.)		8. Performing Organization Report No.	
9. Performing Organization Name and Address University of California at Berkeley Institute of Transportation Studies Berkeley, CA 94720		10. Work Unit No. (TRAIS)	
		11. Contract or Grant No. 65A0048	
12. Sponsoring Agency Name and Address California Department of Transportation Sacramento, California 95814		13. Type of Report and Period Covered Final Report	
		14. Sponsoring Agency Code	
15. Supplementary Notes In cooperation with the U.S. Department of Transportation, Federal Highway Administration			
16. Abstract <p>This report describes the development of a methodology for the evaluation of pavement properties from data collected by high-speed sensors, and the development of pavement performance models that form the basis of the methodology. These include a pavement rutting progression model, a pavement cracking initiation and prediction model system.</p> <p>The report also describes the development of an analytical procedure for inferring pavement resistance by using measurements obtained from high-speed sensors. The procedure is based on Bayesian updating principles, and combines the predictions from the relevant pavement performance model and the measurements obtained from the sensors.</p> <p>The methodology was tested on two different types of field data: a data set obtained from the Mn/Road site, a set of specially built pavement sections, and condition survey data obtained from various sites in the U.S.</p> <p>The results of the tests indicated that the use of the measurements obtained from high-speed sensors in the analytical procedure jointly with the performance prediction models helped improve the precision of pavement rutting progression.</p> <p>The report includes complete documentation of the software that includes the methodology developed in this research, as well as hardware specifications for its future implementation.</p>			
17. Key Words Pavement Condition Assessment, Pavement Performance Prediction, High-Speed Sensors, Statistical Modeling, Pavement Management, Structural Number, Pavement Rutting, Pavement Cracking.		18. Distribution Statement No restrictions. This document is available to the public through: National Technical Information Service Springfield, VA 22161 Ph. (703) 487-4650	
19. Security Classif. (of this report) Unclassified	20. Security Classif. (of this page) Unclassified	21. No. of Pages	22. Price

## **FOREWORD**

This report describes the development of a methodology for the evaluation of pavement properties from data collected by high-speed sensors, and the development of pavement performance models that form the basis of the methodology. These include a pavement rutting progression model, a pavement cracking initiation and prediction model system.

The report also describes the development of an analytical procedure for inferring pavement resistance by using measurements obtained from high-speed sensors. The procedure is based on Bayesian updating principles, and combines the predictions from the relevant pavement performance model and the measurements obtained from the sensors.

The methodology was tested on two different types of field data: a data set obtained from the Mn/Road site, a set of specially built pavement sections, and condition survey data obtained from various sites in the U.S.

The results of the tests indicated that the use of the measurements obtained from high-speed sensors in the analytical procedure jointly with the performance prediction models helped improve the precision of pavement rutting progression.

The report includes complete documentation of the software that includes the methodology developed in this research, as well as hardware specifications for its future implementation.

## **ACKNOWLEDGEMENT**

This work was supported by a research contract from the State of California Department of Transportation, Division of New Technology and Research.

## TABLE OF CONTENTS

Chapter 1: Introduction	2
Overview of Report Contents	2
Problem	3
Background and Literature Review	5
Objectives and Scope	6
Chapter 2: Technical Discussion	7
Development of Pavement Deterioration Models	7
Pavement Rutting Progression Model	7
Pavement Cracking Initiation Model	29
Pavement Cracking Progression Model	47
Analytical Procedure for Inferring Pavement Properties	53
Test Conditions	61
The MnRoads Test Data	61
Field Tests Sites Considered	64
Test Results	71
MnRoads Test Data	71
Field Data	74
Evaluation of Results	88
Pavement Rutting Prediction	88
Pavement Cracking Prediction	89
Chapter 3: Conclusions and Recommendations	91
Chapter 4: Implementation	94
Software Specifications	94
Systems Specifications	106
References	115

## LIST OF FIGURES

Figure 1: GPR Survey Vehicle	4
Figure 2: Typical Output of High-Speed Pavement Thickness Survey	4
Figure 3: Rut depth measurements	12
Figure 4: Relation between the $a_i$ coefficient and pavement strength	16
Figure 5: Thawing index computed at the AASHO road test	20
Figure 6: Observed and predicted rut depth vs. time for two sections used to estimate the model parameters	27
Figure 7: Observed and predicted rut depth vs. time for two sections not used to estimate the model parameters	28
Figure 8: Cracks on asphalt pavements	38
Figure 9: Survival function	45
Figure 10: Cumulative hazard function	45
Figure 11: Bayesian updating of the AASHO performance model	58
Figure 12: MnRoad test facility parallel to interstate I-94	62
Figure 13: Low Volume Loop at MnRoad test facility	63
Figure 14: Sample GPR data from interstate I-25	65
Figure 15: Rut Depth data from I-25 Northbound	65
Figure 16: Sample Plot of Cracked Area vs. Distance for Tamiami Trail	66
Figure 17: GPR Layer Analysis for SH 33 in Wisconsin	67
Figure 18: RMSE for the three prediction methods	72
Figure 19: RMSE for the case of annual inspections	73
Figure 20: RMSE with and without TI coefficient	73
Figure 21: Overall Program Flow	82
Figure 22: Chart of Berkeley Model	83
Figure 23: Modified Rutting Model	84
Figure 24: Model for determination of homogeneous sections	85
Figure 25: Rut Predictions from Various Models for a single cell	86
Figure 26: Rut Predictions vs. Distance and Time- Tamiami Trail	87

## LIST OF TABLES

Table 1: Rutting model estimation result	24
Table 2: Parameter estimates for cracking model #1	44
Table 3: Parameter estimates for cracking model #2	44
Table 4: RMSE of the mean predicted axle load repetitions to cracking	46
Table 5: Continuous model estimation result	52
Table 6: Sample data file for alligator cracking and rutting	68
Table 7: Sample GPR data for Tamiami Trail	69
Table 8: SH33 Condition data	70

## **I. Introduction**

- 1. Overview of Reports Contents**
- 2. Problem**
- 3. Background and Literature Search**
- 4. Objectives and Scope**

## **J. Technical Discussion**

- 1. Development of Pavement Deterioration Models**
- 2. Analytical Procedure for Inferring Pavement Properties from Condition Data**
- 3. Test Conditions**
- 4. Test Results**
- 5. Evaluation**

## **K. Conclusions and Recommendations**

## **L. Implementation**

- 1. Software Specifications**
- 2. Hardware Specifications**

# CHAPTER 1

## INTRODUCTION

### Overview of Report Contents

This report describes the work performed by a research team consisting of Dr. Samer Madanat and his graduate students, of the Department of Civil and Environmental Engineering at the University of California at Berkeley, and Dr. Kenneth Maser and his technical staff, at Infrasense, Inc. The subject of this research is “Pavement Evaluation Using Integrated Data from High-Speed Sensors”.

The report consists of the following chapters. The present chapter, introduction, describes the problem, presents the background and literature review, and lists the objectives and scope of the research.

The technical discussion is contained in chapter 2. It includes a description of the pavement deterioration models that were developed as part of this research, specifically models of rutting progression and cracking initiation. Chapter 2 also includes a description of the analytical procedure used for inferring pavement properties using measurements of pavement conditions from high-speed sensors. This analytical procedure is tested using two types of data that were collected as part of this research: experimentally designed pavement sections subject to actual traffic (the MnRoads data set), and in-service pavement sections (collected from various state agencies’ Pavement Management Systems). These data sets are also described in chapter 2. The chapter closes with a description of the test results and their evaluations.

Chapter 3 describes our conclusions and recommendations on the basis of the research project results.

Finally, Chapter 4 provides specific implementation details that are necessary for successful use of the research results and products by Caltrans, including both software and hardware specifications.

## **Problem**

Pavement maintenance and rehabilitation, and the prediction of future pavement life are heavily dependent on data describing the structure and condition of each pavement segment in the road network. Pavement data for these is typically based on four measures: (1) surface distress and rutting; (2) longitudinal profile (roughness); (3) structural capacity; and (4) skid resistance. These measures were originally developed in conjunction with technologies and surveying systems, which are now over 20 years old. A number of these technologies involve lane closures for detailed pavement measurements, such as visual observation and manual measurement of cracks, and the taking of pavement cores.

Over the past 10-15 years there has been a rapid introduction of continuous automated high-speed pavement condition surveying systems. Commercial systems are now available which can continuously measure and record the following parameters: the type, degree, and intensity of cracking; the width, depth, and profile of rutting; and the pavement layer thickness (Wang, 1998; Iowa State, 1990; Maser, 1996). Systems for evaluating pavement deflections at driving speeds are under development, and prototype systems are being evaluated. These high-speed surveying systems now provide 100% pavement coverage with a level of detail that was previously unattainable.

For example, INFRASENSE has been heavily involved with the applications of ground penetrating radar for the evaluation of pavement layer thickness. Typical equipment used for this type of data collection is shown in Figure 1 below. The data is collected at normal driving speed. Similar equipment for measurement of rut depth and roughness at highway speed has been available on the market for 10 years. More recently, equipment and processing techniques have become available for continuous evaluation of surface distress such as different types of pavement cracking. Each type of equipment can produce some measure of pavement condition as a continuous function of distance. For example, typical results for a thickness survey are shown in Figure 2. It can be assumed that a series of plots, similar to that of Figure 2, will be available as input to the pavement evaluation process.

Up until recently, each data source has been used separately to evaluate one aspect of the pavement's behavior. The goal of the research described herein was to utilize all of the data in a

way that provides a more complete picture of the pavement's current condition and future performance. With such a picture, maintenance and rehabilitation strategies and activities can truly address the real pavement conditions, and can be designed to optimize the remaining life of the pavement at minimal life cycle cost.

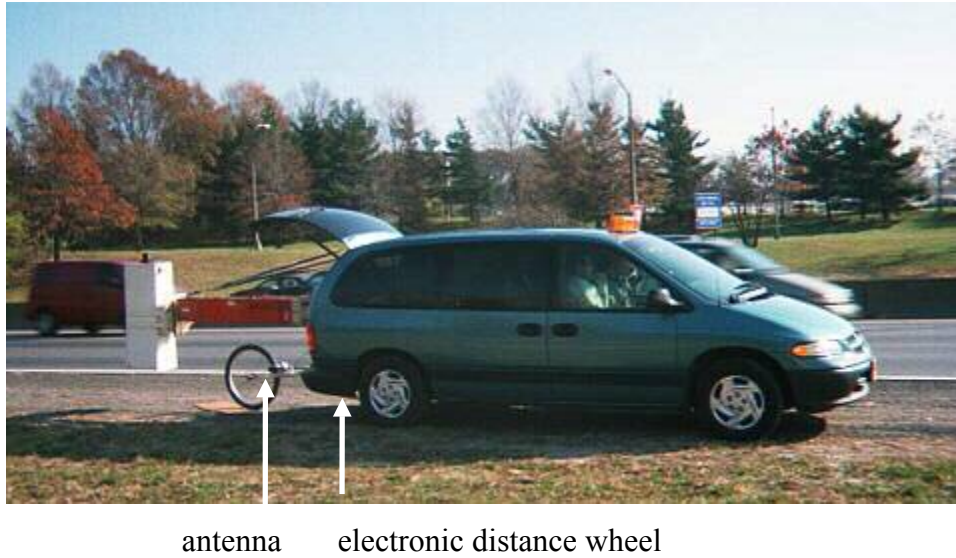


Figure 1 - GPR Survey Vehicle

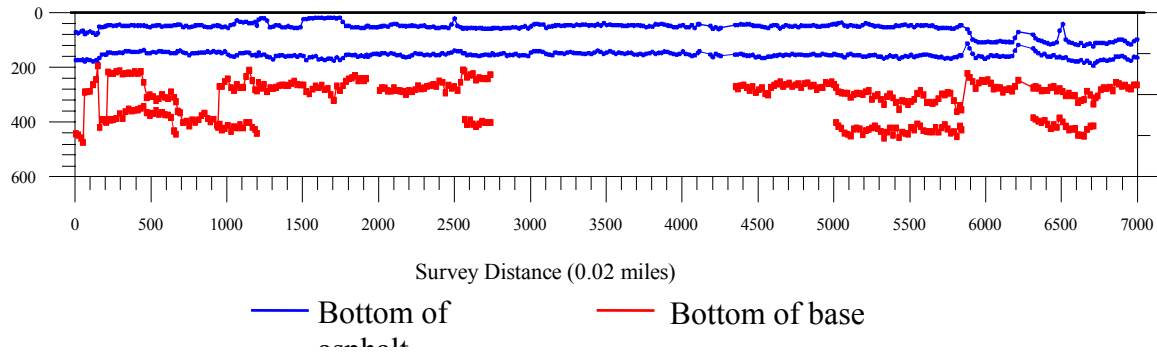


Figure 2 - Typical Output of High-Speed Pavement Thickness Survey

## **Background and Literature Review**

The use of high-speed sensor technology by highway agencies has been limited because there is inadequate means for making use of the large volume of data that they generate. The data that is collected is aggregated into traditional condition and performance indices such as the PCI and the IRI (eg. Shahin and Kohn, 1981) which are then used as a basis for pavement and maintenance management decisions. These indices, although simple and widely used in the past, do not take advantage of the extensive capability available from high-speed pavement sensors. Also, the use of separate indices for different aspects of the pavement behavior fails to treat the pavement as a single physical system with a mechanistic rationale for the observed conditions. Therefore, the index approach does not explain the basic causes of the pavement's behavior, and hence can neither accurately project future behavior nor can it lead to an optimal maintenance and rehabilitation strategy.

With high-speed pavement sensors it is now possible to examine 3 to 4 pavement parameters which are measured independently and continuously along the same length of the pavement. The simultaneous measurement of multiple pavement distresses can provide sufficient information to statistically estimate underlying pavement properties such as layer resistance coefficients (Maser et al 1989). By inferring the values of such variables in-situ, pavement engineers can use them for purposes of deterioration prediction. Furthermore, inferring the causes of the observed deterioration allows pavement engineers to select more effective maintenance strategies. For example, we can now continuously measure pavement cracking (with video processing and/or laser crack detectors), rutting (with optical, laser, or ultrasonic sensors), and layer thickness (with ground penetrating radar). Pavement cracking is caused by fatigue, which is related to the maximum strain in the pavement structure. The strain in the pavement structure is mechanistically related to the load, the layer coefficients, and the layer thickness. Since loads, thickness, and cracking can now be continuously measured, there is enough information to determine the pavement layer coefficients and the cause of cracking, and to predict its future development.

## Objectives and Scope

Pavement represents a physical system characterized by relationships between input (loads, environmental conditions) and observable output (roughness, rutting, cracking, etc.). These relationships involve properties of the pavement system, which can change over time. The pavement maintenance and rehabilitation process involves

- ◇ observations of the pavement condition;
- ◇ calculating or estimating physical properties related to these observed conditions;
- ◇ modeling the remaining life of the pavement based on the estimated pavement properties;
- ◇ implementing maintenance and rehabilitation that maximizes the remaining life of the pavement at minimum cost.

In the context of the above framework, the work described in this report is based on two underlying hypotheses:

1. The key physical properties of the pavement associated with observed pavement conditions can be estimated from the data obtained from a suite of high speed pavement sensors; and
2. These estimates will be sufficiently accurate to lead to more effective maintenance and rehabilitation decisions that are current made with the manner in which the data is currently used.

The long-term objective of the present work is to develop a hardware/software system for automated prediction of pavement life and for selection of the optimum maintenance and rehabilitation. The near-term objective of this research is to develop prototype software, test the software on actual field data, and develop software and hardware specifications for a final system. The prototype software will, at a minimum, produce estimates pavement layer coefficients based on pavement input data (loads and environmental exposure) and on measurements obtained from high-speed pavement sensors. Achievement of this objective will be based on development of a methodology for determining these underlying pavement properties from field observations using the latent variable approach. An additional near term objective is to use the estimated values of the pavement layer coefficients to predict future deterioration and remaining life. This can be achieved by using these estimates as input values (causal variables) in existing mechanistic-empirical deterioration models.

## CHAPTER 2

### TECHNICAL DISCUSSION

#### Development of Pavement Deterioration Models

##### **Pavement Rutting Progression Models**

Rutting, loosely defined as longitudinal depressions in the wheel paths of asphalt concrete pavements, has historically been a primary criterion of structural performance in many pavement design methods. As pointed out by Paterson (1987), other types of permanent deformation are generally much less tractable for direct modeling since they depend to a larger degree on material properties, their local variations, and their interactions with the pavement's microclimate. Rutting is also a serious safety issue for road users. When water accumulates in the ruts, there is a potential for hydroplaning. The hydroplaning phenomenon consists of the buildup of a thin layer of water between the pavement and the tire and results in the tire losing contact with the surface, with the consequent loss of steering control (Yoder and Witczak 1975). With increasing magnitudes and repetitions of loads and increased tire pressures, the rutting problem has become severe in many highway pavements (Haas et. al, 1994). Considerable research has been conducted over the years for developing models to predict the progression of rutting, but with limited success. This report is concerned with the development of an empirical rutting progression model using experimental data. The data set used in this report is taken from the AASHO Road Test (HRB 1962).

The use of experimental data, as opposed to field data collected from condition surveys of in-service pavements, for model development has the following characteristics:

*Advantages:* The main factors affecting rutting such as axle loads and layer thicknesses are carefully controlled, therefore the researcher can capture their effects on rutting progression. This is hardly possible using field data alone. Field data generally involve a distribution of loads whose measurement is not very accurate. Discriminating the effect of each load level from a distribution of loads is a difficult problem, which is not present when each pavement is subjected to a known load level. Further, in field data, the control of constructed layer thicknesses is of lower quality, and the design thicknesses are usually a function of traffic. The latter causes an

econometric problem known as endogeneity. Endogenous variables are determined through the joint interaction with other variables within the model. In field data, layer thicknesses are endogenous since they are usually a function of predicted traffic. Estimation of parameters by Ordinary Least Squares (OLS) regression results in biased and inconsistent results in the presence of endogenous variables. This problem is avoided in experimental data.

*Disadvantage:* The main disadvantage is that experimental data may not represent the true deterioration mechanism of in-service pavements. For example, material aging is not captured in accelerated pavement loading tests.

The salient features of the model specification in this report are:

- 1) no restrictions have been imposed on the values of the parameters representing equivalencies between axles or pavement layer resistance,
- 2) the definition of a thawing index variable that captures the effects of the environmental factors at the AASHO Road Test, and
- 3) the model predicts rut depths by adding predicted values of the increment of rut depth for each time period; this is particularly advantageous in a pavement management context where the engineer is interested in predicting changes in rut depth.

To estimate the model parameters, an unbalanced panel data set with more than 14,000 observations from the AASHO Road Test was used. An unbalanced panel data set consists of observations for different pavement units through time, where the numbers of observations for each pavement section are not necessarily the same. The model is nonlinear in the parameters and the variables so special routines had to be programmed to account for the non linearity of the model and the panel structure of the data.

### Background

There is an extensive body of literature on the rutting of asphalt concrete pavements spanning many decades. Part of this literature is reviewed in the following subsections. First, we identify the factors affecting the rutting performance of asphalt concrete pavements. Then, we review some results from the mechanistic-empirical literature. The information in these two subsections is considered important for the development of a meaningful model specification. Finally, we review significant empirical models that have been developed to date.

Factors that affect rutting.

Rutting is strongly influenced by traffic loading, but climate can also have a large influence especially when the pavement subgrade undergoes seasonal variations in bearing capacity, or when bituminous courses are subjected to high temperatures (OECD 1988). Ruts develop within pavement layers when traffic loading causes layer densification and/or when stresses induced in the pavement materials are sufficient to cause shear displacements within the materials.

Research performed over several decades has shown that the susceptibility to rutting can be linked to the following material attributes: excessive asphalt content, excessive fine-grained aggregate, high percentages of natural sand, rounded aggregate particles, excessive permissible moisture in the mix or in granular materials and soils, temperature susceptible asphalt cement, and cold weather paving leading to low density. Other factors affecting rutting are temperature, precipitation and time, type and extent of loading. These factors can also affect severely the rutting performance of a given mix. The above factors combined also determine the stiffness measures (Hveem and Marshal stability, complex modulus, resilient modulus, etc) and deflection measures that are normally used for pavement distress modeling. Generally, only a few of these factors are measured in experimental data sets, and thus can be used in an empirical model such as the one developed herein.

Evidence from the Mechanistic-Empirical Literature.

The focus of this report is the statistical estimation of models that relate rut depth trends to explanatory variables representing pavement structure, loading and climate. These are described as empirical models in the pavement literature. Despite this focus, relevant results from the literature on the mechanistic-empirical approach to modeling pavement rutting are reviewed so as to identify suitable model forms.

Rutting is the result of the integration of the plastic strains over the pavement structure.

Numerous models have been used to relate plastic strain accumulation to the number of load or stress repetitions. By far, the most common model found in the literature is of the form

$$\varepsilon_p = a N^b \quad (1)$$

where

$\varepsilon_p$  = permanent or plastic strain;

$N$  = number of stress applications;

$a, b$  = estimated coefficients, functions of applied stress, and material characteristics.

The above model form has been proposed for subgrades and unbound materials (Monismith 1976, Behzadi G. and W.O. Yandell 1996, Diylajee and Raymond 1982, Vuong and Armstrong 1991) as well as for asphalt concrete mixes (Khedr 1986).

The following equation form is used by Kenis (1977) and by Ali et al (1997):

$$\varepsilon_p(N) = a' \varepsilon_e N^{b'} \quad (2)$$

where  $\varepsilon_e$  is the elastic strain and  $a'$  and  $b'$  are permanent deformation parameters. This equation is based on the proportionality between the plastic and elastic strains in a pavement structure under traffic loading. Given a level of elastic strain, this equation is equivalent to equation (1).

In the Texas Flexible Pavement System (TFPS) the permanent strain on asphalt concrete mixes is assumed to behave in essentially the same manner as above:

$$\frac{\partial \varepsilon_p}{\partial N} = a'' \varepsilon_e N^{-b''} \quad (3)$$

where  $a''$  and  $b''$  are estimated parameters and  $\varepsilon_e$  is the elastic strain (Button et al 1990).

Obviously, the form in Equation (2) is obtained if this equation is integrated. In the TFPS analysis, the elastic strain is assumed to remain constant throughout the life of the pavement.

The coefficients  $a$  and  $b$  (and also  $a'$ ,  $a''$ ,  $b'$ , and  $b''$ ) are usually considered functions of applied stresses and material properties. Their estimates vary widely among researchers depending on the materials involved and test procedures. In general,  $a$  is influenced by these factors to a greater extent than  $b$ .

Evidence from the empirical literature.

The most common relevant finding in the empirical literature is the concave shapes of rut depth with cumulative number of load repetitions. Such trends have been observed with Heavy Vehicle Simulators by Maree et al (1982) and by Harvey et al (1997) and in other experiments such as

the AASHO Road Test (HRB 1962). Further, most developed models specify such a concave shape (Lister 1981, Paterson 1987).

Most rutting models developed to date have been limited to linear specifications (e.g., Saraf 1982) and do not account for the effects of the environment (e.g., Saraf 1982, Thompson and Nauman 1993). Paterson (1987) developed a non-linear model with data from in-service pavements that included the effect of the environment. Unfortunately, in spite of its complexity, it produced a mediocre fit.

### The AASHO Road Test

To date, the AASHO Road Test remains the most comprehensive controlled experiment performed for evaluating the performance of pavements in the U.S. The test was carried out between 1959 and 1962 near Ottawa, Illinois about 80 mi southwest of Chicago.

All variables for pavement studies were concerned with pavement designs and loads within each of the sections. The sections were subjected to traffic for slightly more than 2 years. Twelve set of sections were subjected twelve different combinations of axle load and axle configuration. The climate of the Road Test area was temperate with an average annual precipitation of about 34 in. The average mean summer temperature was 76 F and the average mean winter temperature 27 F. The soil usually remained frozen during the winter with alternate thawing and freezing of the immediate surface.

The experiment included a total of 234 structural sections or 468 test sections. A majority of the test sections in each of the twelve sets comprised a complete factorial experiment, the design factors of which were surfacing thickness, base thickness and subbase thickness. These experiments were referred to as the main factorial designs. The data that will be used in this research consist of this main factorial design.

The information available for model estimation consists essentially of initial thicknesses of the asphalt concrete, base and subbase layers and biweekly information on axle load and number of repetitions, mean maximum and minimum temperatures, and mean rut depth. The asphalt concrete, base and subbase material characteristics were the same for all sections.

In the AASHO Road Test, the routine biweekly rut measurements were carried out with the device shown in Figure 3. The distance between the legs of this device is 1.2 m (4-ft). This

measurement methodology differs from the one specified in AASHTO (1993), which specifies that a 4-foot (1.2 m) straightedge should be laid across the rut and the maximum depth measured.

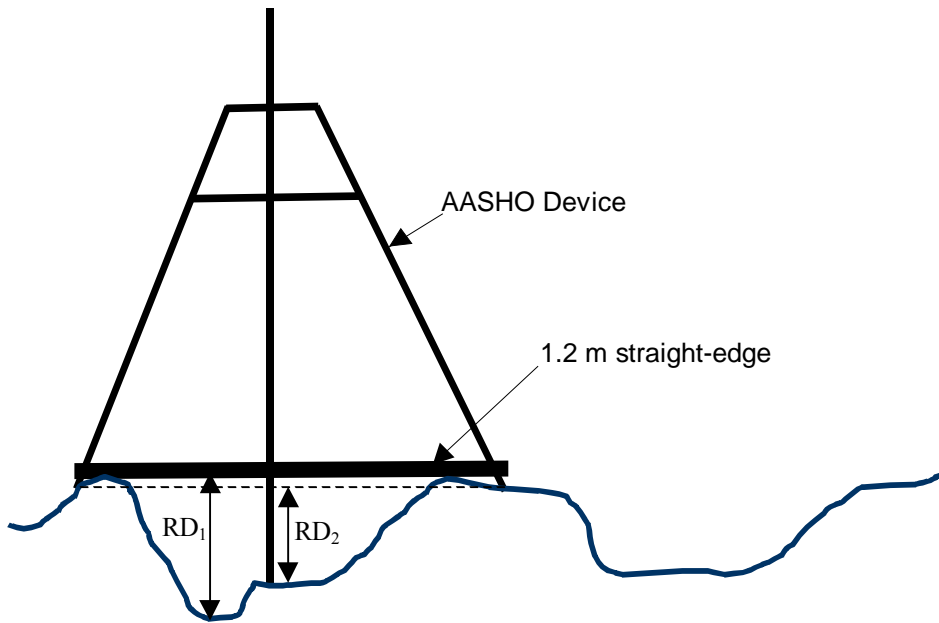


**Figure 3:** Rut depth measurements with a straightedge ( $RD_1$ ) vs. rut depth measurements with AASHO device ( $RD_2$ ).

Nevertheless, for ruts where all the layers are contributing to rutting (the high and low points are far apart transversally and the low point is located near the middle of the rut), the difference should be negligible. According to cross sections shown in the AASHTO Road Test report (HRB 1962), this seems to have been the case for most sections at the AASHTO Road Test.

#### Model specification

The literature revealed that the results of laboratory tests indicate that most materials follow the strain-number of stress repetitions relation given by equation (1). Thompson and Nauman (1993), based on the above observation, argued that it was reasonable to assume that a pavement surface model would be of the same form. They proposed the model given by equation (4).

$$RR = RD/N = A/N^B \quad (4)$$

where

RR = rutting rate,

RD = rut depth (in.)

N = number of repeated load applications, and

A and B = terms developed from field calibration data.

Further, the concave trend of deformation with respect to the number of load applications appears in most empirical and accelerated test studies. Therefore, the same functional form will be the starting point for the model formulation in this section, but instead of a rutting rate as used by Thompson and Nauman (which was in fact a secant rate), rut depth will be used directly. Specifically, the following specification is used:

$$RD_{it} = \beta_{i10} + a_i N_{it}^{b_i} \quad (5)$$

where

$RD_{it}$  = rut depth for section  $i$  at time  $t$  (mm);

$N_{it}$  = a variable representing the cumulative number of load repetitions applied to pavement section  $i$  up to time period  $t$  (a more complete definition is given later);

$a_i$  and  $b_i$  = functions of the characteristics of pavement  $i$  such as layer thicknesses, gradations, etc; and

$\beta_{i10}$  = rut depth immediately after construction for pavement section  $i$  (the reason for using the subscript 10 will be apparent shortly).

For laboratory experiments that are usually carried out at a given stress level, the definition of  $N$  is straightforward, but this is not so for the AASHO Road Test where different pavement sections were subjected to various load levels and different load configurations (single or tandem axles). This is even more complex for actual pavement sections since each section is subjected to a distribution of loads and configurations. A possible solution to this is to use the cumulative number of equivalent single axle loads (ESALs). This is actually what many researchers have done in the past. The problem with this approach is that it is assumed that the load equivalency factors that were based on the serviceability index are appropriate in the case of rutting. This is unlikely, and consequently biases may be introduced in the estimation if this path is followed.

Nevertheless, the concept (if not the specific values) of axle load equivalencies is well accepted in pavement engineering, and thus this concept can be used to define  $N_{it}$  as follows:

$$N_{it} = \sum_{s=1}^t \Delta V_{is} \left( \left( \frac{FL_i}{SAL} \right)^{\beta_5} + R_i \left\{ \left( \frac{AL1_i}{SAL} \right)^{\beta_5} + \left( \frac{AL2_i}{\beta_7 SAL} \right)^{\beta_6} \right\} \right) \quad (6)$$

where

$\Delta V_{is}$  = number of vehicle passes on section  $i$  during period  $s$ ,

$FL_i$  = load in front axle of truck used in section  $i$  (kN or lbs);

$AL1_i$  = load in *single* load axle(s) (rear axle(s)) of truck used in section  $i$  (kN or lbs);

$AL2_i$  = load in *tandem* load axle(s) (rear axle(s)) of truck used in section  $i$  (kN or lbs);

$R_i$  = number of load axles in truck used in section  $i$  ( $R_i=1$  or  $2$ );

$SAL$  = 80 kN if loads are expressed in kN or 18,000 lbs if loads are expressed in lbs; and

$\beta_j$  = parameters to be estimated ( $j=5,6,7$ ). These parameters determine the equivalencies between axle loads.

In equation (6) all the single loads have been standardized to an equivalent 80 kN (18,000 lbs) *single* axle load, which is the standard practice in pavement engineering. Tandem axles have been standardized by  $\beta_7 \cdot 80$  kN, which is the standard *tandem* axle producing the same rutting as a *single* 80 kN axle. This definition of  $N_{it}$  makes it independent of the units being used.

We assumed that the exponent for the front axle load is the same as the exponent for single axle loads ( $\beta_5$ ). The only difference between these axles is that the front axle had a single wheel whereas the rear single axles had double wheels. Certainly, the rutting produced by these two different wheel configurations (for a given load) could be different, but the differences are mostly due to differences in stress distributions in the upper portions of the pavement. In the lower portions of the pavement the distributions of stresses are similar. The separation between tires of dual wheels is of the order of 0.3 m. Also, tire pressures are usually not equal because of temperature differences between the tires, road surface irregularities, bending of the axle, etc (OECD 1988). Thus, although dual wheels distribute the load in a greater area of the pavement surface, the above factors diminish that advantage. Further, the loads in front axles are usually

smaller and thus of lower importance. In any case, although it would be desirable to obtain different coefficients for these two wheel configurations, this was not possible because the ratio of rear single axle load (twin wheel) to front axle load (single wheel) varied only between 3 and 3.5 for the different pavement sections. Nevertheless, it is considered better to include the front axle loads into the model than to neglect them altogether as has been done in previous research.

The identification of a different exponent for tandem axles is considered important. The reason is that the axle separation in tandem axles is large (1.0 to 1.2 m). Thus, the differences in stresses between single and tandem axles are substantial at greater depths. And  $\beta_6$  captures the equivalency between different load magnitudes for tandem axles.

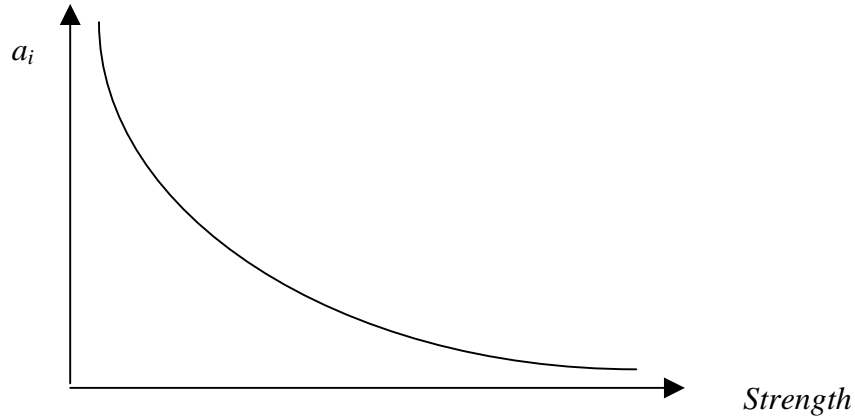
Specifications for  $a_i$  and  $b_i$ :

From the literature review in section 2, it seems that a plausible assumption for  $b_i$  is that is relatively constant or at most that it varies linearly with pavement strength. In this study,  $b_i$  is assumed to be constant for all sections. On the other hand,  $a_i$  seems to vary widely with pavement strength.

Thompson and Nauman (1993), after performing 192 regressions with the specification of equation (4), observed low A's for structural responses less than a certain value, but high magnitudes and erratic trends above that value. Based on these results, they concluded that their A term followed threshold type relations. However, this conclusion is indicative of the inability to estimate the true relation. It is more likely that the relation is rapidly varying near their threshold. The observed trends for weak pavements may be a consequence of their estimation approach, or it may be because the variance of the intercept increases with its mean value.

Thompson and Nauman's results indicate that as the structural response decreases, i.e., as the pavement strength increases, their A term decreases. This means that the  $a_i$  vary with strength in the manner illustrated in Figure 4. This is also what our intuition would suggest.

**Figure 4:** Anticipated relation between the  $a_i$  coefficient and the strength of a pavement.



This simply says that the stronger the pavement, the less the accumulated rut depth for a given traffic.

The exponential function provides a way to obtain such a shape. To model pavement strength, a concept similar to the structural number defined in AASHTO (1993) is used. Specifically, the strength of the pavement is modeled as:

$$RN_i = \beta_1 T_{i1} + \beta_2 T_{i2} + \beta_3 T_{i3} \quad (7)$$

where

$RN_i$  = resistance number for pavement  $i$  (although this is almost identical to the structural number, a different name is used to make explicit that this number is specific to rutting)

$T_{i1}$  = thickness of the asphalt concrete layer for pavement  $i$  (m);

$T_{i2}$  = thickness of the granular base layer for pavement  $i$  (m);

$T_{i3}$  = thickness of the subbase layer for pavement  $i$  (m);

$\beta_j$  = contribution of the  $j^{\text{th}}$  layer to the pavement resistance, where  $j = 1,2,3$  for asphalt concrete, base, and subbase respectively.

The following expression is used to relate  $a_i$  to  $RN_i$ :

$$a_i = \beta_4 e^{-RN_i} = \beta_4 e^{-(\beta_1 T_{i1} + \beta_2 T_{i2} + \beta_3 T_{i3})} \quad (8)$$

The above equation admits the following interpretation. Assume that  $T_{i1} = T_{i2} = T_{i3} = 0$ , that is, traffic loads move over the subgrade material (or over a thin wearing course that does not add structural resistance). In such a situation  $a_i = \beta_4$  represents the rut depth caused by the first standard axle load passage (see equation 5). Now if a thickness  $T_{i3}$  of subbase material is added to the pavement structure, then the rut depth caused by the first standard axle load passage is reduced in a proportion given by  $\exp(-\beta_3 T_{i3})$ . That is, the rut depth caused by the first standard axle load is now  $a_i = \beta_4 \exp(-\beta_3 T_{i3})$ . A similar reasoning for the base and asphalt concrete layers leads to equation (8). These  $\beta$ 's are functions of the subgrade, subbase, base, and asphalt concrete materials. In summary,  $a_i$  represents the rut depth caused in the pavement structure by the first standard axle load.

This is a convenient interpretation because as the pavement becomes more resistant, rut depth approaches zero asymptotically. Of course, it also implies that rut depth could be reduced as much as one wants by using only a low quality subbase material which is not realistic. But, as will be seen later, for common pavement structures, this specification produces reasonable results.

Environmental effects:

Most sections in the AASHO Road Test showed an evident increment in the rate of rut depth progression during the spring months. In what follows, an environmental variable is defined with the information available.

The environmental information available in our database for the AASHO Road Test was very limited. Nevertheless, from the information about the maximum and minimum temperatures, a thawing index is computed with the following reasoning. Freeze will only accumulate when temperatures are below 0°C. Thus an accumulated freeze index for period  $t$  is computed as follows:

$$\begin{cases} AccumFze_t = \max(0, -MeanMinT_t) & t = 1 \\ AccumFze_t = \max(0, AccumFze_{t-1} - MeanMinT_t) & t = 2, \dots, T_i \end{cases} \quad (9)$$

where  $MeanMinT_t$  is the mean minimum temperature ( $^{\circ}C$ ) in the two week period  $t$  (in the AASHO road test there was no freezing in period 1, so it is not necessary to worry about what happened before that) and where  $T_i$  is the number of observations for section  $i$ .

Once the minimum temperature falls below zero, freezing starts to accumulate. At some point in time the minimum temperature again exceeds zero, thus reducing the freezing index. When there are enough periods with temperatures above zero the accumulated freeze index is exhausted and therefore the variable  $AccumFze$  becomes zero again.

The effect of thawing will be the greatest when there is considerable accumulated freeze from previous periods and the temperatures in the current period are substantially above zero. In such cases there will be large amounts of water in the pavement structure with the consequent detrimental effects. Thus, a thawing index representing this interaction of cumulative freeze with temperatures above zero is defined as follows

$$TI_t = AccumFze_t \cdot \max(MeanMaxT_t, 0) \quad (\text{with units of } ^{\circ}C^2) \quad (10)$$

where  $MeanMaxT_t$  is the mean maximum temperature ( $^{\circ}C$ ) in the two week period preceding  $t$ . This thawing index will be zero when the mean maximum temperature in the period is below zero or when there is no accumulated freeze. Thus, as illustrated in Figure 5, when thawing starts, this variable starts increasing, then reaches a maximum and then returns to zero at the end of the thawing period. For freezing to occur in the pavement structure, there should be enough water available. Given the precipitations at the AASHO road test site and water table information, this seems to have been the case.

Having defined the thawing index, we now explain how it is incorporated in the model.

Obviously, thawing alters the materials' properties so one could try to incorporate its effect in  $a_i$ . The problem is that equation (5) is not suitable for this kind of adjustment. The reason is that one would like to obtain a monotonic increasing function with traffic. If during thawing,  $a_i$  increase, then it is possible that the function decreases afterwards when there is no more thawing.

Since the evidence in the literature suggests that equation (5) is a good approximation when the environmental conditions do not change, it is desirable to keep this functional form. Taking a first order Taylor series approximation around the conditions in the previous time period gives

$$RD_{it} \approx RD_{i,t-1} + a_i b_i \frac{\Delta N_{it}}{N_{it}^{1-b_i}} \quad (11)$$

where

$$\Delta N_{i,t} = N_{i,t} - N_{i,t-1} = \Delta V_{it} \left( \left( \frac{FL_i}{SAL} \right)^{\beta_5} + R_i \left\{ \left( \frac{AL1_i}{SAL} \right)^{\beta_5} + \left( \frac{AI2_i}{\beta_7 SAL} \right)^{\beta_6} \right\} \right) \quad (12)$$

With this new formulation, introducing a correction factor for  $a_i$  when the environmental conditions change is done as follows:

$$RD_{it} \approx RD_{i,t-1} + a_i e^{\beta_8 TI_i} \beta_9 \frac{\Delta N_{it}}{N_{it}^{1-\beta_9}} \quad (13)$$

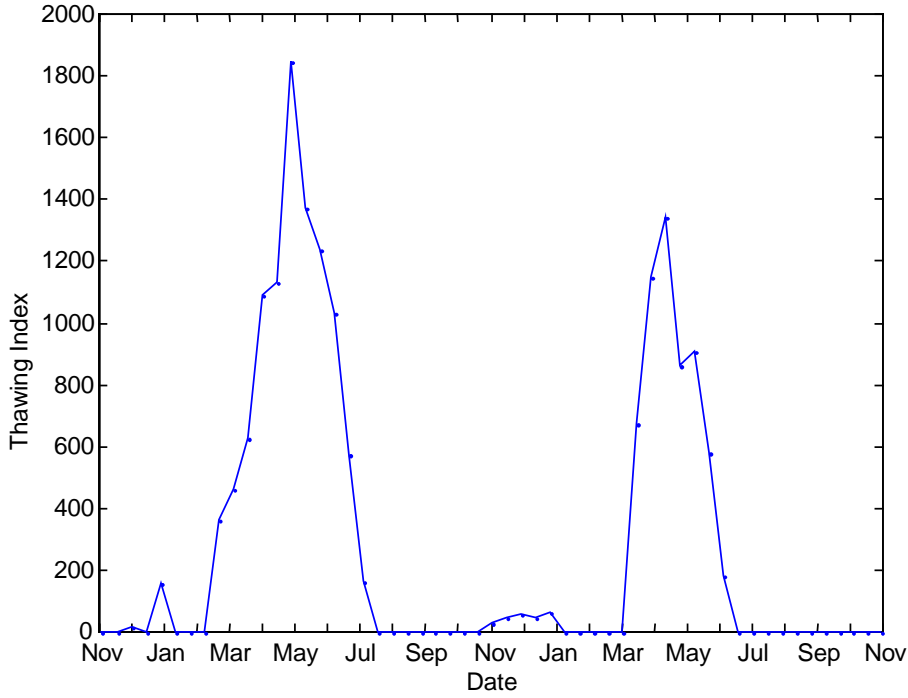
where  $b_i$  has been replaced by  $\beta_9$ . Or, substituting successively the values of  $RD_{i,t-1}$ ,  $RD_{i,t-2}$ , etc,

$$RD_{it} \approx \beta_{i10} + \sum_{s=1}^t a_i e^{\beta_8 TI_s} \beta_9 \frac{\Delta N_{is}}{N_{is}^{1-\beta_9}} \quad (14)$$

Whenever the thawing index is zero, the new multiplicative factor ( $\exp(\beta_8 TI_i)$ ) is 1 and whenever there is thawing the factor is greater than one implying that the pavement will rut faster during the corresponding period. Equation (13), or equivalently equation (14), is the model specification that we used.

It is important to stress that the use of the thawing index is not intended to be a precise description of the freeze-thaw problem in more general cases. However, the intent is to capture most of the freeze-thaw effects at the AASHO Road Test so as not to cause bias in the estimation of the loading and resistance parameters.

**Figure 5:** Thawing index computed at the AASHO Road Test.



### Model estimation results

Equations (13) or (14) are the expressions of the conditional expectation function of rut depth for section  $i$  at time  $t$ ,  $E(RD_{it}|X_{it},\beta)$ . This function gives expected rut depth conditional on the set of regressors  $X_{it} = (1, T_{i1}, T_{i2}, T_{i3}, \Delta V_{i1}, \dots, \Delta V_{it}, FL_i, R_i, AL1_i, AL2_i, TI_t)'$  and on the vector of parameters  $\beta = (\beta_1, \dots, \beta_{11})'$ . The model can be expressed as the following set of regression equations:

$$RD_{it} = E(RD_{it}|X_{it},\beta) + \varepsilon_{it} \quad i = 1, \dots, S, \quad t = 1, \dots, T_i \quad (15)$$

where  $T_i$  is the number of observations for section  $i$  and  $\varepsilon_{it}$  is the error term which is assumed to have mean 0 and constant variance  $\sigma_\varepsilon^2$ . As can be seen from either equation (13) or equation (14) this model is nonlinear in the variables and the parameters. Moreover, the vector  $X_{it}$  contains the whole history of loading through the  $\Delta V$ 's. All these factors make the estimation of the model fairly complex.

When a data set consists of observations for different pavement units through time, several methods of pooling the data can be used. Such data sets are known as panel data sets. One could estimate separate cross-section regressions (each using observations for different pavement sections at the same point in time) or separate time-series regressions (each with observations for a single pavement section over time). However, if the model parameters are constant over time

and over cross-sectional units more efficient parameter estimates (i.e., estimates with lower variance) can be obtained if all the data are combined and a single regression is run. This is the case if all observations are the result of a single underlying deterioration process.

The simplest technique is to combine all cross-section data and time series data and perform ordinary least-squares regression on the entire data set. In the present context, this would mean to perform a regression using equation (15) with  $E(RD_{it}/X_{it}, \beta)$  given by equation (14) and assuming that  $\beta_{i10} = \beta_{10}$  is the same for all  $i$ . The problem with this procedure is that despite the reasonableness of the assumption that all the observations are the result of a single underlying process, some unobserved heterogeneity (unobserved and persistent pavement-specific factors) is still expected among different pavement sections.

Examples of unobserved heterogeneity are the initial cross-section profile and layer compaction. The former directly influences the intercept term in our model. Layer compaction can also influence the intercept term in a more subtle way. For example, a layer that has not been adequately compacted will densify rapidly with the first traffic loads on the wheel paths. This effect will show up mostly in the intercept term, afterward, the conditions are similar to the ones that would have been obtained with good compaction. These are examples of the kind of unobserved heterogeneity that we account for in our model.

The advantage of panel data set over a cross sectional data set is that it allows the researcher greater flexibility in modeling differences in behavior across individual units (Greene 1997). The two most widely used frameworks for modeling unobserved heterogeneity are called fixed and random effects respectively. Both approaches assume that the unobserved heterogeneity can be captured through the constant term. In the *fixed effects* approach, the individual effect ( $\beta_{i10}$ ) is taken to be constant over time and specific to the individual pavement section  $i$ . This approach always produces consistent results (consistent as  $S$ , the number of sections, approaches infinity) but it is costly in terms of the number of degrees of freedom lost, because a different intercept term is required for each pavement section.

An alternative approach is the random effects specification. Since the inclusion of different constant terms ( $\beta_{i10}$ ) represents a lack of knowledge about the model, it is natural to view the section specific constant terms as randomly distributed across pavement sections. Specifically, it is assumed that  $\beta_{i10} = \beta_{10} + u_i$ , where  $u_i$  is a random disturbance characterizing the  $i^{\text{th}}$  section and

is constant through time with mean  $E(u_i) = 0$  and constant variance equal to  $\sigma_u^2$ . With these assumptions the random effects specification is:

$$RD_{it} = \beta_{10} + \sum_{s=1}^t a_i e^{\beta_8 T I_s} \beta_9 \frac{\Delta N_{is}}{N_{is}^{1-\beta_9}} + u_i + \varepsilon_{it} \quad (16)$$

This approach is more appropriate if it is believed that the sampled cross sectional units are drawn from a large population (Greene 1997), which is the case in the AASHO Road Test. However it yields consistent parameter estimates only if the regressors are uncorrelated with the individual effects  $u_i$ . This can be tested using a Hausman specification test (Greene 1997). Both approaches are used to estimate the model parameters in this report. The estimation approach for linear models can be found, for example, in Greene (1997). The estimation of our model parameters is more complicated since our the model is nonlinear in the variables and the parameters, and the panel is unbalanced (that is, there are different number of observations for different pavement sections). Therefore special routines had to be programmed for estimation of the model. The details of the estimation approach are given in Archilla (1999). Initially, the model was estimated separately for the inner wheelpath (IWP) rutting and the outer wheelpath (OWP) rutting using both the fixed and random effects approaches. A total of 7005 observations corresponding to 244 pavement sections were used for the IWP and 7035 observations corresponding to 247 pavement sections were used for the OWP. For each wheel path, the parameter estimates were almost identical from both approaches. Although for both wheel paths, the fits were good and all the parameter estimates were significant (the smallest asymptotic t-statistic was 6.6), there were significant discrepancies between the same parameters for both wheel paths. These differences were not surprising per se, since differences in the mechanism of rutting can be visually observed in plots of rutting trends over time. Further, there are several reasons why this is the case. For example, the state of stresses caused by the same load is different in each wheel path because the boundary conditions are different. One would expect a higher degree of confinement in the IWP than in the OWP and as it is well known from soil mechanics, the shearing resistance of a soil is higher for higher confining pressures. Thus, the different state of stresses and possibly different resistances can lead to different model parameters. For another example, consider the effect of thawing. If the pavement surface is not

cracked, then after a thawing cycle it will take longer for the excess water to leave the pavement structure under the IWP than under the OWP (the drainage path is longer).

Despite the fact that one should expect differences in the parameter estimates for both wheel paths, the differences we obtained were suspiciously high. For example, the estimates for  $\beta_5$  were 2.16 for the IWP and 3.72 for the OWP and the estimates for  $\beta_6$  were 2.92 for the IWP and 4.81 for the OWP. Further, the estimate of  $\beta_9$  was 0.524 for the IWP and 0.377 for the OWP which was inconsistent with the generally observed faster rutting rate for the IWP during periods without thawing.

A possible explanation for the above results is that the objective function is very flat near the optimum along some paths in the parameter hyper-space and therefore the variation in performance between the two wheel paths can cause high differences in the parameter estimates. This may happen despite the high t-statistics, which are computed using partial derivatives of the predicted values of rut depth with respect to each of the parameters. The variation in one parameter alone may have a pronounced effect in the objective function, but the same variation in conjunction with variations from other parameters may have a negligible effect. For example, a high rutting rate could be attained with a high value for  $\beta_4$  (the subgrade coefficient), or high  $\beta_5$  and  $\beta_6$  (the load equivalence coefficients) with a low  $\beta_9$  (the loading exponent), or low  $\beta_5$  and  $\beta_6$  but a high  $\beta_9$  or some other combination. These interactions are believed to cause the differences in the parameter estimates. Since the observations for both wheel paths show similar trends but at the same time some clear differences, combining them can help to reduce the uncertainty of common parameter estimates. This is similar in concept to the effect of the variance of the independent variables in linear regression models. In such models, other things being equal, the larger the variance in the independent variables, the smaller the variance of the parameter estimates.

From a practical point of view, one would like to summarize the effect of traffic in a single variable independently of which wheel path is being considered. This is actually what is done by pavement engineers when they use the concept of an equivalent single axle load (ESAL).

Therefore the model was re-estimated for both wheel paths simultaneously restricting only  $\beta_5$ ,  $\beta_6$ , and  $\beta_7$  to be the same for both wheel paths. The fit was only slightly lower than when the model was estimated separately for each wheel path, thus confirming the suspicions mentioned above.

Table 1 shows the estimation results using the random effects approach. The parameter estimates using the fixed effects approach were practically the same. All the coefficients are statistically significant and have the expected signs. According to these results, the asphalt concrete layer is only 1.68 or 1.53 ( $\beta_1/\beta_2$ ) times more effective in reducing rutting than the base layer for the IWP and OWP respectively. For the OWP the contribution of the base is 1.23 ( $\beta_2/\beta_3$ ) times the contribution of the subbase but this result is reversed for the IWP where the contribution of the base is 0.87 times the contribution of the subbase. The factors affecting the pavement performance on each wheel path mentioned above may play a role in this result. No comparisons are made between  $\beta_1$ ,  $\beta_2$ , and  $\beta_3$  for the different wheelpaths because their values are related to the value of  $\beta_4$ . The estimate of  $\beta_4$  for the OWP is about twice the estimate for the IWP. This is in agreement with the hypothesis that subgrade material is more confined for the IWP. The coefficient  $\beta_7 = 1.81$  indicates that a *tandem* axle load of 145.15 kN (32,659 lbs) has the same effect on rutting as an 80kN (18,000 lbs) *single* axle load. This is in agreement with the assumption made at the AASHO Road Test (HRB 1962) that an 18,000 lbs single axle was equivalent to a 32,000 lbs tandem axle. Notice that the coefficients  $\beta_5$  and  $\beta_6$ , which indicate the equivalencies within axle configurations (single or tandem), are significantly different from each other. Further,  $\beta_5 = 2.98$  is significantly different from 4.0. This illustrates the advantage of not having presupposed a 4-power law for load equivalencies.

**Table 1:** Model estimation results.

Parameter	Parameter Description	$H_0^*$	Inner wheel path		Outer wheel path	
			Parameter Estimate	Asymptotic t-statistic	Parameter Estimate	Asymptotic t-statistic
$\beta_1$	Asphalt concrete coefficient	0	3.34	589.35	5.43	24.8
$\beta_2$	Base coefficient	0	2.07	344.91	3.57	45.81
$\beta_3$	Subbase coefficient	0	2.36	386.23	2.87	43.28
$\beta_4$	Subgrade coefficient	0	0.90	45.30	1.89	84.18
$\beta_5$	Single axle exponent	1	2.98	140.95	2.98	140.95
$\beta_6$	Tandem axle exponent	1	3.89	81.01	3.89	81.01
$\beta_7$	Conversion to standard tandem axle	1	1.81	739.02	1.81	739.01
$\beta_8$	Thawing index coefficient	0	1.96	592.30	1.60	376.18
$\beta_9$	$N_{it}$ exponent	0	0.412	145.43	0.452	78.06
$\beta_{10}$	constant	0	-0.449	-42.25	0.022	2.57
$\sigma_\epsilon^2 = 4.53$ $\sigma_v^2 = 6.17$						
Number of observations = 14042						

\* Null hypothesis for which the asymptotic t-statistics are computed

The significance of  $\beta_8$ , the coefficient of the thawing index, shows that the inclusion of the environmental effects is very important to avoid biasing the other parameters. These estimates are also in agreement with the hypothesis that thawing has a greater proportional effect on the IWP than on the OWP.

The values of  $\beta_9$  are consistent with the concave shapes reported in the literature. This is also a convenient result because, when using such models for prediction, traffic forecasts are usually subject to error, specially for longer planning horizons. Therefore, it is desirable for the model predictions to be robust with respect to traffic forecasting uncertainty. For our model, a 20 % underestimation of  $N_{it}$  causes only a 13 % overestimation of  $\Delta RD_{it}$  whereas a 20 % overestimation of  $N_{it}$  causes a 10 % underestimation of  $\Delta RD_{it}$ .

The estimates of  $\sigma_u^2$ , 6.17 and of  $\sigma_\varepsilon^2$ , 4.53 indicate that the individual effects produce more than 50 % of the variance. This shows that the size of the unobserved heterogeneity is significant. Finally, the estimated standard error of the regression, 3.3 mm, is within the accuracy with which rut depth can be measured. The result is even better in a pavement management context where the random effects are less important since previous observations of rut depth are used to predict the future observations. In this case the estimate of  $\sigma_\varepsilon$  is more relevant which is only 2.1 mm. Figures 6 shows a comparison of the predicted rut depths to the observed rut depths for two of the sections in the estimation sample. As can be observed in the figure the pavement behavior of these sections is replicated quite well for both wheel paths. With a few exceptions, this was generally the case. This was further confirmed by a prediction test with a set of pavements not used for estimation. Figure 7 shows two examples for these sections.

The above results indicate that the model assumptions seem to be generally valid. It should be noticed, however, that the residuals from some sections indicate some heteroskedasticity (variance increasing with thawing index) which leads to some estimation inefficiency.

## Conclusions

The goal of this report was to develop a model of pavement rutting from the AASHO Road Test. A non-linear model was specified and estimated. The model specification uses concepts that are familiar to pavement engineers such as load equivalencies and structural coefficients. However, the model in this report is an improvement over other state of the art empirical models for several reasons. The load equivalence parameters and the resistance parameters were allowed to vary

freely during estimation. This is in contrast with previous research where these coefficients are pre-specified. This is perhaps one reason for the lack of success in developing empirical models to date.

Another important difference with previous research is the introduction of a thawing index. This variable proved to be extremely important to capture the effect of the environment at the AASHO Road Test.

**Figure 6:** Observed and predicted rut depth vs. time for two sections used to estimate the model parameters. The design in the figure caption indicates the thicknesses (meters) of asphalt concrete, base, and subbase respectively. The axle loads are expressed in kN (KiloNewtons) and S or T indicate single or tandem axle respectively.

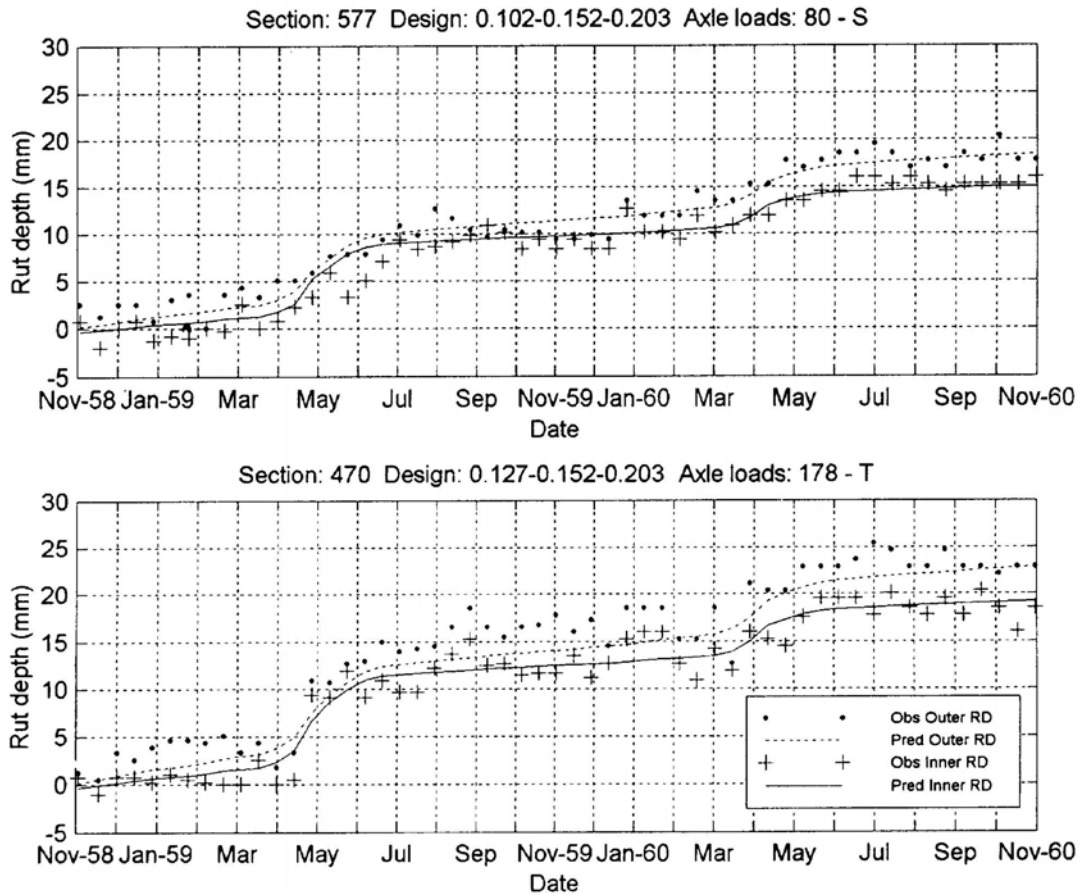
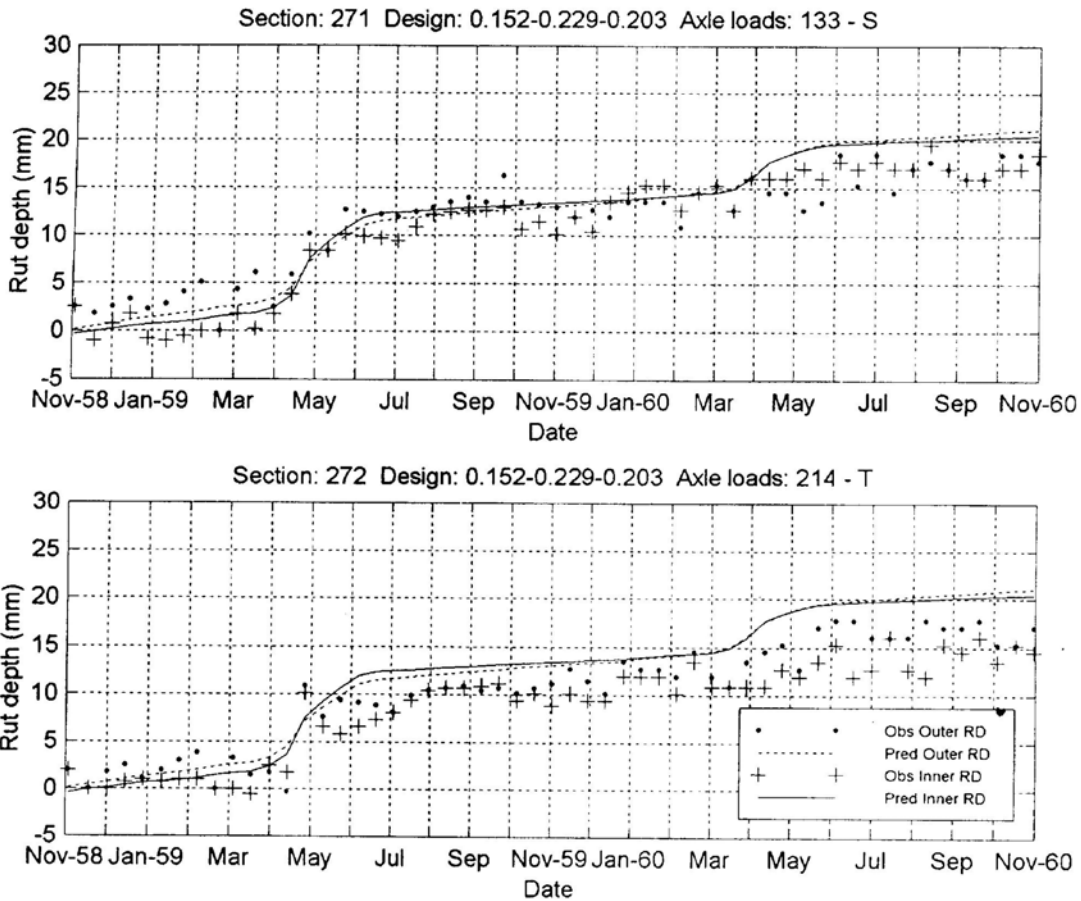


**Figure 7:** Observed and predicted rut depth vs. time for two sections not used to estimate the model parameters. The design in the figure caption indicates the thicknesses (meters) of asphalt concrete, base, and subbase respectively. The axle loads are expressed in kN (KiloNewtons) and S or T indicate single or tandem axle respectively.



The model fits were good, especially considering the number of sections and observations that were used for their estimation. Both fixed effects and random effects specifications were used to account for unobserved heterogeneity. The results showed that the size of the unobserved heterogeneity was significant.

The specification of a non-linear model allowed a good fit. However, it also called for a more careful analysis of the estimation results even when all the statistics indicated no problems. In particular, our model contained several parameters that interacted so as to capture similar effects. By estimating the model parameters for both wheel paths jointly, we were able to reduce the uncertainty in these parameters' estimated values.

Finally, a prediction test with a set of pavements not used for estimation confirmed that the model replicates well the pavement behavior at the AASHO Road Test.

## **Pavement Cracking Initiation Model**

### Cracking Mechanisms

#### Fatigue Cracking

Fatigue cracking generally occurs at low to moderate pavement temperatures, after the pavement has been in service for a period of time. It results from the cumulative effects of repeated loading cycles. The most critical stress is the tensile stress at the bottom of the layer. Fatigue cracks normally start at the underside of the asphalt treated layer and progress to the pavement surface. An advanced stage of fatigue cracking is called alligator cracking, where cracks are plentiful and join in an alligator scale pattern. Fatigue cracking can be caused by excessive heavy load applications, a thin asphalt treated layer, or high pavement deflections. The stiffness of the asphalt mix plays a major role in its fatigue behavior. Since the aggregate and the asphalt influence mix stiffness, both materials are important contributors to the fatigue resistance of an asphalt mix. Normally, more flexible, elastic materials provide longer fatigue life while stiff, brittle materials are more prone to cracking. One exception to this rule is with thick asphalt pavements where higher stiffness mixes will produce longer fatigue life. Transition areas between thin and thick asphalt pavement are about 50 to 100 mm.

#### Thermal Cracking

Depending on the climate, two mechanisms of thermal cracking may be involved:

- Low temperature cracking; and
- Thermal fatigue cracking.

Low temperature transverse cracking has been recognized as the most common non-traffic associated failure mode and is a serious problem in Northern parts of the world including the United States and Canada (OECD, 1988). Low temperature cracking occurs when the tensile stress caused by cold or rapidly declining temperatures exceeds the strength of an asphalt pavement. Low temperature cracking appears as nearly equally spaced transverse cracks on the pavement surface. The asphalt binder plays a major role in low temperature cracking. Hard asphalt or excessively aged asphalt is prone to low temperature cracking. Waxy asphalt concrete mixes are also susceptible to low temperature cracking.

The second mechanism is thermal fatigue cracking. In hot climates, especially where there are long periods of sunshine, daily temperature variations give rise to repeated thermal stresses in the surfacing, which in conjunction with the stresses produced by traffic, lead to failure through fatigue. Such cracks develop at a slower rate. This is generally referred to as thermal fatigue cracking. Block cracking is the usual consequence. In such hot climates, the aging of asphalt through oxidation and the evaporation of volatile oils further aggravate the situation. This increases the stiffness of the surfacing and intensifies thermal stresses. Note that the mechanism of failure is the same for low temperature cracking as for thermal fatigue cracking; the only difference is in the rate at which cracking occurs. Thus, one may refer to both phenomena as thermal cracking. (Hiltunen and Roque, 1994)

#### Causes of Cracking: Material Characteristics, Climate, and Loading

Cracking performance depends on many factors, including

- The thickness of various pavement layers;
- The quality of the construction materials and practices;
- Environmental considerations, such as temperature and moisture; and
- The axle loads and axle configurations to which the pavement is subjected.

The importance of layer thickness is evident: thicker pavements deflect less under load, and thus are less susceptible to fatigue cracking. Previous research, starting before the AASHO Road Test (HRB, 1962) has shown that the thickness of the asphalt concrete layer is more important than that of the unbound layers in retarding pavement cracking initiation.

Material characteristics also play an important role in pavement performance. It is generally believed that a dense aggregate gradation gives better cracking performance. It is also believed that good compaction is necessary for better cracking resistance, while more asphalt content gives better resistance to cracking. On the other hand, excessive asphalt content leads to lower rutting resistance.

Climatic factors can also affect to a large extent the performance and mechanical properties of pavement components and hence the pavement structure's ability to withstand traffic loads. The reason is that seasonal weather variations introduce variations of material properties and therefore periodic changes of the specific pavement characteristics (OECD, 1988). Moisture has a significant impact on the cracking resistance of the asphalt mix. Excessive moisture in a pavement can reduce the strength of underlying layers, weaken the bond between the asphalt and aggregate, and reduce the stiffness or strength of the asphalt treated layer.

The aging of the asphalt mix can accelerate cracking. Because asphalt cements are composed of organic molecules, they react with oxygen from the environment. This reaction is called oxidation and it changes the structure and composition of asphalt molecules. Oxidation causes the asphalt cement to become more brittle, generating the term oxidative hardening or age hardening. Oxidative hardening happens at a relatively slow rate in a pavement and it is not the main cause of cracking, although it occurs faster in warmer climates and during warmer seasons. Because of this hardening, old asphalt pavements are more susceptible to cracking.

Finally, the distribution of axle loads and configurations to which a pavement is subjected affects its cracking resistance. Previous research has shown that the effect of increasing axle loads on pavement life is highly non-linear (HRB 1962). Pavement engineers typically assume that the functional form relating axle load to damage is convex, with the equivalence between two different loads being represented by a transformation raised to the fourth power. Previous research has also indicated that, for a given load, tandem axles are about 40% less detrimental to pavement condition than single axles.

### Modeling Approaches

This section reviews how pavement engineers have modeled pavement cracking in the past. The modeling approaches are generally divided into the following two categories:

- Mechanistic–Empirical Models; and

- Empirical Models

The focus of this research is on the statistical estimation of empirical models that relate field data on crack initiation to explanatory variables representing the pavement structure, traffic loading, and climate. However, mechanistic-empirical models will also be reviewed since (1) useful information can be obtained by studying other approaches, and (2) it will help to explain why an empirical approach was adopted.

### Mechanistic-Empirical Models

Analytical methods refer to the numerical calculation of the stress, strain, or deflection in a multi-layered system, such as a pavement, when subjected to external loads, or the effects of temperature or moisture. Mechanistic methods or procedures refer to the ability to translate the analytical calculations of pavement response to performance such as cracking or rutting.

Mechanistic pavement design methods are based on the assumption that a pavement can be modeled as a multi-layered elastic or visco-elastic structure on an elastic or visco-elastic foundation. Assuming that pavements can be modeled in this manner, it is possible to calculate the stress, strain, or deflection (due to traffic loading and/or environments) at any point within or below the pavement structure. However, researchers recognize that pavement performance will likely be influenced by a number of factors that will not be precisely modeled by mechanistic methods. It is, therefore, necessary to calibrate the models with observations of performance, i.e., empirical correlation. The resulting model is referred to as a mechanistic-empirical model. (AASHTO, 1993) Mechanistic-empirical models have the advantage of representing a wide range of traffic compositions and environmental conditions.

The use of mechanistic-empirical models to predict fatigue cracking performance for asphalt concrete pavement has been investigated by various researchers throughout the world over the past 40 years. From initial understanding of the critical mechanisms responsible for this distress has come development of pavement response calculation methods and statistical transfer functions to relate calculated responses to observed pavement performance (Long et al, 1996). This subsection reviews the mechanistic-empirical models since the principles of mechanistic modeling can identify suitable model forms and variables for specifying empirical models.

Deacon et al (1997) evaluated the effects of binder loss stiffness on pavement performance. In their research, regression models of laboratory fatigue life versus tensile strain of the following form were used:

$$N_f = K_1(1/\varepsilon)^{K_2} \quad (17)$$

where

$N_f$  = laboratory fatigue life;

$\varepsilon$  = tensile strain; and

$K_1$  and  $K_2$  = regression coefficients.

Crack initiation times observed in the field differ widely from laboratory test results because of such factors as crack propagation, traffic wander, and intermittent loading. Finn et al (1977) and Harvey et al (1997) used similar equations to represent fatigue lives for laboratory data but also developed a shift factor to provide results compatible with field observations.

Tayebali et al (1994) examined the effects of various mix properties on fatigue life. They explored the effects of mode-of-loading on in-situ mix performance. The mode-of-loading analysis was based on models of the following type:

$$N_f = a \exp(b MF) \exp(c V_0) (\varepsilon_0 \text{ or } \sigma_0)^d (S_0)^e \quad (18)$$

where

$N_f$  = cycles to failure;

MF = mode factor assuming variables of 1 and -1 for controlled-strain and controlled-stress loading, respectively;

$V_0$  = initial air-void content in percent;

$\varepsilon_0$  = initial flexural strain in in/in;

$\sigma_0$  = initial flexural stress in psi;

$S_0$  = initial mix stiffness in psi; and

a, b, c, d, e = regression coefficients.

While such studies have provided rich understanding of pavement failure under idealized conditions (i.e., laboratory tests), they required empirical studies using field data for calibration and validation purposes.

## Empirical Models

The AASHO Road Test, which is described in some detail in Appendix A, was an accelerated loading test experiment. A crack initiation model was developed as part of the test. The crack initiation model uses traffic repetitions as the dependent variable and pavement thickness and load type as explanatory variables. Though the AASHO cracking model's functional form was apparently arbitrary, the model has been widely accepted. It forms the basis for most current pavement design procedures in the world today. The AASHO Road Test Report 5 proposed the following crack initiation equation.

$$W_c = \frac{A_0 (a_1 D_1 + a_2 D_2 + a_3 D_3 + a_4)^{A_1} L_2^{A_3}}{(L_1 + L_2)^{A_2}} \quad (19)$$

where

$W_c$  = number of weighted axle applications sustained by the pavement before appearance of Class 2 Cracking;

$D_1, D_2, D_3$  = thickness of surfacing, base and sub-base respectively, in inches;

$L_1$  = nominal axle load, in kips;

$L_2 = 1$  for single axle configuration and 2 for tandem axle configuration;

$a_1, a_2, a_3, a_4$  = coefficients that were assigned earlier; and

$A_0, A_1, A_2, A_3$  = regression coefficients.

The AASHO model suffered from severe problems. These are discussed below. First, the analysis did not account for censoring. The data are considered censored when cracking is not actually observed. In the case in which the section had cracked before the first inspection, the observation is left censored, or if it had yet to crack at the last inspection, it is considered right censored. In the AASHO Road Test, there were several sections that had not cracked by the time the experiment ended, and these constitute right-censored data. If censoring is not accounted for correctly in the statistical estimation of model parameters, the estimates can be expected to be biased (Greene, 1997). Second, the model form was arbitrary. One specific problem is the variable  $(L_1 + L_2)$ , which consists of the sum of two quantities with different units. Finally, the coefficients,  $a_1$  to  $a_4$ , were determined a-priori instead of being estimated simultaneously with the other parameters. The pre-determined parameters were used to compute the Structural Number of the pavement.

The Structural Number is related to the thickness of flexible pavement layers through the use of layer coefficients that represent the resistance of the material being used in each layer of the pavement structure. The following general equation for structural number reflects the relative impact of the layer coefficients ( $a_i$ ) and thickness ( $D_i$ ):

$$SN = \sum_{i=1}^3 a_i D_i \quad (20)$$

The estimated values of the coefficients,  $a_1$ ,  $a_2$  and  $a_3$ , were: 0.33, 0.10, and 0.08 respectively. The Queiroz-GEIPOT models (Queiroz, 1981; GEIPOT, 1982) have separate regression equations that predict crack initiation and the rate of crack progression. The crack initiation model used the number of equivalent single axles to initiation as the dependent variable and the structural number as the explanatory variable. The equation for the crack initiation model is as follows:

$$\log_{10} N_c = \alpha + \beta \log_{10} SN \quad (21)$$

where

$N_c$  = the number of Equivalent Single Axle Loads (ESAL) needed to initiate cracking;

SN = structural number; and

$\alpha$ ,  $\beta$  = regression coefficients.

The World Bank's Highway Design and Maintenance (HDM) models (Paterson, 1987) predict the initiation and progression of various pavement distresses such as cracking, rutting, raveling and roughness. Each distress model includes a number of explanatory variables such as age, traffic, design parameters, environmental factors and other distresses. A probabilistic parametric duration model represented crack initiation, where the dependent variable is the probability distribution of the time to cracking. The basic concepts of probabilistic duration models will be described in section 4 of this report. The HDM-III crack initiation model used a hazard function,  $h(t)$  of the following form:

$$h(t) = \gamma \exp(-\gamma\mu) t^{\gamma-1} \quad (22)$$

When  $\gamma < 1$ , the hazard function is decreasing through time; when  $\gamma = 1$ , it is a constant; and when  $\gamma > 1$ , the hazard function is increasing. In the analysis of crack initiation, the parameter  $\mu$  is replaced by a linear function of explanatory variables  $\underline{x}$ ,  $\mu = \underline{x}'\beta$ .

The resulting model for prediction of expected cumulative traffic loading to crack initiation is:

$$TE_{CR2} = \beta_1 SN^{\beta_2} e^{\beta_3 SY} \quad (23)$$

where

$TE_{CR2}$  = mean cumulative traffic loading at initiation of narrow cracking (in millions of ESAL);

SN = structural number;

$SY = SN^4 / (1,000 YE_4)$ , where  $YE_4$  is the annual traffic loading (in millions of ESAL/lane/year);

and

$\beta_1, \beta_2, \beta_3$  = regression coefficients.

Several deterioration models reviewed above include separate equations for distress initiation and progression. Most crack initiation models were developed without accounting for censoring, which may introduce bias in the parameter estimates.

Madanat et al (1995) applied a structured econometric method for developing deterioration models of pavement crack initiation and progression. A model system consisting of a discrete model for distress initiation and a regression model for distress progression was developed. The estimation sample for the progression model is self-selected, as it contains a disproportionately large fraction of weaker pavements, because they are more likely to have already started cracking (they have lower initiation times). This selectivity bias was corrected by using Heckman's sequential procedure. Madanat and Shin (1998) extended this research to account for unobserved heterogeneity in the panel data set, using random-effects specifications in both the discrete and continuous models.

### Measurement of Cracking

One early method used to standardize crack measurements was used at the AASHO Road Test. Cracking was divided into three categories: Class 1, Class 2, and Class 3, as illustrated in Figure 8. Class 1 cracking was the earliest type observed and consisted of fine disconnected hairline cracks. As distress increased, the cracks lengthened and widened until cells formed into alligator cracking. Such cracking was called Class 2 cracking. When the segments of the Class 2 cracks spalled more severely at the edges and loosened until the cells rocked under traffic, the situation was called Class 3 cracking. Class 1 cracking was not included in the evaluation of serviceability of the pavement. Therefore, the AASHO Road Test engineers defined crack initiation as the appearance of Class 2 cracking.

This classification was modified for use in the Brazil United Nations Development Program (UNDP) road cost study. Paterson (1987) used the modified classification as the basis for the formulation of the cracking models in HDM-III. This method identifies cracking by type, severity (class), and extent (area) summarized as follows (Paterson, 1987):

- Severity: Class 1, cracks < 1mm wide; Class 2, cracks 1 to 3 mm wide; Class 3, cracks > 3mm wide without spalling; Class 4, spalled cracks.
- Area: the sum of rectangular cracked areas (in m<sup>2</sup>) reported as a percentage of the total section surface area. Linear crack lengths were converted to area by multiplying by a standard width of 0.5 m.
- Type: the following types were identified: crocodile, irregular, block, transverse, and longitudinal.

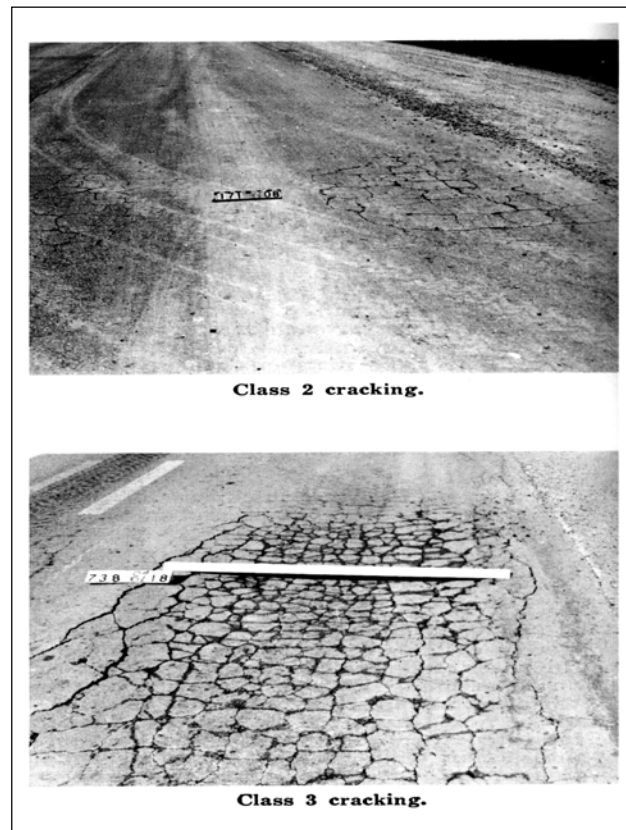


**Figure 8: Cracks on asphalt pavements (HRB, 1962)**

The Brazil UNDP study indexed cracking to normalize the sum of the various AASHO class cracks, weighting wider cracks more heavily to reflect their ability to allow for water ingress into the pavement structure.

There have been some problems in using this method in practice because it is difficult to observe Class 1 cracks and differentiate between cracks of different severity. It is also important to realize that aging had little effect on the pavements at the AASHO Road Test, because the test covered only 2 years. As a result, the cracking observed was primarily load related. The absence of transverse cracking is consistent with the Brazil UNDP data, but is not typical of many pavements located in colder climates.

As part of the SHRP Long Term Pavement Performance (LTPP) program, a slightly different approach to crack identification was developed on the basis of three crack attributes: type, severity (low, moderate, or high), and extent (linear or area). Though details are not presented here, the manual gives thorough guidelines (SHRP, 1993).

In the Brazil UNDP study, initiation was defined by a cracking area of 0.5 percent for practical reasons. First, this helped to ensure that the cracking was not due to a local flaw

unrepresentative of the pavement as a whole but was caused by the mechanism of interest. Second, it represents the minimum size (about 5m<sup>2</sup> on the standard 320 m by 3.5 m subsection) for which a condition survey observation could be expected to be reliably consistent. Because the surveys were made at intervals of four to six months, the first recorded observation was not always 0.5 percent. By convention, the initiation date was regarded as the survey date if the first observation was in the range of 0.5 to 5 percent (Paterson, 1987).

In this research, initiation was defined by a cracking of five percent, which is believed to represent Class 2 Cracking. This criterion was also used because it was stable. When we used a two to three percent criterion, a crack sometimes disappeared after it appeared.

### Model Formulation

#### Stochastic Duration models

Let  $T$  denote the time to cracking of a pavement in a test experiment.  $T$  is a random variable that takes values in  $(0, \infty)$ . Its continuous distribution is specified by a cumulative function  $F(t)$  with a density function  $f(t)$ . The cumulative distribution function is

$$F(t) = \int_0^t f(s) ds = \text{Prob}(T \leq t) \quad (24)$$

The probability that the pavement cracks after  $t$  is given by the survival function,

$$S(t) = 1 - F(t) = \text{Prob}(T \geq t) \quad (25)$$

Since we collect data at specific times, and we know the condition of pavements at these times, the hazard rate is a more useful function than the cumulative density function or the survival function. The probability that a pavement cracks in the next small interval,  $\Delta t$ , given it lasts at least until time  $t$ , is given by

$$g(t) = \text{Prob}(t \leq T < t + \Delta t | T \geq t) \quad (26)$$

The hazard function,  $h(t)$ , which is the instantaneous rate of change of  $g(t)$ , is defined as:

$$h(t) = \lim_{\Delta t \rightarrow 0} \frac{\text{Prob}(t \leq T < t + \Delta t | T \geq t)}{\Delta t} \quad (27)$$

The hazard function quantifies the instantaneous risk that the pavement sections crack at time  $t$ .

The cumulative (or integrated) hazard function is expressed as

$$H(t) = \int_0^t h(u) du \quad (28)$$

The density function, the survival function, and the hazard function are all related;

$$h(t) = \frac{f(t)}{S(t)} \quad (29)$$

The following relationships between these functions also hold:

$$H(t) = -\log S(t) \quad (30)$$

and

$$S(t) = e^{-H(t)} \quad (33)$$

Right censoring of the data occurs when the test ends at time  $C$ , before all pavement sections have failed. For each section  $i$ , we either know  $T_i$ , if  $T_i \leq C$ , or that  $T_i > C$ , in which case the time to cracking for pavement  $i$  is censored. The time recorded is  $\min(T_i, C)$  together with the censoring indicator variable  $\delta_i$ , which is a dummy variable that takes the value 0 if the observation (pavement section) is censored and 1 otherwise.

The full likelihood function is obtained by multiplying the respective contributions of values of density function  $f$  for uncensored observations and values of survival function  $S$  for censored observations. In the presence of right censoring the likelihood for all observations in a sample of size  $n$  is (Kalbfleisch and Prentice 1980):

$$l = \prod_{\delta_i=1} f(t_i) \prod_{\delta_i=0} S(t_i) = \prod_{i=1}^n [f(t_i)]^{\delta_i} [S(t_i)]^{1-\delta_i} \quad (32)$$

To estimate the parameters of the distributions, we maximize the log likelihood function,

$$L = \log l = \sum_{i=1}^n \{ \delta_i \log[f(t_i)] + (1 - \delta_i) \log[S(t_i)] \} \quad (33)$$

Upon choosing a particular distribution, we can substitute the appropriate expressions for the density function and the survival function.

### The Weibull Hazard Model

Though the hazard function  $h(t)$  can be assumed to be constant over time, there are many situations in which it is more realistic to suppose that  $h(t)$  either increases or decreases over time.

A flexible form for such a hazard function is given by

$$h(t) = \alpha \gamma t^{\gamma-1} \quad t > 0 \quad (34)$$

where  $\alpha$  and  $\gamma$  are positive constants. The hazard function given by Equation (34) is called the Weibull hazard function with parameters  $\alpha$  and  $\gamma$ . The parametric model that follows the

Weibull hazard function is called the Weibull model. Note that  $h(t)$  increases when  $\gamma > 1$ ; decreases when  $\gamma < 1$ ; and is constant when  $\gamma = 1$ .

The Weibull distribution function obtained from Equation (34) is:

$$\begin{aligned} F(t) &= 1 - \exp\left(-\int_0^t h(s)ds\right) \quad t > 0 \\ &= 1 - \exp(-\alpha t^\gamma) \end{aligned} \quad (35)$$

Its density function is:

$$f(t) = \alpha \gamma t^{\gamma-1} \exp(-\alpha t^\gamma) \quad t > 0 \quad (36)$$

The survival function is thus:

$$S(t) = 1 - F(t) = \exp(-\alpha t^\gamma) \quad (37)$$

If a vector of explanatory variables  $\underline{x}$  is observed with the duration data, the Weibull hazard function is written as:

$$\begin{aligned} h(t, \underline{x}, \underline{\beta}) &= e^{-\gamma \underline{\mu}} \gamma t^{\gamma-1} \\ &= e^{-\gamma \underline{x} \underline{\beta}} \gamma t^{\gamma-1} \end{aligned} \quad (38)$$

where  $\underline{\mu} = \underline{x} \underline{\beta}$ . Then, the distribution function, density function, and survival function are as follows:

$$F(t, \underline{x}, \underline{\beta}) = 1 - \exp\left(-e^{-\gamma \underline{x} \underline{\beta}} t^\gamma\right) \quad (49)$$

$$f(t, \underline{x}, \underline{\beta}) = e^{-\gamma \underline{x} \underline{\beta}} \gamma t^{\gamma-1} \exp\left(-e^{-\gamma \underline{x} \underline{\beta}} t^\gamma\right) \quad (50)$$

$$S(t) = \exp\left(-e^{-\gamma \underline{x} \underline{\beta}} t^\gamma\right) \quad (41)$$

The parameters  $\gamma$  and  $\underline{\beta}$  of the model can be estimated by maximum likelihood. In the Weibull model, the expected time to cracking initiation is given by (Meeker and Escobar 1998):

$$\begin{aligned} E[t|\underline{x}] &= e^{\underline{\mu}} \Gamma\left(1 + \frac{1}{\gamma}\right) \\ &= e^{\underline{x} \underline{\beta}} \Gamma\left(1 + \frac{1}{\gamma}\right) \end{aligned} \quad (42)$$

where the gamma function,  $\Gamma(z)$ , is defined as

$$\Gamma(z) = \int_0^\infty w^{z-1} e^{-w} dw \quad (43)$$

for  $z > 0$ .

Furthermore, because the model is not a linear regression model, there is no obvious equivalent to the conventionally reported standard error.

### Model Specification and Estimation Results

#### Model Specification

The AASHO Road Test Data were used for development of the pavement cracking initiation model. We have a total of 252 observations (test sections). The number of sections that had cracked by the end of the test was 185. The remaining 67 observations were censored (i.e., cracking had not occurred yet by the time of the test). The model shown in this section used right wheel path cracking as the dependent variable. The variables included are:

- avt: number of accumulated load repetitions in the traffic lane before crack initiation (the dependent variable);
- D1: surface thickness in inches (1 to 6 inches);
- D2: base thickness in inches (0, 3, 6, and 9 inches);
- D3: sub-base thickness in inches (0, 4, 8, 12, and 16 inches);
- LOAD: nominal axle load (in kips); and
- TYPE: single dummy variable, 1 for single axle and 0 for tandem axle.

We estimated a Weibull model using two different model specifications. Our first specification (Model 1) was a modified version of the original AASHO model, which was presented earlier (equation 19). The function  $\mu$  (of the hazard model in equation 38), using this first specification, is shown below:

$$\mu = \beta_1 + \beta_2 D_1 + \beta_3 D_2 + \beta_4 D_3 + \beta_5 L_2 + \beta_6 (L_1 + L_2) \quad (44)$$

where  $L_1$  and  $L_2$  are defined after equation (3). Essentially, this is similar to the AASHO specification, with the predetermined coefficients of the structural number in equation (19) replaced by parameters to be estimated.

Our second model specification improved on the original AASHO specification, which is problematic because it assumes that the effects of  $L_1$  and  $L_2$  are separable and additive. This is physically unrealistic for two reasons. First, it assumes a constant rate of substitution between axle load and axle type, which is inconsistent with pavement engineering knowledge. Pavement engineers typically use nonlinear equations to convert between single and tandem axle loads.

Second, the specification involves an addition of two variables with different units ( $L_1$  is in units of kips while  $L_2$  is in units of axles).

Our improved specification accounts for the difference in the effects of a single axle and a tandem axle of equal load through the use of interaction terms. The function  $\mu$  in the hazard model with the improved specification (Model 2) is:

$$\mu = \beta_1 + \beta_2 D_1 + \beta_3 D_2 + \beta_4 D_3 + \beta_5 \text{TYPE} * \text{LOAD} + \beta_6 (1 - \text{TYPE}) * \text{LOAD} \quad (45)$$

Note that we use two interactive terms for LOAD and TYPE: the first interactive term is  $\beta_5 \text{TYPE} * \text{LOAD}$  and the second interactive term is  $\beta_6 (1 - \text{TYPE}) * \text{LOAD}$ . In this specification,  $\beta_5$  is the effect of 1 unit of a single axle load, while  $\beta_6$  is the effect of 1 unit of a tandem axle load.

### Estimation Results

It is expected that an increase in pavement layer thickness increases the time to cracking of the pavements, and that an increase in axle load, of either type, will decrease the time to pavement crack initiation. The effect of the surface layer should be greater than the effects of the two unbound layers, and the effect of the sub-base should be the smallest. Moreover, the effect of single loads should be greater than that of tandem loads. The dependent variable in the model is hazard rate, not the time to cracking of the pavements, so the parameters should be interpreted accordingly.

Table 2 presents the results of the Weibull model using the first specification. The t-statistics show that each variable is a significant explanatory variable of crack initiation at one percent significance level. Furthermore, it can be seen that the coefficients have the correct signs, which confirm our a priori hypotheses. The ratio of the estimated resistance of the asphalt concrete to that of the base is less than 3, which is lower than what was obtained in the original AASHO model. On the other hand, the ratio of the estimated resistance of the base to that of the sub-base is about 1.5, which is higher than what was obtained in the original AASHO model. The estimated value of the parameter  $\gamma$  is close to 1.0, which seems to indicate a relatively constant hazard rate in terms of load repetitions.

**Table 2: Parameter Estimates for Model 1**

Variable	Coefficient	t-statistic
Constant	7.225	15.458
D <sub>1</sub>	0.706	8.954
D <sub>2</sub>	0.255	9.785
D <sub>3</sub>	0.172	7.439
L <sub>2</sub>	3.331	9.439
L <sub>1</sub> +L <sub>2</sub>	-0.180	-12.694
$\gamma$	0.924	16.366

Table 3 presents the results of the Weibull model using our second specification. Again, the t-statistics show that each variable is a significant explanatory variable of crack initiation at one percent significance level. Again, it can be seen that the coefficients have the expected signs.

**Table 3: Parameter Estimates for Model 2**

Variable	Coefficient	t-statistic
Constant	10.788	60.435
D <sub>1</sub>	0.783	11.521
D <sub>2</sub>	0.253	12.620
D <sub>3</sub>	0.191	10.658
TYPE*LOAD	-0.230	-21.522
(1-TYPE)*LOAD	-0.124	-18.850
$\gamma$	0.727	17.502

The ratios of the estimated resistances of the three layers are close to those obtained in the original AASHO model. The results indicate that the asphalt concrete layer is about 3.1 times more effective in reducing the rate of crack initiation than the base layer, and the base layer is about 1.3 times more effective than the sub-base layer. The AASHO results indicated that the asphalt concrete layer is about 3.3 times more effective in reducing crack initiation than the base layer, and the base layer is about 1.3 times more effective than the sub-base layer (HRB 1962).

The coefficients of the two interactive load terms indicate that a tandem axle load of 1.85 kip has the same effect on crack initiation as single axle load of 1 kip. These relative magnitudes are consistent with pavement engineering knowledge. Finally, note that the estimated value of the parameter  $\gamma$  is less than one, indicating a decreasing hazard rate with load repetitions.

The Survival function and the cumulative hazard function computed at the means of the explanatory variables are shown in Figure 9 and Figure 10.

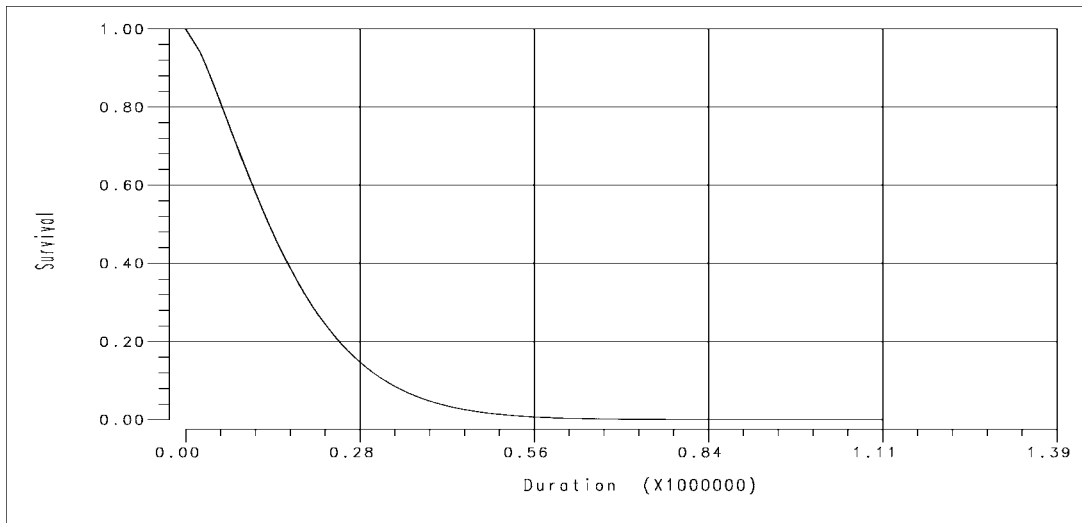


**Figure 9: Survival Function**

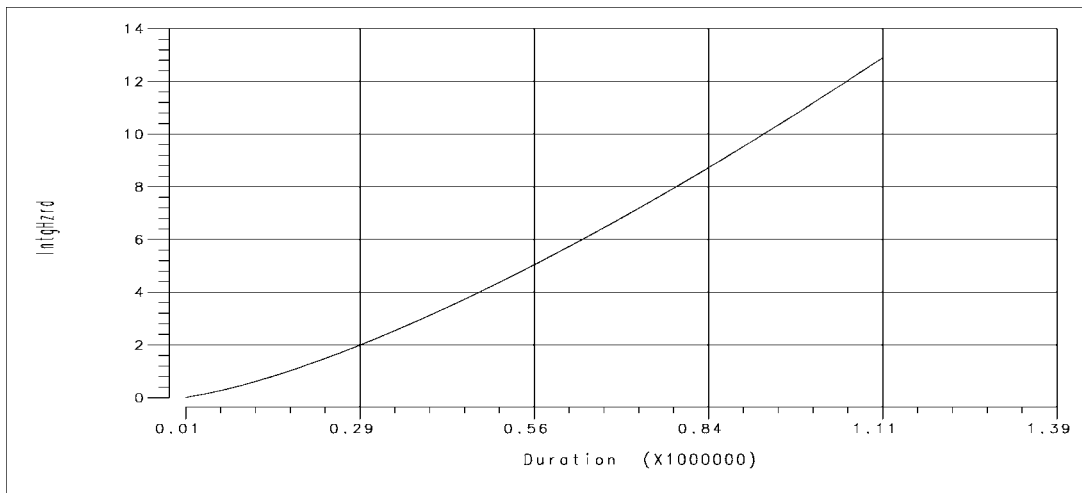


**Figure 10: Cumulative Hazard Function**

The prediction accuracies of the three models (AASHO, Model 1 and Model 2), for the sample of observations used in estimating the parameters, were compared by computing the Root Mean Squared Error (RMSE) of the mean axle load repetitions until cracking initiation, as predicted

with each model. The results are shown in Table 4. The entries in the table are the RMSE of the predicted mean time to cracking in units of axle load repetitions. It can be seen that Model 1 achieves about 10% improvement in the prediction accuracy over the original AASHO model, while Model 2 is 20% more accurate than the AASHO model. In other words, for this data set, almost equal improvements in prediction accuracy can be attributed to the two contributions of this research: a rigorous statistical method (stochastic duration techniques) and an improved model specification.

**Table 4: RMSE of the Mean Predicted Axle Load Repetitions to crack initiation**

AASHO	Model 1	Model 2
3.09 E+5	2.80 E+5	2.46 E+5

Conclusion

In this study, an analysis of the pavement cracking initiation data collected during the AASHO Road Test was conducted. This analysis is based on the use of probabilistic duration modeling techniques. Duration techniques enable the stochastic nature of pavement failure time to be evaluated as well as censored data to be incorporated in the statistical estimation of the model parameters. Due to the nature of pavement cracking initiation, the presence of censored data is almost unavoidable and not accounting for such data would produce biased model parameters. The main advantages that distinguish this stochastic duration model from the original AASHO model are as follows. First, the duration model explicitly recognizes the stochastic variations in the pavement cracking initiation process. Second, the stochastic duration model accounts for the fact that some of the data are censored. Third, our specification was more realistic than that used in the AASHO model, in that it did not assume that the effects of axle type and load were separate and additive. Finally, the predictions obtained with our hazard rate model, using our improved specification, were about 20% more accurate than those obtained using the original AASHO model.

## **Pavement Cracking Progression Model**

### Introduction

Pavement management decisions are based on several data items, such as the available budget, the cost and effectiveness of different activities, and the current and projected levels of usage; among these, the most important piece of information is the performance of the facilities in the system. Two forms of information on pavement performance are used in maintenance and rehabilitation decision-making: information on current (measured) performance, which is obtained through facility inspection, and information on future (predicted) performance, which is obtained using deterioration models. Deterioration models provide predictions of pavement condition over time, which are necessary inputs for planning maintenance and rehabilitation activities.

Pavement deterioration models relate indicators of pavement condition to explanatory variables such as traffic loads, age and environmental factors. The most common indicators of pavement condition are surface distresses, such as longitudinal and transverse cracking, rutting, potholes, etc. These surface distresses are caused by load, moisture, temperature, construction defects or a combination of the above. Most of the engineering knowledge of pavement behavior under traffic loading has been based on mechanistic analyses of pavement structures. While such studies have provided a rich understanding of pavement failure under idealized conditions, they had to be complemented by empirical studies using field data for calibration and validation purposes. Empirical methods, when combined with mechanistic knowledge, have the advantage of representing a wide range of traffic compositions and environmental conditions.

A summary of relevant previous research aimed at developing models of pavement cracking progression and initiation is given below. The ARE study (Butler et al., 1985) developed models of pavement distress and serviceability as a function of explanatory variables. The distress types modeled in the ARE study are cracking, raveling, potholes, rut depth and roughness. Two different sets of models were developed for the initiation and progression phases of the deterioration process. For each time period and distress type, these models predict the change in the extent of distress. The EAROMAR model system (Markow and Brademeyer, 1981) predicts pavement performance, as well as maintenance and rehabilitation costs. The

EAROMAR model differs from the ARE model in that deterioration is predicted by modeling the change in the material properties as a result of traffic loads and precipitation, rather than simply specifying the condition as a function of a vector of explanatory variables. The Queiroz-Geipot models (Queiroz, 1981) have separate regression equations which predict cracking initiation and the rate of crack progression. The cracking initiation model used the number of equivalent single axles to initiation as the dependent variable and the modified structural number as the explanatory variable, while cracking progression was specified to be a function of both structural and age parameters of the pavement. The RITM2 team (Hodges et al., 1975), (Peirsly and Robinson, 1982) also developed separate models for cracking initiation and progression. The cracking initiation model predicts the amount of cumulative equivalent single axles applied during the period before cracking initiation for a given modified structural number. The cracking progression model predicts the incremental change in the area of cracking as a function of the modified structural number and the incremental cumulative traffic loading since the most recent resurfacing. The HDM models developed by the World Bank (Paterson, 1987) predict the initiation and progression of various pavement distresses namely cracking, rutting, potholing, raveling and roughness. Each distress model includes a number of explanatory variables such as age, traffic, design parameters, environmental factors and other distresses.

Several deterioration models reviewed above consist of separate equations for distress initiation and progression. For example, in the World Bank study, cracking initiation was represented by a duration model, where the dependent variable is the probability distribution of the time to cracking. Cracking progression was developed as a regression model, where the estimation sample consisted only of pavement sections that had cracked at the time of the survey. Such an estimation procedure is subject to selection bias, which is introduced by non-random sampling of observations in the progression model. This non-random sampling leads to data sets that are said to be self-selected. Effectively, the data subset used in the estimation of the progression model is likely to differ significantly from the entire data set in its coverage. As such, these progression models are not representative of the entire pavement population from which the sample was drawn.

This report applies a structured econometric method for developing deterioration models of cracking initiation and progression. A model system consisting of a hazard rate model for cracking initiation and a regression model for cracking progression is developed. The estimation

sample for the progression model is self-selected, as it contains a disproportionately large fraction of weaker pavements, because they are more likely to have already started cracking (they have lower initiation times). This selectivity bias is corrected by using Heckman's sequential procedure (Greene, 1993) to obtain consistent coefficient estimates. The methodology for model estimation with self-selected samples is first described. The data set used in this study is then discussed, and empirical results are presented. The report concludes by discussing the importance of these modeling techniques in the field of pavement management.

### Model Development Using Self Selected Samples

When developing continuous models using self selected samples, it is essential to account for the process by which observations are selected into the estimation sample. This is accomplished by representing the sample selection process by a hazard rate model. In this study, the initiation of cracking forms the hazard rate model and the progression of cracking forms the regression model. In this situation, the estimation of the regression model is likely to suffer from selectivity bias. Econometrically, selectivity bias occurs because the error terms of the two models are correlated due to common unobserved effects. In the pavement deterioration context, such unobserved effects may include materials variations that affect the mechanics of both cracking initiation and progression.

The regression model presented in this report was developed using a panel data set of pavements, and therefore had to account for the presence of unobserved heterogeneity, which is likely to exist in such data. Unobserved heterogeneity refers to the presence of persistent facility-specific but unobserved factors, such as variations in construction quality and materials characteristics from one facility to the next. If not corrected for, unobserved heterogeneity may lead to biased model coefficient estimates (Heckman, 1981). The development of the hazard rate model was described in the previous section. The regression model is formulated as follows.

Continuous (cracking progression) model:

$$Y_{it} = \beta' X_{it} + \varepsilon_i + \xi_{it}; \quad \text{if } Z_{it} = 1 \quad (46)$$

where:

$X_{it}$  = a vector of independent variables specific to pavement section  $i$  in period  $t$ ,

$\beta$  = a vector of coefficients to be estimated,

$Y_{it}$  = the dependent variable representing the extent of cracking on pavement  $i$  in time period  $t$ ,  
 $\varepsilon_i$  = a pavement specific term, assumed normally distributed across the population of pavements,  
with mean zero and variance  $\sigma_\varepsilon^2$ , and  
 $\xi_{it}$  = a random error term, varying across both pavements and time periods, assumed normally  
distributed with mean zero and variance  $\sigma_\xi$ .

Clearly, the above equation holds only for those pavements for which cracking is observed at the  
time of the survey.

It can be expected that the pavement-specific random terms of the cracking initiation and  
progression models are correlated, since whatever unobserved pavement-specific factors that  
affected pavement cracking initiation will probably have an effect on cracking progression as  
well. We represent this correlation by the coefficient  $\rho_2$ .

The two equations are now combined to obtain a model that applies to the observations in the  
progression model data set (Greene 1993):

$$E[Y_{it} | Y_{it} \text{ is observed}] = \underline{\beta}' \underline{X}_{it} + \beta_\lambda [\phi(\underline{\mu}' \underline{w}_{it}) / \Phi(\underline{\mu}' \underline{w}_{it})] \quad (47)$$

where:

$\phi$  = the standard normal probability density function,

$\beta_\lambda$  = a coefficient to be estimated.

Equation (5) can thus be written as:

$$E[Y_{it} | Y_{it} \text{ is observed}] = \underline{\beta}' \underline{X}_{it} + \beta_\lambda \lambda_{it} \quad (48)$$

where,

$$\lambda_{it} = \phi(\underline{\mu}' \underline{w}_{it}) / \Phi(\underline{\mu}' \underline{w}_{it}) \quad (49)$$

The parameters of this model system can be estimated by Heckman's procedure which is  
a sequential estimation technique. This method estimates the parameters of the hazard rate  
probabilities and those of the continuous model sequentially, using a three step procedure as  
given below:

1. Estimate the parameters of the hazard rate model by using the method of maximum  
likelihood (this was done in the previous section);
2. For each observation in the selected sample, the correction term given by equation (49) is  
computed.

3. Estimate  $\underline{\beta}$  and  $\beta_\lambda$  by generalized least square regression of equation (48) on the self-selected sample as follows:

$$Y_{it} = \underline{\beta}' \underline{X}_{it} + \beta_\lambda \lambda_{it} + \gamma_{it} \quad (50)$$

where,  $\gamma_{it}$  is now a random error term with zero expected value due to the presence of the correction term in equation (9), but that is still serially correlated because it includes  $\epsilon_i$ . This necessitates the use of a generalized least squares procedure (instead of the usual ordinary least squares) to cleanse the data from the effects of this serial correlation. The details of the GLS procedure are given in (Greene, 1993).

The second term in the right hand side ( $\beta_\lambda \lambda_i$ ) of equation (50) is the correction term for selectivity bias in this regression equation (Train, 1986). If this term is not included in this model, the GLS estimation will result in biased and inconsistent estimates of the vector  $\underline{\beta}$ . This is a typical case of bias due to missing relevant explanatory variables. It can be shown that, if  $\rho_2 > 0$ , this results in an upward bias in the estimated value of  $\underline{\beta}$  (Greene, 1993). Clearly, this bias increases with the absolute magnitude of  $\beta_\lambda$ , which is an estimate of the size of the common unobserved effects among the initiation and progression models.

### Empirical Case Study

The data set was taken from the AASHO road test, which was described in the previous section. To correct for sample selectivity bias, the correction term derived earlier ( $\beta_\lambda \lambda$ ) was included in the cracking progression model, which was estimated by GLS. The estimated regression model with the correction term is as follows:

$$E [\log(\text{cracking}) \mid \text{initiated}] = 4.36 - 1.45 \log(\text{SN}) + 0.22 \log(\text{ESAL}) + 0.14 \log(\text{TD}) \quad (51)$$

Where:

SN: Structural Number of pavement

ESAL: Number of Equivalent Single Axle Loads

TD: Average Temperature Difference between Maximum and Minimum Daily Temperatures in the Previous Time period.

**TABLE 5: Continuous model estimation**

Dependent Variable: log(cracking)		
Observations: 754		
R-squared: 0.713		
Variable	Coefficient	t-statistic
constant	4.365	21.047
Log(SN)	-1.451	-15.386
Log(ESAL)	0.226	17.138
Log(TD)	0.136	2.591

It can be seen that the t-statistics of all the variables are significant, and that the signs of all the coefficients conform to our prior expectations.

### Conclusions

In this report, a structured econometric approach for modeling the initiation and progression of pavement cracking has been presented. Using OLS regression for modeling cracking progression leads to biased and inconsistent estimates as the sample contains only facilities for which cracking has been initiated, thereby introducing selectivity bias in the estimation. A better approach consists of developing separate but interrelated models for cracking initiation and progression, which recognizes and corrects for the presence of selectivity bias by using appropriate correction terms. The coefficients of the model system can be estimated by using a sequential procedure. Finally, the models presented in this report also accounted for possible unobserved heterogeneity in the panel data set, by using a random-effects specification.

## **Analytical Procedure for Inferring Pavement Properties from Condition Data**

In this section, some background on the subject of Bayesian updating will be presented. The proposed procedure for pavement performance model parameter updating will be described. The pavement performance model chosen to illustrate the application of Bayesian updating is the AASHO rutting model developed by Archilla and Madanat (1999a).

### **Bayesian Updating**

In classical statistics, it is assumed that the parameters of a population are constants and sample statistics are used as estimators of these parameters. Because the estimators are invariably imperfect and errors of estimation are unavoidable, the classical statistical approach uses confidence intervals to express the degree of these errors. When the observed data are limited, the statistical estimates have to be supplemented by judgmental information or prior information. With the classical statistical approach there is no provision for combining prior information with observed data in the parameter estimation (Ang and Tang 1975). For example, in a pavement performance model, the only way to utilize new information is to re-estimate all parameters using previous and new data. This would not be cost-effective if the new measurements can be obtained by using high-speed sensor technologies at a higher measurement frequency. On the other hand, the Bayesian approach treats the parameters as random variables and the measurements are sampling results. The Bayesian updating approach provides a way to systematically combine the prior information and new measurement to improve the precision of pavement performance models.

The parameters of the state-of-the-art rutting models that were presented in section 2 were estimated using classical statistics. We can apply Bayesian updating using new observations to update the parameters of these models. The model form stays the same, but the parameters of interest are updated. The standard deviation of the parameters will be reduced, and hence the prediction precision will be improved. The following sections present an overview of the Bayesian Updating Approach. This overview is based on the presentation given in Ang and Tang (1975). Depending on the distribution of the parameters, there are two cases: discrete case and continuous case.

### Discrete Case

Suppose that the possible values of a parameter  $\theta$  are assumed to be a set of discrete value  $\theta_i$ ,  $i = 1, 2, \dots, n$ , with relative likelihoods  $p_i = P(\Theta = \theta_i)$ . If additional information becomes available, the prior assumptions on the parameter  $\theta$  may be modified through Bayes' theorem as follows: Let  $\varepsilon$  denote the new observation, we can update the PMF for  $\theta$  as

$$P(\Theta = \theta_i | \varepsilon) = \frac{P(\varepsilon | \Theta = \theta_i)P(\Theta = \theta_i)}{\sum_{j=1}^n P(\varepsilon | \Theta = \theta_j)P(\Theta = \theta_j)} \quad i=1,2, \dots, n \quad (52)$$

where

$P(\varepsilon | \Theta = \theta_i)$ : the likelihood of the experimental outcome (observation)  $\varepsilon$  if  $\Theta = \theta_i$ ;

$P(\Theta = \theta_i)$ : the prior probability of  $\Theta = \theta_i$ ;

$P(\Theta = \theta_i | \varepsilon)$ : the posterior probability of  $\Theta = \theta_i$ .

Denoting the prior and posterior probabilities as  $P'(\Theta = \theta_i)$  and  $P''(\Theta = \theta_i)$  respectively, we have:

$$P''(\Theta = \theta_i) = \frac{P(\varepsilon | \Theta = \theta_i) P'(\Theta = \theta_i)}{\sum_{i=1}^n P(\varepsilon | \Theta = \theta_i) P'(\Theta = \theta_i)} \quad (53)$$

The expected value of  $\theta$ , called the Bayesian estimator, is expressed as:

$$\hat{\theta}'' = E(\Theta | \varepsilon) = \sum_{i=1}^n \theta_i P''(\Theta = \theta_i) \quad (54)$$

This estimator is based on prior information and updated information.

### Continuous Case

If the distribution of the parameter is continuous, Bayes' theorem gives the posterior probability that  $\theta$  will be in  $(\theta_i, \theta_i + \Delta\theta)$  as

$$f''(\theta_i)\Delta\theta = \frac{P(\varepsilon | \theta_i) f'(\theta_i)\Delta\theta}{\sum_{i=1}^n P(\varepsilon | \theta_i) f'(\theta_i)\Delta\theta} \quad (55)$$

where

$$P(\varepsilon | \theta_i) = P(\varepsilon | \theta_i < \theta \leq \theta_i + \Delta\theta).$$

In the limit, this yields:

$$f''(\theta) = \frac{P(\varepsilon | \theta) f'(\theta)}{\int_{-\infty}^{\infty} P(\varepsilon | \theta) f'(\theta) d\theta} \quad (56)$$

The denominator is independent of  $\theta$  and is replaced by a notation  $k$ .  $P(\varepsilon | \theta)$  is a function of  $\theta$  and is commonly referred to as the likelihood function of  $\theta$  and denoted  $L(\theta)$ . Now we have:

$$f''(\theta) = kL(\theta) f'(\theta) \quad (57)$$

Analogous to the discrete case, we have:

$$\hat{\theta}'' = E(\Theta | \varepsilon) = \int_{-\infty}^{\infty} \theta f''(\theta) d\theta \quad (58)$$

Examples of the application of Bayesian updating include the study by Ang (1973) in the inspection and detection of material defects and the study by Lu and Madanat (1994) in infrastructure deterioration models.

### Pavement Performance Model Parameter Updating

In the proposed research, Bayesian methods will be used to update the parameters of a pavement performance model. In this section, the rutting model developed by Archilla and Madanat (1999a) based on the AASHO road test data, reproduced below, is used to illustrate the parameter updating procedure:

$$RD_{i,t} \approx \beta_{i,10} + \sum_{s=1}^t a_i e^{\beta_8 T_{i,s}} \beta_9 \frac{\Delta N_{i,s}}{N_{i,s}^{1-\beta_9}}$$

$$a_i = \beta_4 e^{-RN_i}$$

$$RN_i = \beta_1 T_{i,1} + \beta_2 T_{i,2} + \beta_3 T_{i,3}$$

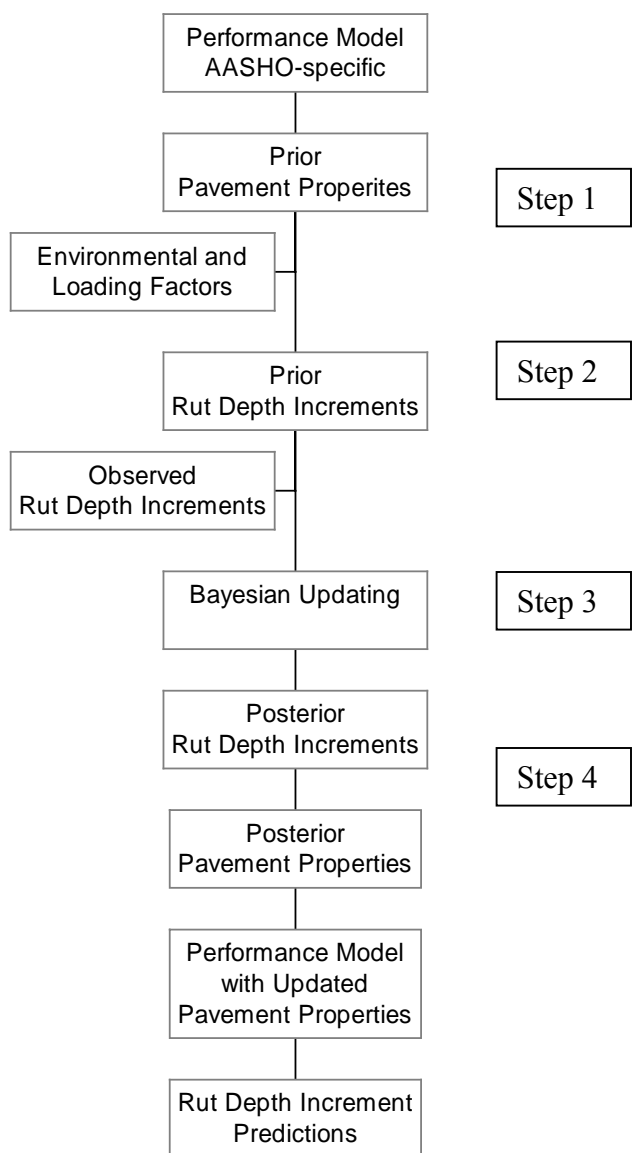
$$N_{i,t} = \sum_{s=1}^t \Delta V_{i,s} \left[ \left( \frac{FL_i}{SAL} \right)^{\beta_5} + R_i \left\{ \left( \frac{AL1_i}{SAL} \right)^{\beta_5} + \left( \frac{AL2_i}{\beta_7 SAL} \right)^{\beta_6} \right\} \right]$$

Pavement sections in the field lack either initial construction data or complete performance history or both, and the accuracy of data is lower than that of experimental data. Due to the constraints above, a complete re-calibration of model parameters using field data is infeasible. A possible approach would be to re-calibrate one or some important model parameters based on available data, while assuming that the other parameters are constant. The AASHO Road Test is a well-designed experiment and very comprehensive in terms of loading factors, environmental factors, and pavement layer structure. The parameters in the AASHO model are either related to environmental factors (such as  $\beta_8$ ), loading (such as  $\beta_5, \beta_6, \beta_7, \beta_9$ ), or pavement properties (such as  $\beta_1, \beta_2, \beta_3, \beta_4$ ). The data on environmental factors and loading factors are easier to obtain for field pavement sections and the effects of these factors are well captured in the performance model. Hence, when choosing an important parameter in the performance model to update, the focus is on the parameters related to pavement properties. In other words, the feasibility of transferring the AASHO model to other locations depends on the updating of the parameters representing the pavement properties. In the AASHO model, the parameters  $\beta_1, \beta_2, \beta_3$  are used to calculate the resistance number ( $RN_i$ ). The parameter  $\beta_4$  and  $RN_i$  are used to calculate the parameter  $a_i$ . Thus, the parameter  $a_i$  is a function of the parameters  $\beta_1, \beta_2, \beta_3, \beta_4$  and the pavement layer thicknesses  $T_{i1}, T_{i2}, T_{i3}$ . To apply the AASHO model to other locations such as the Mn/Road test site, we need to estimate the parameters  $a_i$  for the pavements in that location. The thickness can be measured by using Ground Penetrating Radar (GPR), but the parameters  $\beta_1, \beta_2, \beta_3, \beta_4$  estimated in the AASHO Road Test may not apply for the Mn/Road pavements. In this research, instead of updating these four parameters, the parameter  $a_i$  will be updated directly. For the purpose of rutting prediction, it is sufficient to know the parameter  $a_i$  for each pavement section. It is not necessary to update the individual parameters  $\beta_1, \beta_2, \beta_3, \beta_4$ .

In the AASHO performance model, the variable  $a_i$  plays the role of pavement property and it is related to the structural number ( $SN$ ) which is used by pavement engineers to characterize the strength of pavements. Therefore, if we can obtain an accurate estimate of the variable  $a_i$  for the pavement sections of interest, then the prediction of rut depth increment is straightforward. To

use the performance model, which was developed based on the AASHO Road Test data, for in-service pavement sections, we must obtain an estimate of the value of  $a_i$  for these pavement sections. The Bayesian updating approach is one way to systematically update the values of  $a_i$ . The estimated parameters in the AASHO model of Archilla and Madanat (1999a) can be safely assumed to be normally distributed because the sample size used for the estimation was very large. The procedure used for updating the AASHO performance model parameter is illustrated in Figure 11 and described below:

**Figure 11: Bayesian Updating of the AASHO Performance Model**



Step 1. Prior distribution of  $a_i$  :

The thickness data,  $T_{i1}$ ,  $T_{i2}$ ,  $T_{i3}$ , can be obtained either from construction records, or measured by using GPR. The distribution of the variable  $a_i$  can be approximated by a normal distribution as suggested by a simulation based on the model estimation results (related to  $\beta_1$ ,  $\beta_2$ ,  $\beta_3$ ,  $\beta_4$ ) given in Table 3. This distribution is the prior distribution of  $a_i$  and is denoted as  $f'(a_i)$ .

Step 2. Prior distribution of  $\Delta RD_{it}$  :

The parameter we want to update is the structural number  $a_i$  but what we observe in the field are rut depth increments that are manifestations of the underlying pavement property interacting with loading and environmental factors. This necessitates the derivation of the prior distribution of rut depth increment from the prior distribution of the structural number  $a_i$  based on the relationship given by the performance model. The distribution of rut depth increment at time  $t$ ,

$\Delta RD_{it}$ , is a function of  $a_i$  and a time-dependent constant  $K_{i,t}$  ( $K_{i,t} = e^{\beta_8 T I_t} \beta_9 \frac{\Delta N_{i,t}}{N_{i,t}^{1-\beta_9}}$ ).

Thus, the parameters of the distribution of rut depth increment (also a normal distribution whose parameters are denoted by  $\Delta RD'_{it}$  and  $\sigma_{it}^2$ ) can be derived, provided the loading data and environment data are known (to calculate the constant  $K_{i,t}$ ).

Step 3. Information from new observations:

Automated sensing technologies such as the PASCO multifunction survey vehicle measure the mean rut depth increment ( $\overline{\Delta RD}$ ) and standard error ( $\sigma/\sqrt{n}$ ) for pavement section  $i$  at time  $t$ . The standard error depends on the precision of measurement equipment and the number of observations made ( $n$ ).

Step 4. Parameter updating:

The posterior estimate of the parameter, obtained by Bayesian updating is a weighted average of the prior information and new information. The weights are proportional to the precision of each source of information (i.e. inversely proportional to the respective variances). In this case, since both the prior information and the observations are normally distributed, they are shown (Ang and Tang, 1975) to be conjugate distributions and the resulting posterior distribution is also a normal distribution with the parameters given below:

$$\Delta RD_{it}'' = \frac{\Delta RD_{it}' (\sigma^2/n) + \overline{\Delta RD} \sigma_{it}^2}{\sigma^2/n + \sigma_{it}^2} \quad (59)$$

$$\sigma_{it}'' = \sqrt{\frac{\sigma_{it}'^2 (\sigma^2/n)}{\sigma_{it}'^2 + (\sigma^2/n)}} \quad (60)$$

After estimating the updated rut depth increment  $\Delta RD_{it}''$ , we can update the pavement property  $a_i$  for pavement section  $i$  using following relation:

$$a_i'' = \frac{\Delta RD_{it}''}{K_{i,t}} \quad (61)$$

Afterwards, the updated pavement property  $a_i''$  will be used instead of  $a_i'$  in the pavement performance model, for prediction purposes.

The 4-step procedure above shows how new information obtained by automated sensing technologies can be used to apply a pavement performance model to a specific pavement section. This approach, although illustrated with a rutting model, can be applied to other types of distresses such as cracking and roughness, if good performance models for these distresses exist.

## **Test Conditions**

### **The MnRoads Test Data**

The AASHO Road Test equations provided adequate knowledge of pavement design for the time period in which they were developed and tested but there were several shortcomings. The AASHO Road Test was conducted over a two-year period, so while the loading effect to pavement was well addressed, the contribution of climate was minimized and the interaction between traffic and climate was not fully related. The changing conditions in traffic loads and new materials could not be incorporated in the design procedure due to the empirical nature of these equations. For example, the use of higher pressure tires (from 75 psi in the late 50's to 105 psi in the late 80's), higher volumes of truck traffic, and new material such as polymer modified asphalt binder cannot be accommodated in the models developed in AASHO Road Test (Stroup-Gardiner *et al.* 1997).

Recognizing the need to address this situation, Mn/DOT cooperated with the University of Minnesota in the late 80's to develop a new pavement design method. In order to better understand the effects the increased traffic loads and volumes have on pavement performance in Minnesota, Mn/DOT decided to build a new full scale pavement test facility to evaluate the current pavement performance and develop the desired pavement design method (Burnham *et al.* 1997).

The Minnesota Road Research Project, known as Mn/Road, constructed a test facility located approximately 40 miles northwest of Minneapolis in Otsego, Minnesota. The facility contains 4.8 km (3 miles) of two-lane interstate as well as 4 km (2.5 miles) of closed-loop low volume track and is divided into forty 150 m (500 ft) long instrumented test sections or "cells" arranged into two different groups of traffic loading and three different periods of service life (see Figure 12 and 13). The groupings are as follows:

- (1) Nine 5 year design life "mainline" cells which carry the high volume interstate (I-94) traffic loads,
- (2) Fourteen 10 year design life "mainline" cells which also carry the high volume I-94 traffic,
- (3) Seventeen 3 year design life "low volume" cells which receive loading from a test truck driven on a closed loop.

Figure 12: Mn/Road Test Facility Parallel to Interstate I-94  
(Source: Mn/ROAD webpage).



Figure 13: Low Volume Loop at Mn/ROAD Test Facility (Source: Mn/ROAD webpage).



The I-94 traffic was about 14,000 vehicles per day (15 percent truck) and is diverted onto the high volume facility where the 23 heavily instrumented test sections are subjected to real traffic loads. The remaining 17 sections in the low volume facility are subjected to the loading from a test truck.

Among these forty sections, twenty two are bituminous surfaced, fourteen are Portland Cement Concrete (PCC) surfaced, and four are aggregate surfaced. Facility construction started in 1990 and electronic instrumentation and paving of the cells occurred in 1992 to 1993. The test cells were opened to traffic loading in August of 1994.

The test sections are heavily instrumented and these sensors can be classified into two groups according to Mn/ROAD team: pavement sensors and subsurface sensors. Pavement sensors contain 13 types of sensors including Concrete Embedment Strain Gage (CE) to monitor dynamic strains, Dynamic Soil Pressure Cell (PK) to measure vertical pressure data that will be used to determine the vertical stress distribution in the base and subgrade layers, and Transverse Embedment Strain Gage (TE) to measure horizontal strains in asphalt concrete which is related to the current failure criteria used in mechanistic-empirical pavement design procedures.

14 types of sensors serve as subsurface sensors which contain Thermocouple (TC) which is used to measure the temperature in the pavement surface layers, the base and subgrade and Moisture Block (WM) for subsurface unfrozen moisture content. Generally speaking, Mn/ROAD test facility has the most sophisticated sensor systems to monitor pavement properties and behaviors (Stroup-Gardiner *et al.* 1997, Burnham *et al.* 1997, Garg *et al.* 1998).

### **Field Tests Sites Considered for Data Analysis**

#### 1) I25/225, Denver, CO

Description of Test Area:

10 miles of I-25, 4 miles of I-225

I-25 section went from MP 194.6 to MP 204.1

Pavement construction:

According to the state records, all of I-25 was asphalt over concrete, except for 0.7 miles at the north end, where it was full depth asphalt. The records show that the asphalt section was constructed in 1996. The GPR data confirms the general composite structure, with 4-8 inches of asphalt overlay. The GPR data shows a full depth asphalt for 0.62 miles beginning at 201.825 to 202.44, a slightly different location than shown in the state records. State records show all of I-225 to be full depth asphalt, constructed in August of 1999. The GPR data confirms the full depth asphalt construction.

Data Collected on both of these sections included longitudinal cracking and rutting, and GPR. Rutting and cracking are reported every 75 feet. Raw GPR data is available every foot, and was processed every 75 feet to coincide with the rutting and cracking data. The full depth asphalt section of I-25 was used for rutting evaluation. Since alligator cracking was not reported, the cracking model could not be applied to this data. The rut data from I-225 was very low and uniform, due to the fact that the pavement was very new, and therefore it was not used for data analysis.

A sample of the GPR data on the full depth asphalt section of I-25 is shown in Figure 14. The asphalt thickness is approximately 32 cm. A sample of the rutting data vs distance is shown in Figure 15.

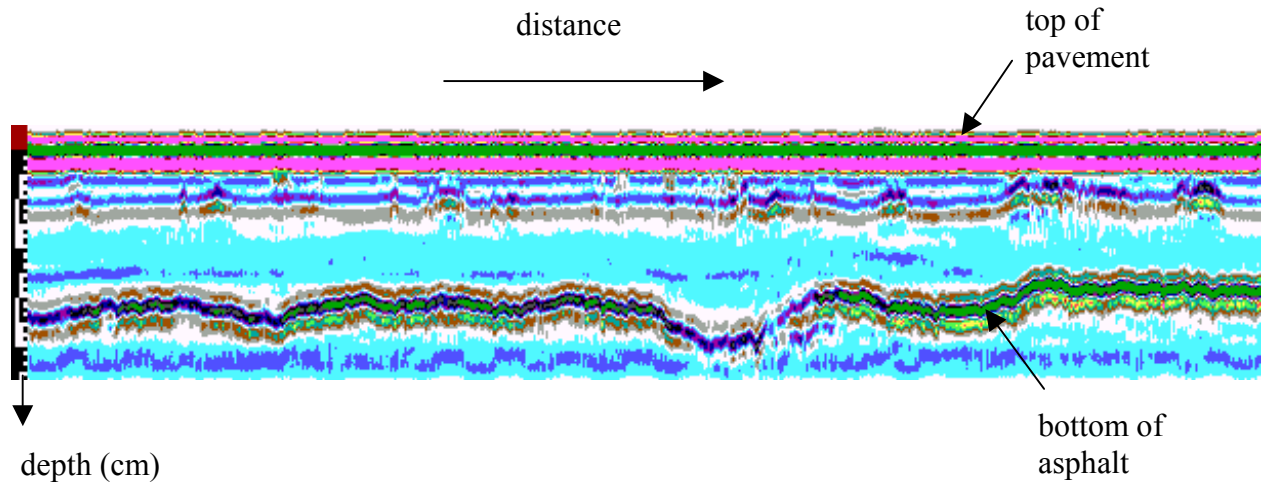


Figure 14 – Sample GPR Data from Interstate 25, Full Depth Asphalt Section

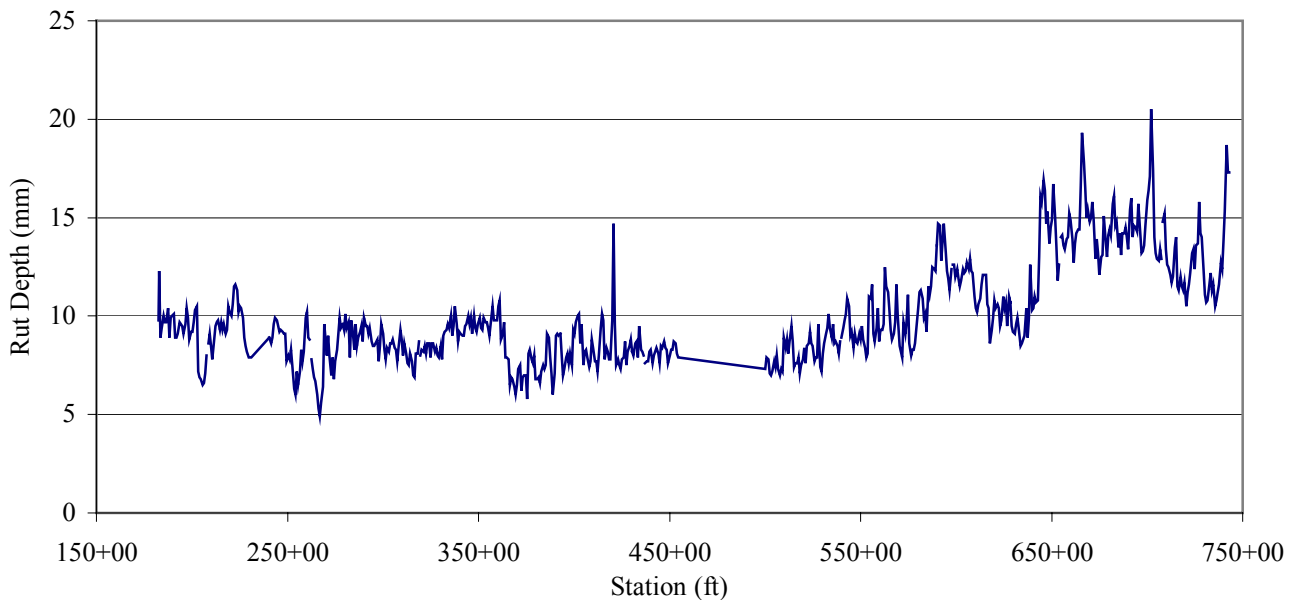


Figure 15 - Rut Depth Data from I-25 Northbound

## 2) Tamiami Trail, US 41, South Florida

The test area was a 10 mile section of US 41 in south Florida. The data collected this section included longitudinal cracking and rutting, and GPR Rutting and cracking are reported every 75 feet. Raw GPR data is available every foot, but thickness has been processed every 500 feet to coincide with the location of FWD tests. A sample of the available rut depth and cracking data is shown in Table 6. A sample of the GPR thickness data is shown in Table 7. Figure 16 shows a plot of the cracking data.

No construction history or traffic information could be obtained for this site.

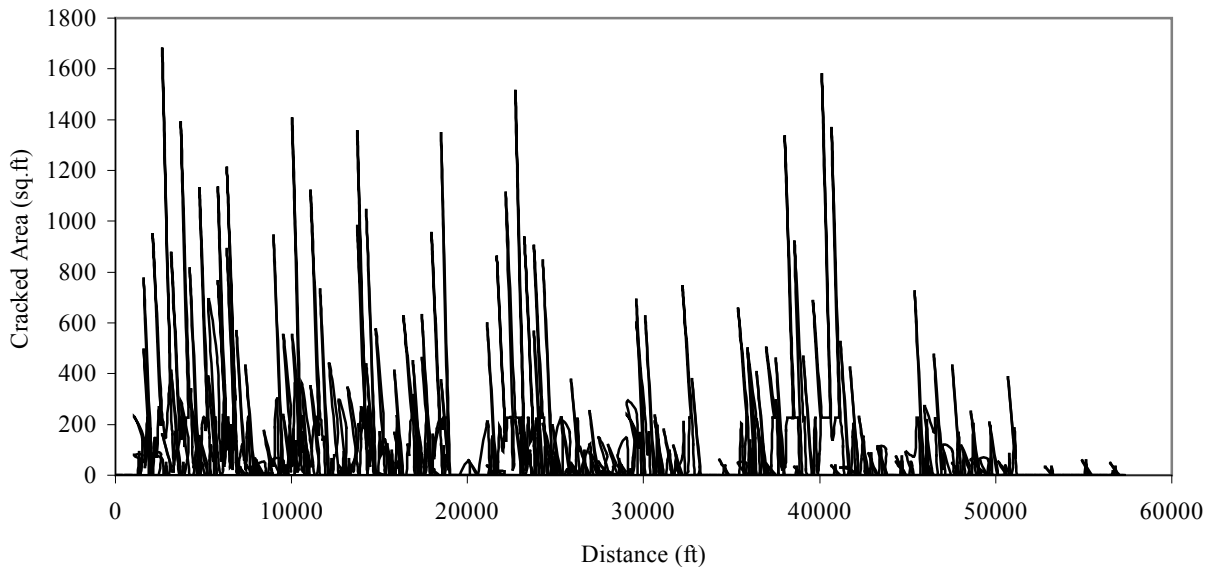


Figure 16 – Sample Plot of Cracked Area vs. Distance for Tamiami Trail

### 3) SH33 near West Bend, WI

This is an old pavement with the following history:

1930 - 9" Jointed Plane PCC (mesh and dowel), joint spacing unknown, probably 40') on a soil base of indeterminate depth. The pavement structure was 20' wide on two lanes. This was a typical depression era public works project from the effort to get rural (farm-market) transportation improved.

1983 - A pavement improvement project widened the road to 24' (two lanes) on the old centerline. The overlay was 5" of recycled AC hot mix. The project included base widening to support the wider pavement structure and shoulders.

1995 - A pavement overlay probably 2-3" (data not available) with no improvement in cross section width.

The pavement performance since 1995 has been very typical. There is no rutting and the transverse and longitudinal cracking are narrow and of a pattern consistent with cold weather cracking (tight cracks, no less than 20' spacing transversely and nothing beyond centerline cracking longitudinally). Nothing out of the ordinary for heavy freeze thaw state.

GPR data was collected on this site based on WisDOT initial description of its suitability for the project. WisDOT initially indicated that they had detailed condition data on this pavement.

However, when pressed for details the data they provided was qualitative, as shown in Table 8, and not directly usable for the quantitative models being investigated under this project. Figure 17 shows the results of the GPR layer thickness analysis of the section.

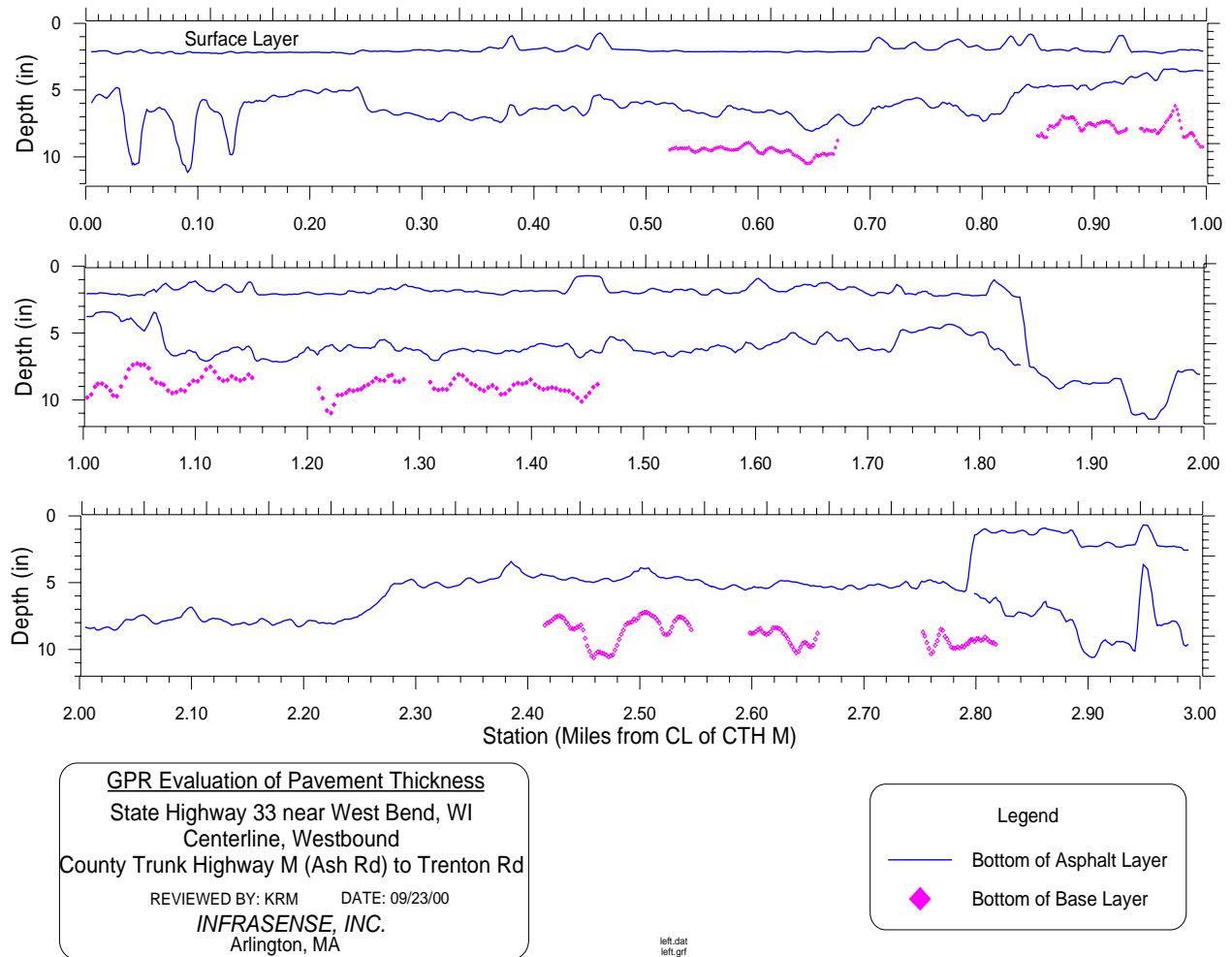


**Figure 17: GPR Layer Analysis for SH 33 in Wisconsin**

Table 6 - Sample Data File for Alligator Cracking and Rutting – Tamiami Trail

RSTNUM	Object	Beg Station	End Station	Alligator Cracking (sf)	rut depth (in.)
1	352	0	75	0	0.14
2	352	75	151	0	0.15
3	352	151	226	0	0.15
4	352	226	302	0	0.14
5	352	302	377	0	0.13
6	352	377	453	0	0.14
7	352	453	528	0	0.17
<b>352 Total</b>		<b>0</b>	<b>528</b>	<b>0</b>	<b>0.15</b>
8	353	528	603	0	0.17
9	353	603	679	0	0.15
10	353	679	754	0	0.17
11	353	754	830	0	0.17
12	353	830	905	0	0.22
13	353	905	981	0	0.22
14	353	981	1056	0	0.18
<b>353 Total</b>		<b>528</b>	<b>1056</b>	<b>0</b>	<b>0.18</b>
15	354	1056	1131	0	0.20
16	354	1131	1207	0	0.24
17	354	1207	1282	0	0.25
18	354	1282	1358	0	0.25
19	354	1358	1433	91	0.27
20	354	1433	1509	0	0.21
21	354	1509	1584	140	0.28
<b>354 Total</b>		<b>1056</b>	<b>1584</b>	<b>231</b>	<b>0.24</b>
22	355	1584	1659	145	0.25
23	355	1659	1735	32	0.19
24	355	1735	1810	91	0.21
25	355	1810	1886	226	0.20
26	355	1886	1961	0	0.16
27	355	1961	2037	0	0.18
28	355	2037	2112	0	0.21
<b>355 Total</b>		<b>1584</b>	<b>2112</b>	<b>494</b>	<b>0.20</b>
29	356	2112	2187	0	0.20
30	356	2187	2263	0	0.16
31	356	2263	2338	0	0.19
32	356	2338	2414	0	0.19
33	356	2414	2489	0	0.23
34	356	2489	2565	0	0.24
35	356	2565	2640	84	0.23
<b>356 Total</b>		<b>2112</b>	<b>2640</b>	<b>84</b>	<b>0.20</b>
36	357	2640	2715	63	0.24
37	357	2715	2791	0	0.22
38	357	2791	2866	0	0.28
39	357	2866	2942	48	0.19
40	357	2942	3017	0	0.19
41	357	3017	3093	0	0.19
42	357	3093	3168	50	0.17
<b>357 Total</b>		<b>2640</b>	<b>3168</b>	<b>161</b>	<b>0.21</b>
43	358	3168	3243	32	0.21
44	358	3243	3319	16	0.23
45	358	3319	3394	16	0.21
46	358	3394	3470	165	0.26
47	358	3470	3545	143	0.17
48	358	3545	3621	38	0.19
49	358	3621	3696	0	0.17
<b>358 Total</b>		<b>3168</b>	<b>3696</b>	<b>410</b>	<b>0.21</b>
50	359	3696	3771	7	0.22

Table 7 - Sample GPR Thickness Data for Tamiami Trail

FWD Station (ft)	GPR Station (ft)	GPR Thickness (in)	GPR Thickness (m)
Eastbound			
0	58019	10.3	0.26162
250	57767	7.5	0.1905
750	57262	7.7	0.19558
1250	56758	7	0.1778
1750	56254	7	0.1778
2176	55824	8.4	0.21336
2184	55816	8.4	0.21336
2191	55809	8.2	0.20828
2250	55749	7.2	0.18288
2750	55245	6.7	0.17018
3250	54741	7	0.1778
3750	54237	7.5	0.1905
4250	53732	5	0.127
4750	53228	6.5	0.1651
5250	52724	6.5	0.1651
5750	52219	6.7	0.17018
6250	51715	5.5	0.1397
6750	51211	6.9	0.17526
7250	50706	7.7	0.19558
7750	50202	7.5	0.1905
8250	49698	6.7	0.17018
8750	49193	6.2	0.15748
9250	48689	7.4	0.18796
9750	48185	9.6	0.24384
10250	47680	8.7	0.22098
10750	47176	8.7	0.22098
11250	46672	9.6	0.24384
11750	46168	9.3	0.23622
12250	45663	9.4	0.23876

Table 8 – SH33 Condition Data

Survey Year		1986	1988	1990	1992	1994	1996	1998*
Spring Distress Survey	PDI	13	13	27	13	36	19	87
Transverse								
	Extent	1	1	1	1	1	1	2
	Severity	1	1	1	1	2	1	2
Longitudinal								
	Extent	1	1	1	1	2	2	1
	Severity	1	1	1	1	2	1	2
Rutting								
		0	0	1	0	0	0	2
Fall Ride Survey	Rutting (")	0.00	0.00	0.18	0.23	0.21	0.19	0.10

Explanation of Distress Survey Values

- Cracking Severity      1 - tight/sealed cracks  
                                  2 - wide Cracks  
                                  3 - dislodgement in cracks
- Transverse Extent      0 - none  
                                  1 - 1-5 per 100' station  
                                  2 - 6-10 per 100' station  
                                  3 - 11+ per 100' station
- Longitudinal Extent    0 - none  
                                  1 - 1-100' per station  
                                  2 - 101-200' per station

Rutting is assigned severity levels only. The extent is assumed to be 100 percent of the segment.

The four severity levels are:

- 0 = rutting not represent or insignificant in amount
- 1 = rutting 1/4- to 1/2-inch in depth
- 2 = rutting 1/2- to 1 inch in depth
- 3 = rutting greater than 1 inch in depth

## **Test Results**

### **Results of Applying the Analytical Procedure to the MnRoads Test Data**

#### Tests Using the Pavement Rutting Model

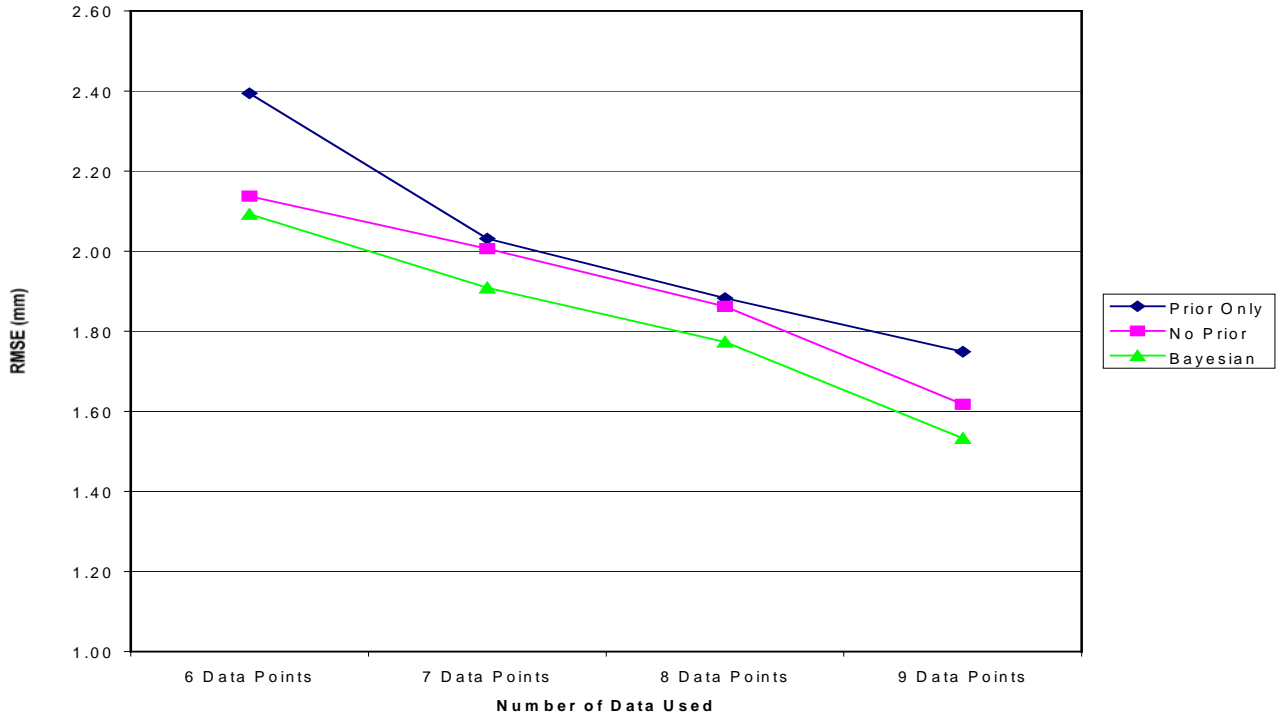
We performed two different tests of the analytical procedure using the rutting model with the MnRoads test data. The first test focused on the effect of the number of measurements used on the prediction precision of the analytical procedure. Toward that end, we performed the following experiment. For each pavement cell in the MnRoads data set for which we have a total of  $N$  observations, we used the first  $M$  observations to compute the statistics of the likelihood function in the Bayesian updating formula. These statistics (as described in the previous chapter) were then used, together with the prior statistics, to compute the relevant pavement properties. On the basis of these computed properties, we predicted that pavement cell's rut depths for the remaining  $(N-M)$  observations. We then compared these predictions to the observed rut depths for these observations. The precision was represented by the Root Mean Squared Error (RMSE) of the predicted rut depths.

The results are depicted in Figure 18, which shows three curves, one corresponding to the RMSE obtained using the prior information only case, one for the no-prior case (likelihood function only), and one for the Bayesian case that combines both sources of information. For each curve, we show four data points, corresponding to the RMSE obtained with 6, 7, 8 and 9 observations respectively.

Two conclusions can be readily made:

1. The Bayesian analytical procedure outperforms both the prior-only and the no-prior methods for predicting pavement rutting;
2. Increasing the number of data points improves the rut depth prediction precision, irrespective of the prediction method used.

Figure 18: RMSE for the three prediction methods



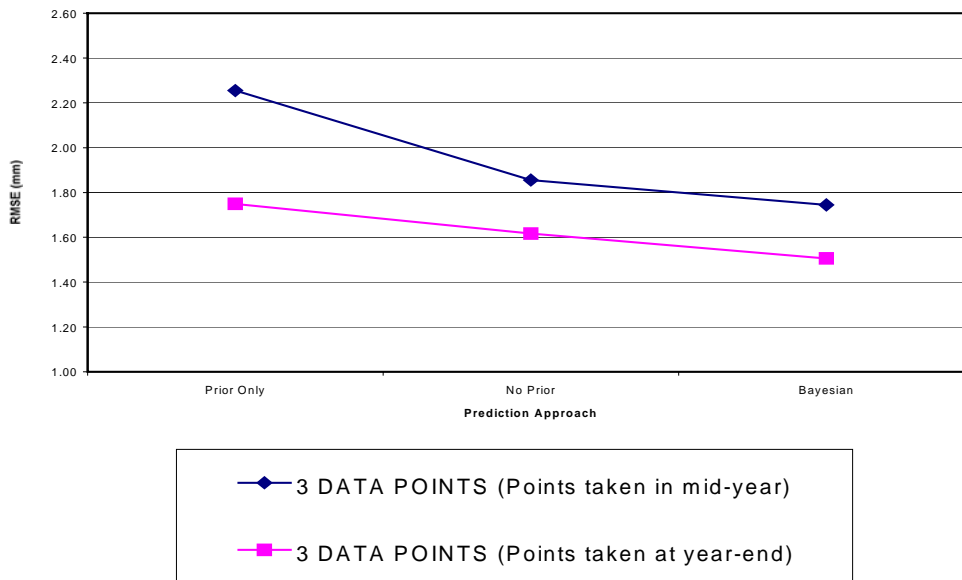
Both conclusions are consistent with statistical theory and with engineering intuition. What we did not expect, however, is that the addition of measurements does not yield a very significant increase in precision. By incorporating three more observations, the RMSE is not reduced by more than one millimeter for any of the three methods. In fact, the predictions based on 6 measurements have high precision (low RMSE), which is sufficient for most pavement management applications.

The second test aimed at evaluating the precision of the analytical approach in cases where the inspection frequency is lower. In a realistic pavement management context, rutting measurements are taken at a lower frequency than in the MnRoads data set. Instead, pavement condition data will likely be collected annually. To test the performance of the Bayesian approach in this context, two simulations were conducted. In the first simulation, the

measurements collected in mid-year were used. In the other, the measurements collected at the end of the year were used. Figure 19 summarizes the results.

As can be seen, the RMSE obtained are small in both cases, even relative to the cases used in the first test, where more measurements were taken. Both the mid-year and the year-end cases perform better than the cases with 6 measurements. This is due to the fact that the three annual measurements cover a longer span of the pavement life than the six consecutive measurements. Effectively, the three annual measurements provide an average of a larger data set, and thus yield

**Figure 19: RMSE for the case of annual inspections**



better results.

### Tests Using the Pavement Cracking Models

The methods used for classifying pavement cracking, and for measuring cracking initiation and progression at the MnRoads test site were totally different from those used in the AASHO test. Therefore, it was not possible to use the MnRoads data set to test the accuracy of our AASHO based cracking initiation and progression models, or of the analytical procedure that uses these models as input.

## **Results of Applying the Analytical Procedure to Field Data**

### Rut Prediction Software (RUT)

The program RUT is a Windows based implementation of both the Berkeley Rutting Model and the Infrasense Rutting Model. The Berkeley Rutting Model is the Pavement Rutting Model described earlier in this report with Bayesian updating added to incorporate the observed rutting behavior into the model. The Infrasense Modified Rutting Model modifies the Pavement Rutting Model to incorporate spatial variability where temporal measurements are unavailable.

Figure 21 depicts the main program flow. The initial choices available to the program user are to either enter project information into the tabbed data screens manually, or to use the pull down menu to retrieve project information from a previously stored project information file. Once project information is retrieved and/or manually modified, it may be saved to a project information file by using the pull down menu.

Data input to the program is in ASCII file formatting (text files). Four data files are required, one for each type of information used by the model: Weather data, Rutting data, Traffic (ESAL) data, and Thickness data. Each line in the files represents a new set of data. The data values for each data set are separated into fields on each line by spaces, tabs or commas.

The specific format for each file is entered into the program on the appropriate tabbed sheet – Weather Data, Rutting Data, ESAL Data and Thickness Data. On each of the tabbed sheets, the user specifies the input file name, the location of each data field in the file, and the number of lines to skip when reading in the input data. Skip lines allows the header information to be ignored by specifying how many lines must be skipped when reading the file before the data set is encountered. The specific requirements for each type of data file are defined in the Berkeley Rutting Model Program Implementation Documentation.

Once the data files and their input specifications have been entered, the user can model the rutting in each cell by selecting the Data Set tab. Here a data directory is specified where the results will be stored. If the rutting distance values and the radar (thickness) distance values are in different scales or directions, the user can check the 'Perform Distance Calibration' box and enter the distance values of two corresponding points in each file in order to calibrate the

thickness data to the rutting cell data locations. Finally, on this tab, the user will choose to model the cells using the Berkeley Model or the Modified Model.

Figure22 depicts the Berkeley Model program flow and Figure23 depicts the Infrasense Modified Model program flow.

Rutting data is provided as the measured rutting value (depth) per cell. Each “cell” is a defined area of pavement. The rutting increases between the date of pavement creation (new pavement or resurfacing) and the date of rutting measurement are interpolated using an exponential function:

$$\text{RutDepth} = \text{alpha} \times \left( N^{\text{beta}} \right)$$

Where N is the number of accumulated load applications. Beta is a fixed coefficient entered by the user, and the program estimates alpha by fitting the curve through the starting and ending rut values. Future versions of the program will allow additional (“intermediate”) rutting values to be entered. These values, when available, will be used to determine the value of the observed rut progression curve. However, because of the cost and annoyance of obtaining rut values, there tends to be, in practice, little or no information about the progression of rut depth over time. Hence, the Modified Rutting Model or the INFRASENSE model, introduces the concept of homogenous sections (explained below) in order to use spatial variation in rutting to supplement the absent (or, at best, sparse) measure of temporal variation originally used in the Berkeley Model for performing Bayesian updating of the pavement model parameters.

In both models, the data files are read using the filenames and formats specified by the user on the tabbed data input screens. Data units are converted, and, if required, a distance is calibrated in order to match rutting data up with the appropriate thickness data. For the Modified Model, the user inputs homogeneous section specifications. A loop is then entered in which the rutting calculations are made for each cell.

As depicted in Figure22, the Berkeley Model loop is as follows:

- interpolate ESALS:  
Daily ESALS for the initial time period and the daily ESALS at the time of the last rut depth study performed on the cell are linearly interpolated over the entire time period. Cumulative 2-week values are obtained from the interpolated daily values.
  
- interpolate rutting

$$\text{RutDepth} = \alpha \times \left( N^{\beta} \right)$$

- calculate the Thermal Index (TI)  
Daily weather data is averaged to obtain mean 2-week maximum and mean 2-week minimum daily temperature values.

$$\text{accFz}_i = \text{Max}(0, \text{accFz}_{i-1} - \text{MinTemp}_i)$$

$$\text{TI}_i = \text{accFz}_i * \text{Max}(\text{MaxTemp}_i, 0)$$

where

accFz<sub>i</sub>=Accumulated Freeze in the current time period

accFz<sub>i-1</sub>=Accumulated Freeze in the previous time period

TI<sub>i</sub>=Thermal Index in the current time period

MinTemp<sub>i</sub>=Average Daily Minimum Temperature in the current time period

MaxTemp<sub>i</sub>=Average Daily Maximum Temperature in the current time period

- Calculate a  
In the model, a, the rut depth caused by the first standard axel load, is defined as follows:

$$a = \beta_4 * \varepsilon^{-(\beta_1 * T_1 + \beta_2 * T_2 + \beta_3 * T_3)}$$

where

β<sub>1</sub>, β<sub>2</sub>, β<sub>3</sub> and β<sub>4</sub> are parameters of the model based upon materials properties

T<sub>1</sub>, T<sub>2</sub> and T<sub>3</sub> are the three pavement layer thicknesses

- calculate a from Monte Carlo simulation  
An average thickness is calculated for T1, T2 and T3 for the cell interval.  
Simulation is implemented using the Box-Muller-Marsaglia method. N samples (N = number of simulation samples) are obtained for the parameters β<sub>1</sub>, β<sub>2</sub>, β<sub>3</sub> and β<sub>4</sub> based on each parameter's given standard deviation, assuming a normally distributed population. If required, the user can change the materials parameters Beta1 though Beta4 and/or their standard deviations, by modifying them on the Simulation tab. On this tab, the user can also change the number of samples used to perform the simulation (N), although 1000 is the recommended value to use.

The value of a is calculated for each simulated sample. The mean and standard deviation for the simulated a values ( $a_{sim}$ ) are obtained:

$$\bar{a}_{sim} = \text{mean}\left[\beta_4 * \varepsilon^{-(\beta_1 * T_1 + \beta_2 * T_2 + \beta_3 * T_3)}\right]$$

$$\hat{a}_{sim} = \text{stdev}\left[\beta_4 * \varepsilon^{-(\beta_1 * T_1 + \beta_2 * T_2 + \beta_3 * T_3)}\right]$$

- calculate a observed

An estimate of a is obtained for each 2 week time interval during the interval between the initial time period and the time of the last rut depth study performed. Then the mean and standard deviation of the observed a values are calculated.

$$a_i = \frac{\Delta \text{RutDepth}_i}{\varepsilon^{\beta_8 * \left(\frac{T_{i1}}{1000}\right)} * \beta_9 * \left(\frac{\Delta \text{ESAL}_i \div 1000}{\text{ESAL}_i^{(1-\beta_9)} \div 1000}\right)}$$

$$\bar{a}_{obs} = \text{mean}(a)$$

$$\hat{a}_{obs} = \text{stddev}(a)$$

- calc a posterior

Bayesian updating provides a Bayesian posterior  $a_{post}$ .

$$a_{post} = \frac{\bar{a}_{sim} * (\hat{a}_{obs})^2 + \bar{a}_{obs} * (\hat{a}_{sim})^2}{(\hat{a}_{obs})^2 + (\hat{a}_{sim})^2}$$

- Calculate the Bayesian model results

Rutting predictions are obtained for each future weather interval provided in the input file using the Bayesian value of a ( $a_{post}$ ).

$$\text{RutDepth} = a_{post} * \left[ \varepsilon^{\beta_8 * \left(\frac{T_{i1}}{1000}\right)} * \beta_9 * \left(\frac{\Delta \text{ESAL}_i}{1000} / \left(\frac{\text{ESAL}_i}{1000}\right)^{(1-\beta_9)}\right) \right]$$

- Save the model constraints and the rutting prediction data

When the user selects the Modified Model, homogeneous sections are defined based on common thickness values. The variation in thickness in these sections as well as the variation in rutting within a section is used to refine the calculation of the posterior a value.

Figure24 shows the flow chart of the process used to define and create homogeneous sections. As seen in Figure24, the user must first enter the defining characteristics of the homogeneous section - which layer to use, the minimum acceptable segment length, maximum difference in average thickness between segments, and a minimum and maximum range value to use when reading in the input data.

Once these definitions are provided, the thickness data is read in and truncated at the maximum and minimum range values. Truncation provides a means to deal with anomalies in the data set so that unusually large or small incorrect values will not unduly influence the section's average value calculation. Thence, defining homogeneous sections proceeds as follows:

- A weighted area is defined for each distance interval (x)

$$A_x = (\text{dist}_x - \text{dist}_{x-1}) * T_x$$

- The average response is calculated

$$\text{rhat} = (A_x - A_0) / (\text{dist}_x - \text{dist}_0)$$

- The cumulative difference slope is defined

<p>Cumulative Area: <math>A_{\text{hat}_x} = (\text{dist}_x - \text{dist}_{x-1}) * \text{rhat} + A_{\text{hat}_{x-1}}</math>          Cumulative Difference: <math>Z_x = A_x - A_{\text{hat}_x}</math>          Slope: <math>mZ_x = (Z_x - Z_{x-1}) / (\text{dist}_x - \text{dist}_{x-1})</math></p>
--

- Segments are initially defined by the minimum acceptable segment length set by the user
- Segments are combined to form homogeneous sections based on the following rules

<p>Combine adjacent segments having the same sign slope          Combine adjacent segments having common averages          Combine segments which are &lt; min segment size w/ the adjacent segment of closest average value          Combine adjacent segments having common averages</p>
--

Once the sections are created, the spatial variance in the measured thickness for each section is then used in the simulation process in the estimate of  $a$ . Hence, when rutting is estimated for each cell, a prior (which will now contains an estimate of the spatial variance in the thickness of the homogeneous section) is combined with the observed  $a$  values (which will now contain an estimate of the variability of rutting within the homogeneous section) to create a new posterior  $a$ .

As depicted in Figure23, the Modified Model loop is as follows:

- Define Homogeneous Sections
- For each homogeneous section, calculate  $a$  from Monte Carlo simulation  
Use the mean and standard deviation of section thickness, as well as the statistical beta parameters, to obtain values of beta and thickness for each sample.

The value of  $a$  is calculated for each simulated sample. The mean and standard deviation for the simulated  $a$  values ( $a_{sim}$ ) are obtained:

$$\bar{a}_{sim} = \text{mean} \left[ \beta_4 * \varepsilon^{-(\beta_1 * T_1 + \beta_2 * T_2 + \beta_3 * T_3)} \right]$$

$$\hat{a}_{sim} = \text{stdev} \left[ \beta_4 * \varepsilon^{-(\beta_1 * T_1 + \beta_2 * T_2 + \beta_3 * T_3)} \right]$$

- interpolate ESALs for each cell in the homogeneous section
- interpolate rutting for each cell in the homogeneous section

$$\text{RutDepth} = \text{alpha} \times \left( N^{\text{beta}} \right)$$

- calculate Thermal Index (TI) for each cell in the homogeneous section  
Daily weather data is averaged to obtained mean 2-week maximum and mean 2-week minimum daily temperature values.

$$\text{accFz}_i = \text{Max}(0, \text{accFz}_{i-1} - \text{MinTemp}_i)$$

$$\text{TI}_i = \text{accFz}_i * \text{Max}(\text{MaxTemp}_i, 0)$$

where

- accFz<sub>i</sub>=Accumulated Freeze in the current time period
- accFz<sub>i-1</sub>=Accumulated Freeze in the previous time period
- TI<sub>i</sub>=Thermal Index in the current time period
- MinTemp<sub>i</sub>=Average Daily Minimum Temperature in the current time period

MaxTemp<sub>i</sub>=Average Daily Maximum Temperature in the current time period

- calculate a observed for each cell in the homogeneous section

An estimate of a is obtained for each 2 week time interval during the interval between the initial time period and the time of the last rut depth study performed. Then the mean and standard deviation of the observed a values are calculated.

$$a_i = \frac{\Delta \text{RutDepth}_i}{\epsilon^{\beta_8 * \left(\frac{\text{TI}_i}{1000}\right) * \beta_9 * \left(\frac{\Delta \text{ESAL}_i \div 1000}{\text{ESAL}_i^{(1-\beta_9)} \div 1000}\right)}}$$

$\bar{a}_{\text{obs}} = \text{mean}(a)$   
 $\hat{a}_{\text{obs}} = \text{stddev}(a)$

- Calculate the mean a observed and the standard deviation of a observed for all cells in the homogeneous section.

$$\bar{a}_{\text{obs\_h}} = \text{mean}(\bar{a}_{\text{obs}})$$

$$\hat{a}_{\text{obs\_h}} = \text{stddev}(\bar{a}_{\text{obs}})$$

- calc a posterior for the homogeneous section  
 Bayesian updating provides a Bayesian posterior  $a_{\text{post}}$ .

$$a_{\text{post}} = \frac{\bar{a}_{\text{sim}} * (\hat{a}_{\text{obs\_h}})^2 + \bar{a}_{\text{obs\_h}} * (\hat{a}_{\text{sim}})^2}{(\hat{a}_{\text{obs\_h}})^2 + (\hat{a}_{\text{sim}})^2}$$

- Calculate the Bayesian model results for each cell in the homogeneous section  
 Rutting predictions are obtained for each future weather interval provided in the input file using the homogeneous section Bayesian value of a ( $a_{\text{post}}$ ).

$$\text{RutDepth} = a_{\text{post}} * \left[ \varepsilon^{B_8 * \left( \frac{\text{TI}_i}{1000} \right) * \beta_9 * \left( \frac{\Delta\text{ESAL}_i}{1000} / \left( \frac{\text{ESAL}_i}{1000} \right)^{(1-\beta_9)} \right)} \right]$$

- Save the model constraints and the rutting prediction data
- Repeat the calculations for the next homogeneous section...

Figure 21 Overall Program Flow

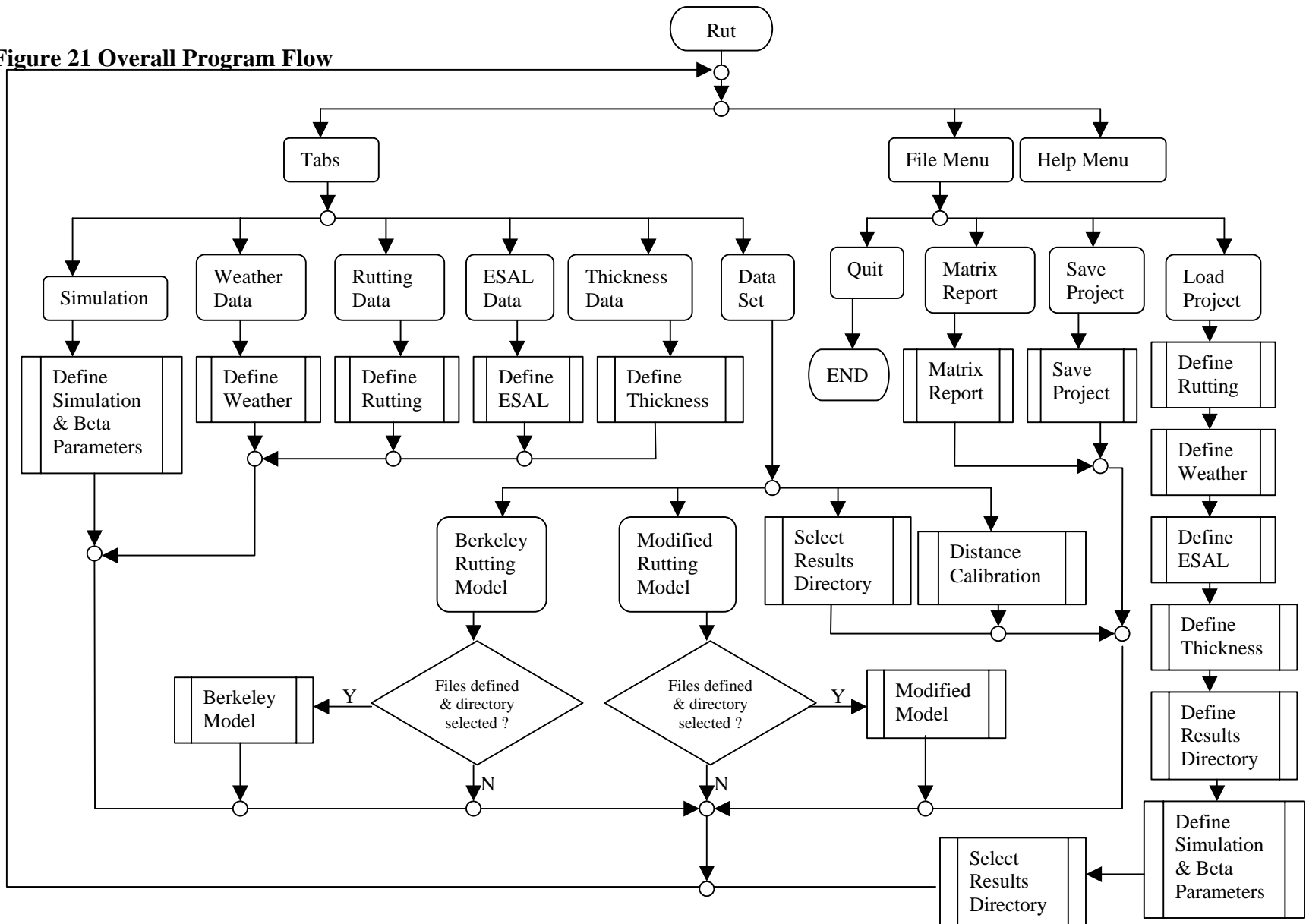


Figure 22-Chart of "Berkeley" Model

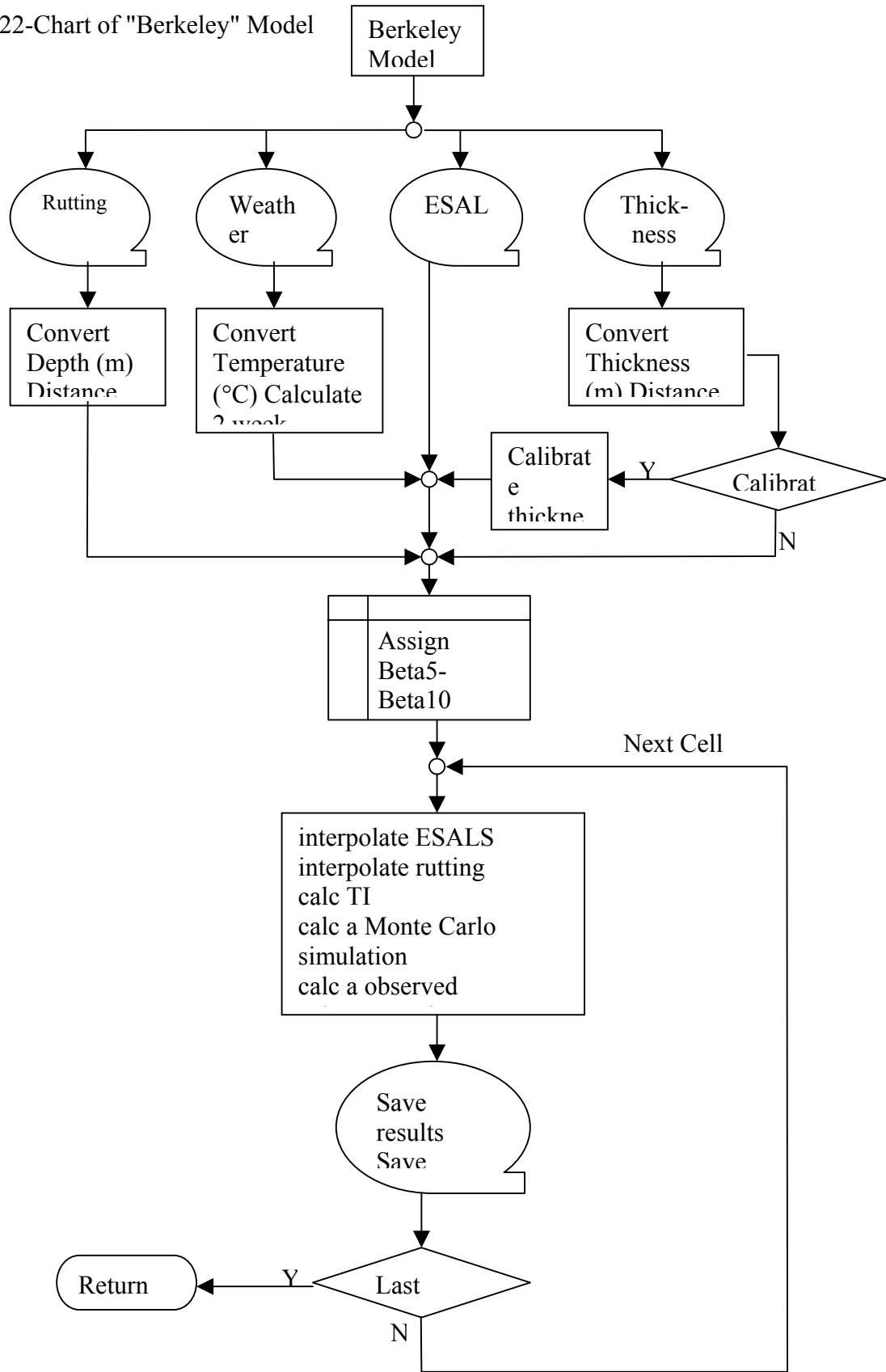


Figure 22

Figure 23 – "Modified" Rutting Model

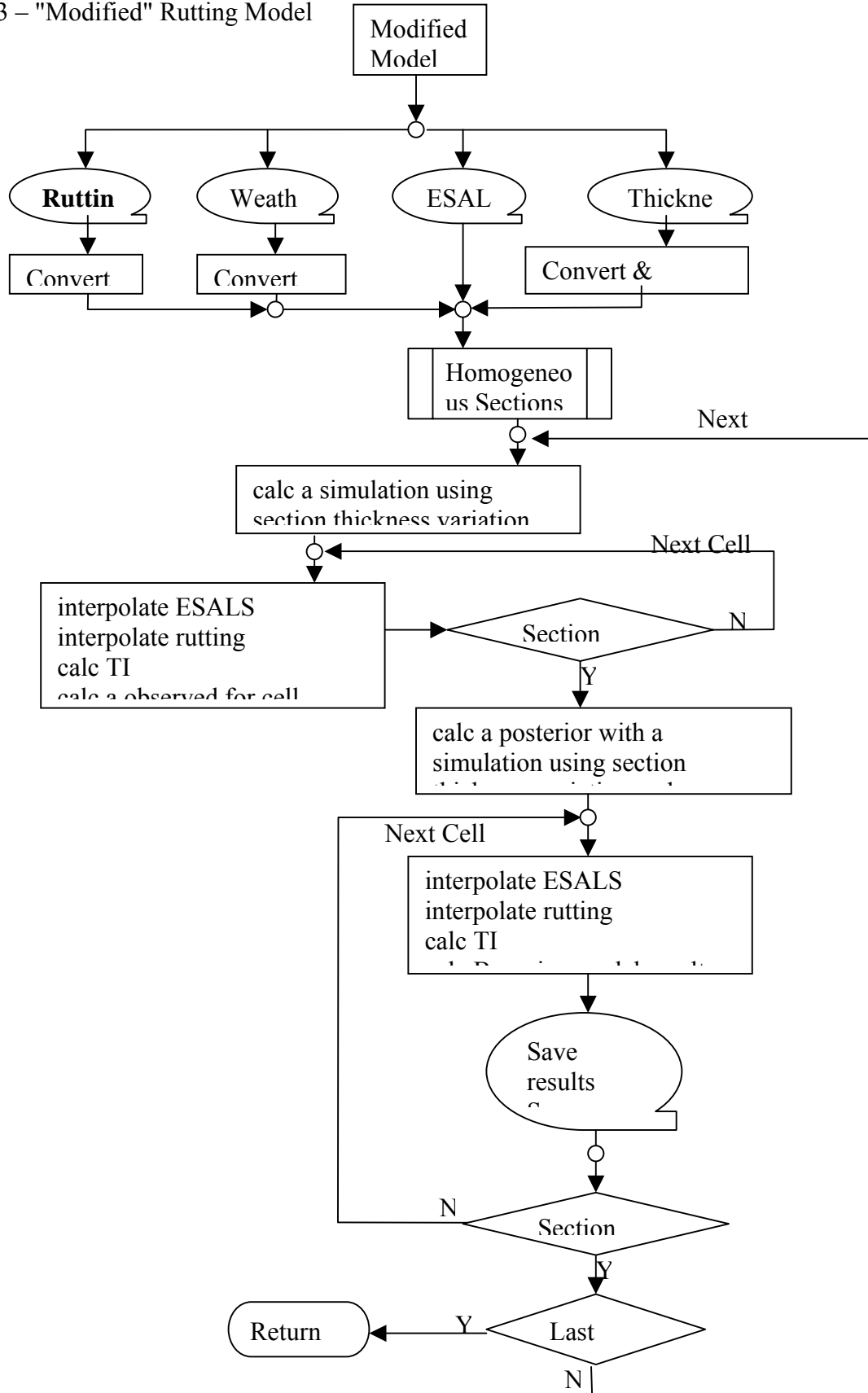
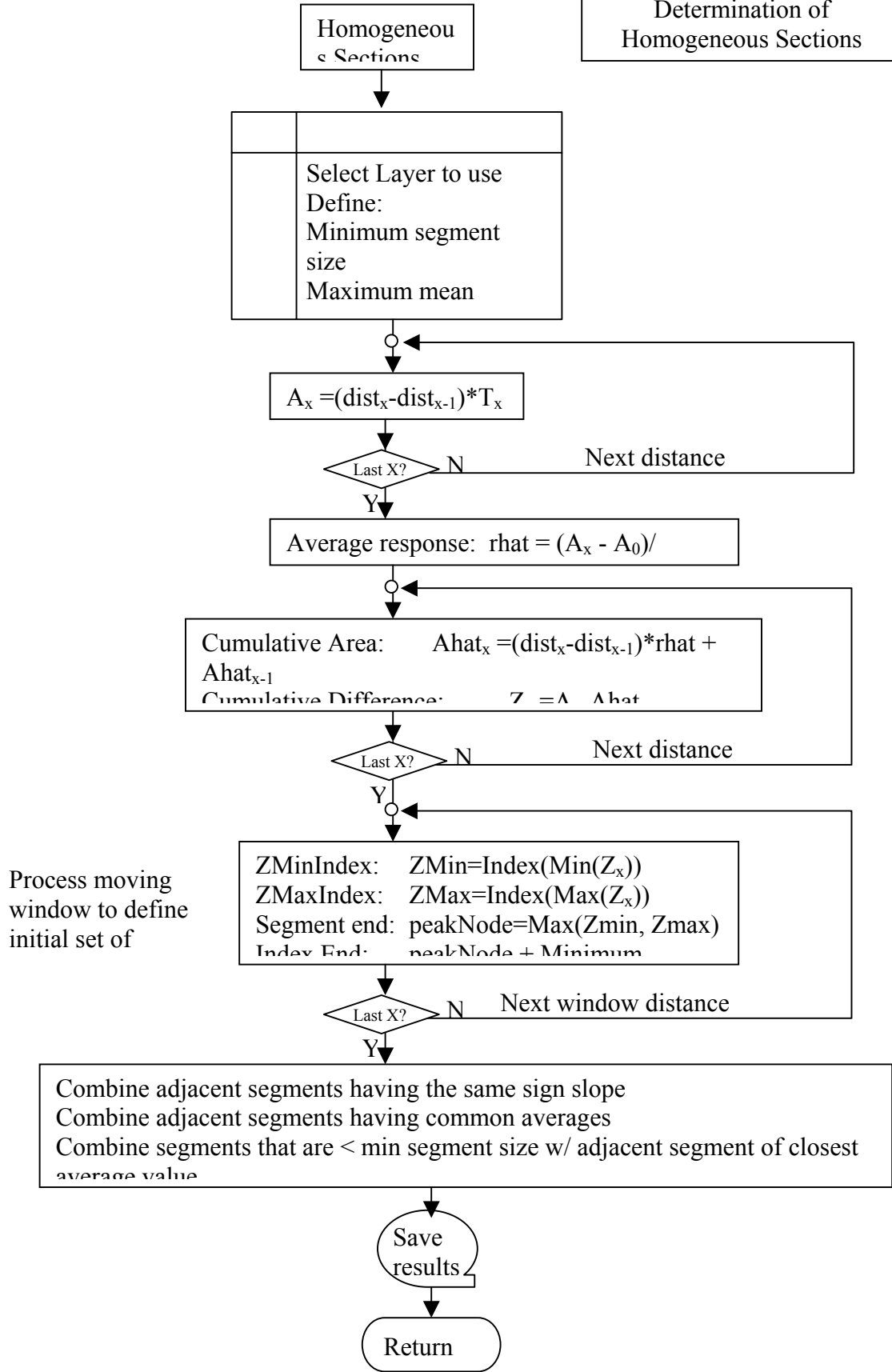


Figure 23

Figure 24 – Model for Determination of Homogeneous Sections



## Model Simulations

Model simulations have been carried out using data from I25 in Denver and the Tamiami Trail in Florida. Initial simulations were carried out on the I25 data by aggregating the pavement into structurally homogeneous sections, and evaluating the thickness in those sections. The modified model, which is based on pavement variability of thickness within these sections, could not be applied to this data unless a more detailed thickness analysis were conducted.

The Tamiami trail data provided a sufficient level of detail to allow the modified model to be implemented. Figure 25 below shows the various models applied to a single cell of the Tamiami pavement. The plot shows the development of rutting over time using the various model predictions incorporated into this work. Figure 26 shows the spatial variability of rutting vs distance (horizontal axis) and vs. time. Both of these output formats are produced directly by the RUT program.

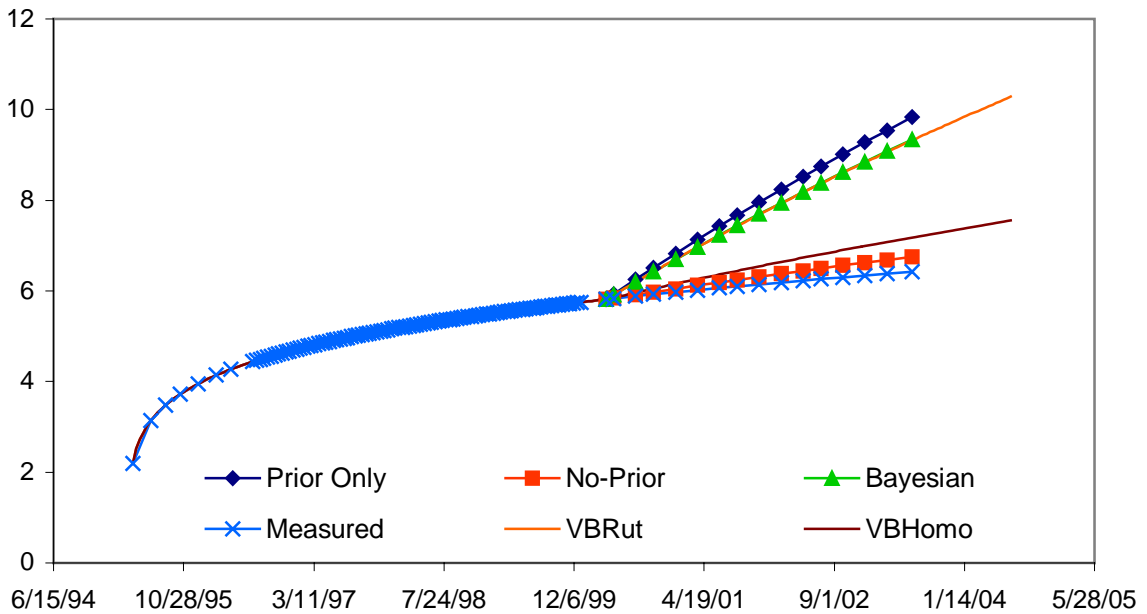


Figure 25 Rut Predictions from Various Models for a Single Cell – Tamiami Trail

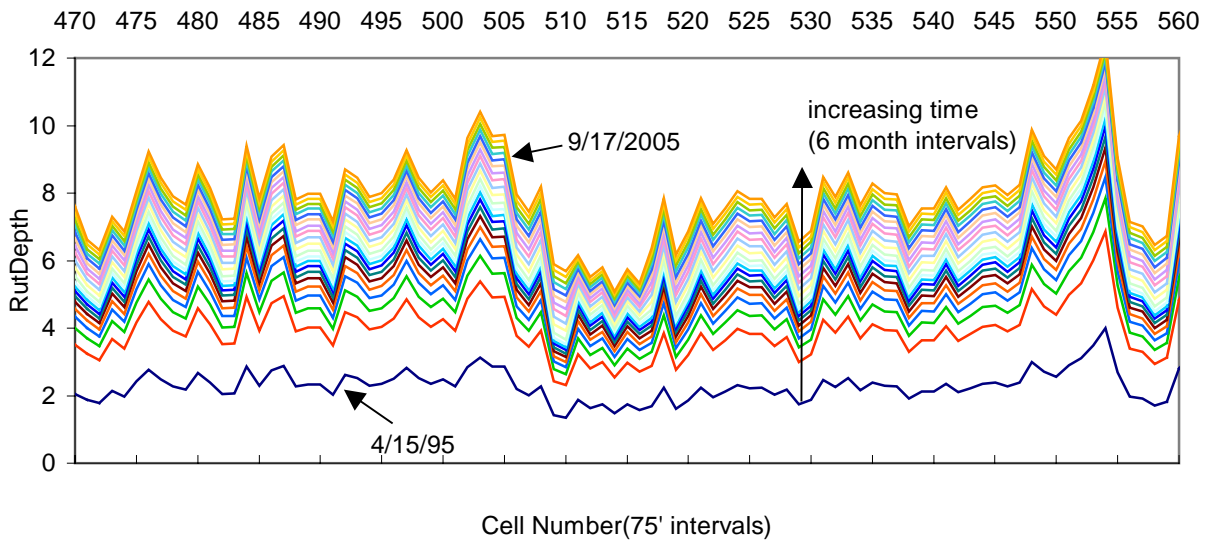


Figure26 Rut Predictions vs. Distance and Time – Tamiami Trail

## **Evaluation of Results**

### **Pavement Rutting Prediction**

The goal of this part of our research was to develop a model of pavement rutting from the AASHO Road Test. A non-linear model was specified and estimated. The model specification uses concepts that are familiar to pavement engineers such as load equivalencies and structural coefficients. However, the model in this report is an improvement over other state of the art empirical models for several reasons. The load equivalence parameters and the resistance parameters were allowed to vary freely during estimation. This is in contrast with previous research where these coefficients are pre-specified. This is perhaps one reason for the lack of success in developing empirical models to date.

Another important difference with previous research is the introduction of a thawing index. This variable proved to be extremely important to capture the effect of the environment at the AASHO Road Test.

The model fits were good, especially considering the number of sections and observations that were used for their estimation. Both fixed effects and random effects specifications were used to account for unobserved heterogeneity. The results showed that the size of the unobserved heterogeneity was significant.

The specification of a non-linear model allowed a good fit. However, it also called for a more careful analysis of the estimation results even when all the statistics indicated no problems. In particular, our model contained several parameters that interacted so as to capture similar effects. By estimating the model parameters for both wheel paths jointly, we were able to reduce the uncertainty in these parameters' estimated values.

Finally, a prediction test with a set of pavements not used for estimation confirmed that the model replicates well the pavement behavior at the AASHO Road Test.

Our analytical approach for using the predictions of the pavement rutting model, together with measurements of pavement rutting for predicting future rutting also provided good results. From the tests performed using the field data from MnRoads, two conclusions were made:

1. The Bayesian analytical procedure outperforms both the prior-only and the no-prior methods for predicting pavement rutting;
2. Increasing the number of data points improves the rut depth prediction precision, irrespective of the prediction method used.

Both conclusions are consistent with statistical theory and with engineering intuition. What we did not expect, however, is that the addition of measurements does not yield a very significant increase in precision. By incorporating three more observations, the RMSE is not reduced by more than one millimeter for any of the three methods. In fact, the predictions based on 6 measurements have high precision (low RMSE), which is sufficient for most pavement management applications.

### **Pavement Cracking Prediction**

In this part of our study, an analysis of the pavement cracking initiation data collected during the AASHO Road Test was conducted. This analysis is based on the use of probabilistic duration modeling techniques. Duration techniques enable the stochastic nature of pavement failure time to be evaluated as well as censored data to be incorporated in the statistical estimation of the model parameters. Due to the nature of pavement cracking initiation, the presence of censored data is almost unavoidable and not accounting for such data would produce biased model parameters.

The main advantages that distinguish this stochastic duration model from the original AASHO model are as follows. First, the duration model explicitly recognizes the stochastic variations in the pavement cracking initiation process. Second, the stochastic duration model accounts for the fact that some of the data are censored. Third, our specification was more realistic than that used in the AASHO model, in that it did not assume that the effects of axle type and load were separate and additive. Finally, the predictions obtained with our hazard rate model, using our improved specification, were about 20% more accurate than those obtained using the original AASHO model.

While we were successful in developing accurate models of cracking initiation and progression, we were unable to test our analytical procedure for using these models together with field measurements of pavement cracking to improve the prediction accuracy of cracking progression. The reason for this is that the methods of measuring

cracking vary widely among experimental sites and state agencies. As a result, it was not possible to identify any field data site where the measurement of cracking was consistent with the definition used in the AASHO road test.

## **CHAPTER 3**

### **CONCLUSIONS AND RECOMMENDATIONS**

The work carried out in the first Phase of this project demonstrated how newly formulated models for pavement rutting and cracking can be implemented using data from current high speed pavement survey technology. The demonstrated effort showed how data from conventional high speed rutting, cracking, and pavement thickness (GPR) sensors can be integrated into the models to predict future performance of pavement sections. The demonstration also showed how compensation could be made for the absence of historical condition data (as is often the case) by using spatial variability in structurally homogeneous sections, as identified through the GPR thickness data. Software was developed for implementation of the portion of the rutting and simulations were conducted to predict future rutting using current condition data from an in-service pavement. Software was also developed for implementation of the cracking model.

The three areas for recommended future work are:

- 1) Complete the development and testing of the rutting and cracking models and conduct trial simulations using the software developed in Phase I
- 2) Apply the rutting and cracking models to pavement sections in California representing a range of structural, traffic, and environmental conditions
- 3) Correlate the model predictions with actual changes in surface conditions.

#### Recommended Task 1. Model Simulations

##### 1.1 Rutting Model

The rutting simulations in Phase I utilized the portion of the model that represented rutting in the base layer. The portion of the model that represents rutting in the asphalt layer was combined with the base rutting model toward the end of the project. The combined model needs to be incorporated into simulation software and simulations need to be carried out using actual pavement data.

## 1.2 Cracking Model

In Phase I the cracking model was programmed into the simulation software but there was not adequate time to run simulations. Such simulations will be carried out on one of the Phase I data sets to insure proper performance of the software and reasonableness of results.

## Recommended Task 2. Application of Models to California Pavement Sections

The objective of this task is to apply the cracking and rutting model software to pavement sections representing typical California conditions. This task will include selection of test sections, collection of surface and GPR data on these sites, and application of prediction models to the data.

### 2.1 Selection of Test Sites

The plan is to selection approximately 30 pavement sections for detailed evaluation. These can include special test sites in California that are currently being intensely monitored. Sections can also be selected in conjunction with a current Caltrans program to assess pavement design procedures. Under this Caltrans program, Stantec, under contract with Caltrans, is collecting surface condition data on 1000 pavement sections throughout California. In addition to the condition data, information on traffic (ESALs), pavement structure, and construction history are being assembled into a database. We will utilize this database to provide a set of sites with representative set of pavement age, construction history, structure, traffic, and environmental exposure.

### 2.2. Collection of Data on Test Sites

Arrangements will be made to collect rutting, cracking, and GPR data on each test section. Data will be collected and processed for utilization in the cracking and rutting prediction software.

### 2.3 Data Processing

Data from the test sites will be processed to yield predictions of cracking and rut depth for future time horizons and future conditions (i.e., changes in traffic, climactic events, etc.). The processed data will be evaluated to insure that reasonable results are obtained.

#### Recommended Task 3 – Correlation of Predictions to Actual Condition

The test sections will be re-surveyed for rutting and cracking after one year and again after two years. The results of these follow up surveys will be correlated with the model predictions.

## CHAPTER 4

### IMPLEMENTATION

#### Software specifications

Input format: comma separated ASCII text files

Input files:

Weather data

month/day/year/maximum and minimum daily temperature values

Rutting/Cracking Data

month/day/year/cell/from station/to station/rut depth

Layer thickness data

Distance/Thickness Layer 1/Thickness layer 2/ Thickness layer 3

ESAL data

month/day/year/cell/esal

Distance Calibration

GPR layer thickness stationing is adjusted to distances for rut depth and cracking

Rut Model Implementation

Option 1 – Original Berkeley Model

Assumes that rutting data is available vs. time

- a) simulate “a” and  $\sigma_a$  for each cell using  $\beta$  statistics and layer thicknesses
- b) calculate “a” for each time that rut depth data is available using rut model over two week intervals, and calculate  $\sigma_a$  from this data
- c) use Bayesian updating to obtain “a” for future prediction

Option 1a – Modified Berkeley Model

(for situations where rut depth measurements are available at only one point in time)

- b) select a function for extrapolating rut depth history to time zero, and use this function to calculate bi-weekly “a”. Calculate mean “a”. Calculate  $\sigma_a$  or use  $\sigma_a$  from other historic data set

other steps remain the same

### Option 2 – Infrasense modified Berkeley Method

(uses concept of homogenous sections to introduce spatial variation for rut depth and thickness. These spatial variations generate  $\sigma_a$  from spatial rather than historic data)

- a) divide the pavement into homogeneous sections
- b) simulate “a” and  $\sigma_a$  for each cell using  $\beta$  statistics and layer thicknesses statistics over the homogeneous section
- c) calculate “a” for each cell from current rutting data and functional fit to time zero.
- d) calculate  $\sigma_a$  from all of the “a” values in the homogeneous section
- e) use Bayesian updating to obtain “a” for future prediction within each homogeneous section
- f) apply “a” to each cell for local prediction of future rutting.

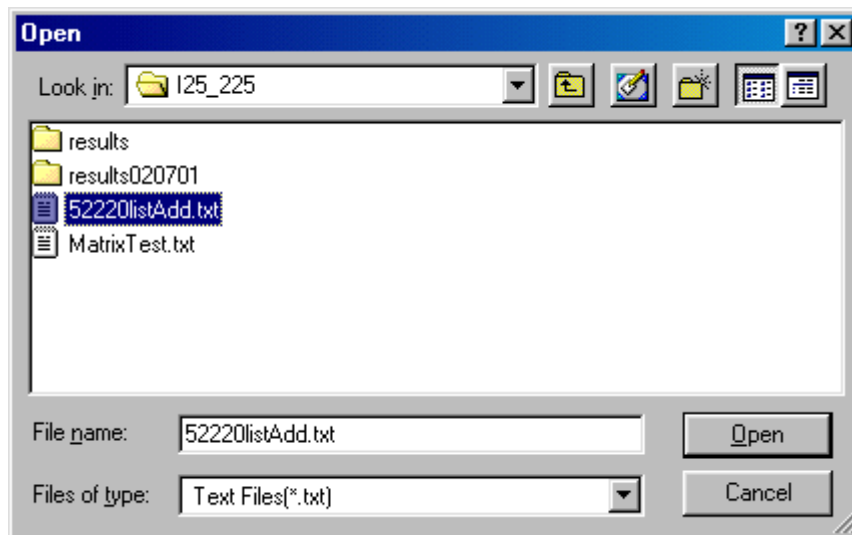
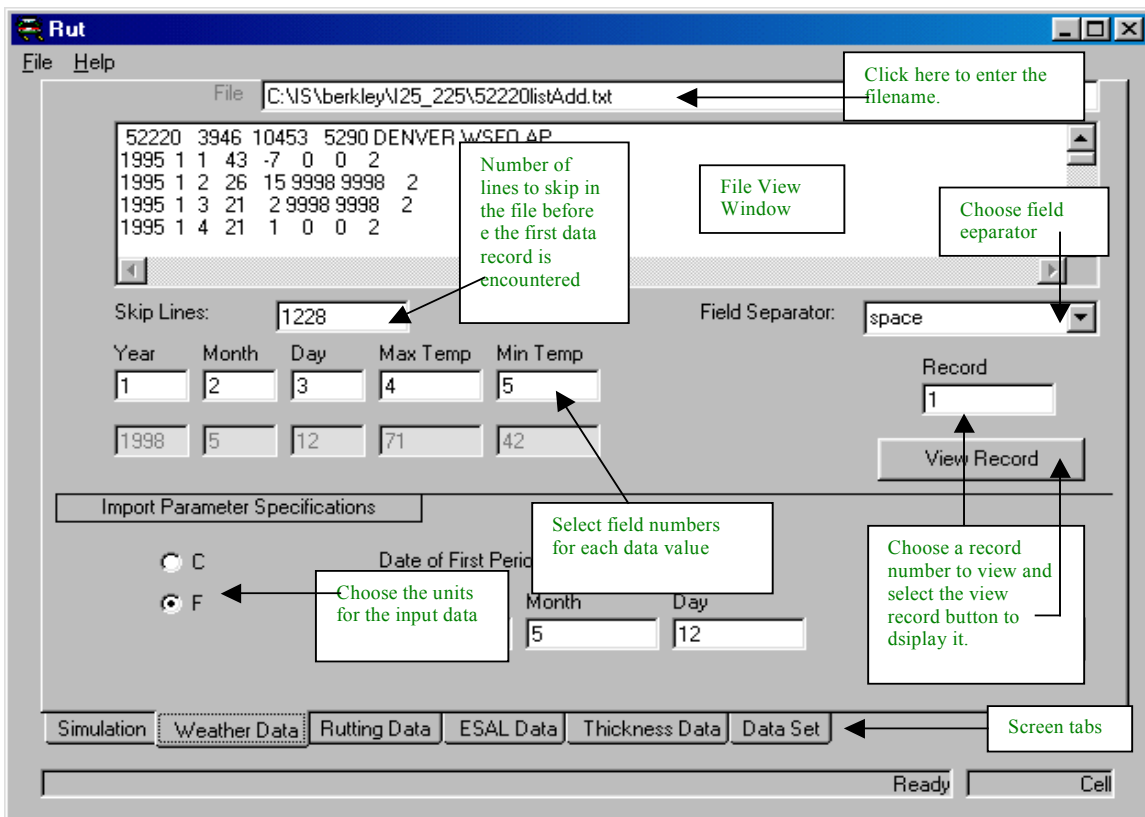
Model Output:

Text file of rut depth vs. time for each cell

Text file of rut depth vs. station for selectable future times.

### **Rutting Model Software Documentation**

Data input to the program is in ASCII file format (text files). Four data files are required, one for each type of information used by the model: Weather data, Rutting data, Traffic (ESAL) data, and Thickness data. Each line in the files represents a new set of data. The data values for each data set are separated into fields on each line by spaces, tabs or commas. Header information is allowed in the files.



The specific format for each file is entered into the program on the appropriate tabbed sheet – Weather Data, Rutting Data, ESAL Data and Thickness Data. On each of the four data input sheets, the user specifies the input file name, the location of each data

field in the file, and the number of lines to skip when reading in the input data. Skip lines allows the header information to be ignored by specifying how many lines must be skipped when reading the file before the data set is encountered.

Weather data is used to input maximum and minimum daily temperature values:

```
52220 3946 10453 5290 DENVER WSFO AP
```

```
1995 1 1 43 -7 0 0 2
1995 1 2 26 15 9998 9998 2
1995 1 3 21 2 9998 9998 2
1995 1 4 21 1 0 0 2
1995 1 5 39 5 9998 9998 1
1995 1 6 30 16 9998 1 1
1995 1 7 55 14 0 0 1
1995 1 8 58 32 0 0 9998
1995 1 9 57 31 0 0 0
1995 1 10 66 33 0 0 0
1995 1 11 58 28 0 0 0
1995 1 12 50 26 0 0 0
1995 1 13 51 27 0 0 0
1995 1 14 61 26 0 0 0
1995 1 15 64 33 0 0 0
1995 1 16 44 27 9998 9998 0
1995 1 17 41 20 0 0 0
1995 1 18 39 14 0 0 0
1995 1 19 49 20 0 0 0
1995 1 20 44 22 0 0 0
1995 1 21 45 15 0 0 0
```

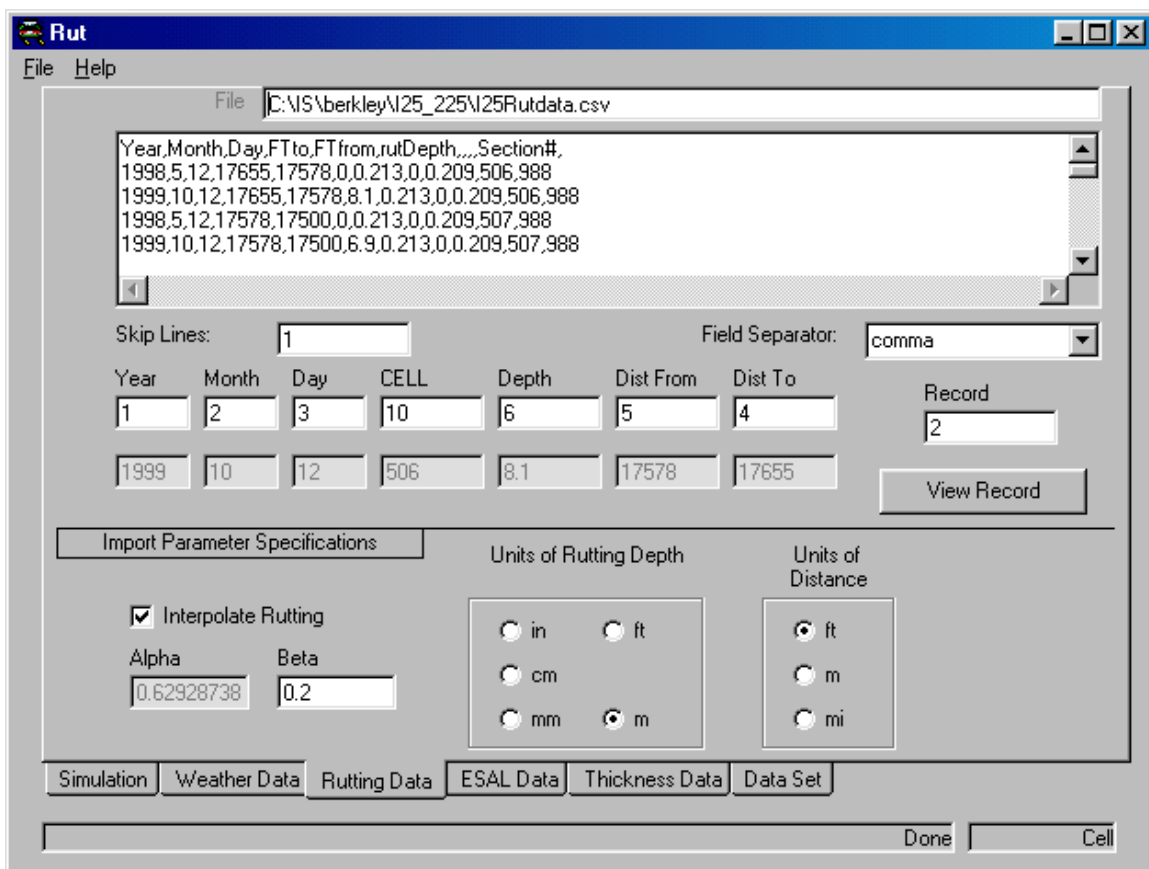
Each line of data contains a date (year, month, and day) and the daily minimum and maximum temperatures recorded at the weather station. The user needs to specify how the data is arranged into fields and the field (column) number for the required data. As shown in the input screen, the weather data are separated by spaces, and the required

fields are found in these columns: the year is in column (or field) 1, the month in column 2, the day of the month is in column 3, daily minimum temperature and daily maximum temperature are in columns 4 and 5. By specifying these values, entering in the number of lines to skip, choosing a record to view, and selecting the View Record button, the data read from the file will be shown in the boxes below the field selection values. This method allows the user to specify a data input format and to verify that the correct data will be read into the program.

In the case of weather data, the skip lines field should move the location of the first record to the date of the initial cell rutting value. The data then displayed in the year, month and day fields when Record is set to 1 should be the same data as the date of the initial rutting. Enough weather data needs to be entered so that there are daily values beyond the date of the final rutting analysis. The rutting model will extrapolate data into the future for as long as there is weather data available.

Units of the input values must be specified for daily temperature, distance, rutting depth and layer thickness.

The rutting data file specifies the measured rutting values (depth) per cell. Each “cell” is

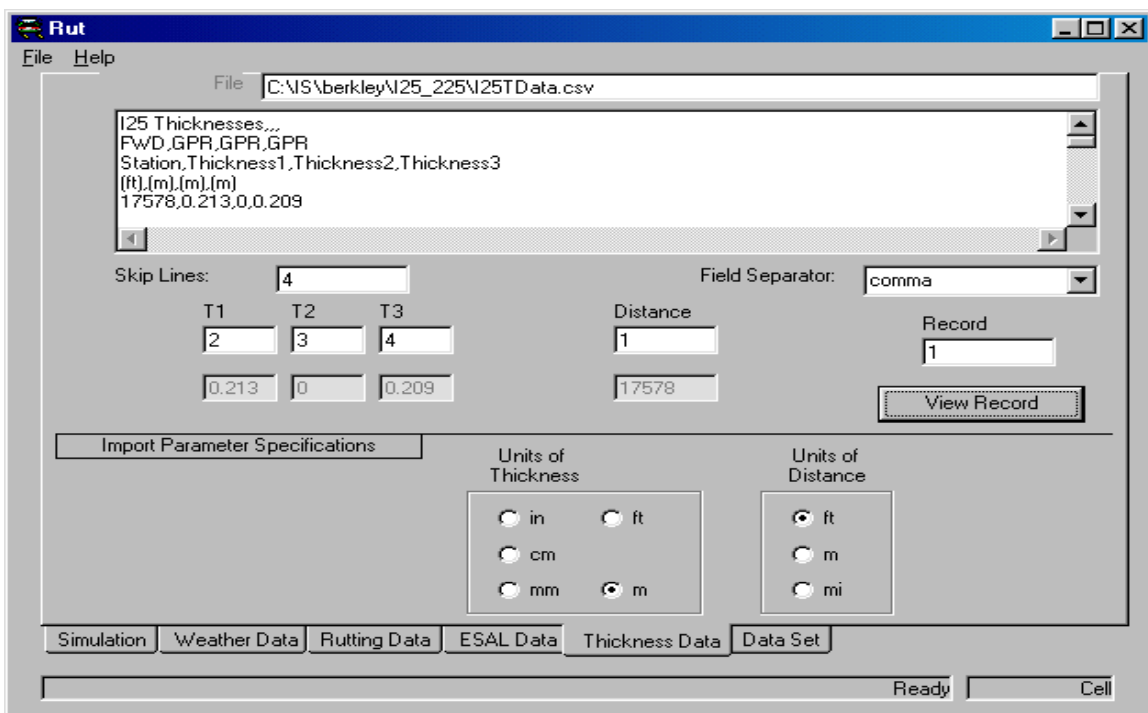


a defined area of pavement. Date, cell ID and the location of the start and end points of the cell are also required. Each line of data represents the rutting depth of a particular cell at a particular date. Data for each cell are arranged in contiguous lines in order of increasing time (date). The current program accepts two input values for each cell. The first line of data is the amount of rutting for the first measured interval. This value is usually a rutting value of 0 on the date that the road was constructed or last resurfaced. The second line is the date and amount of rutting determined from the last rut depth study performed on the cell. Rutting increases between the start and end points are interpolated using an exponential function:

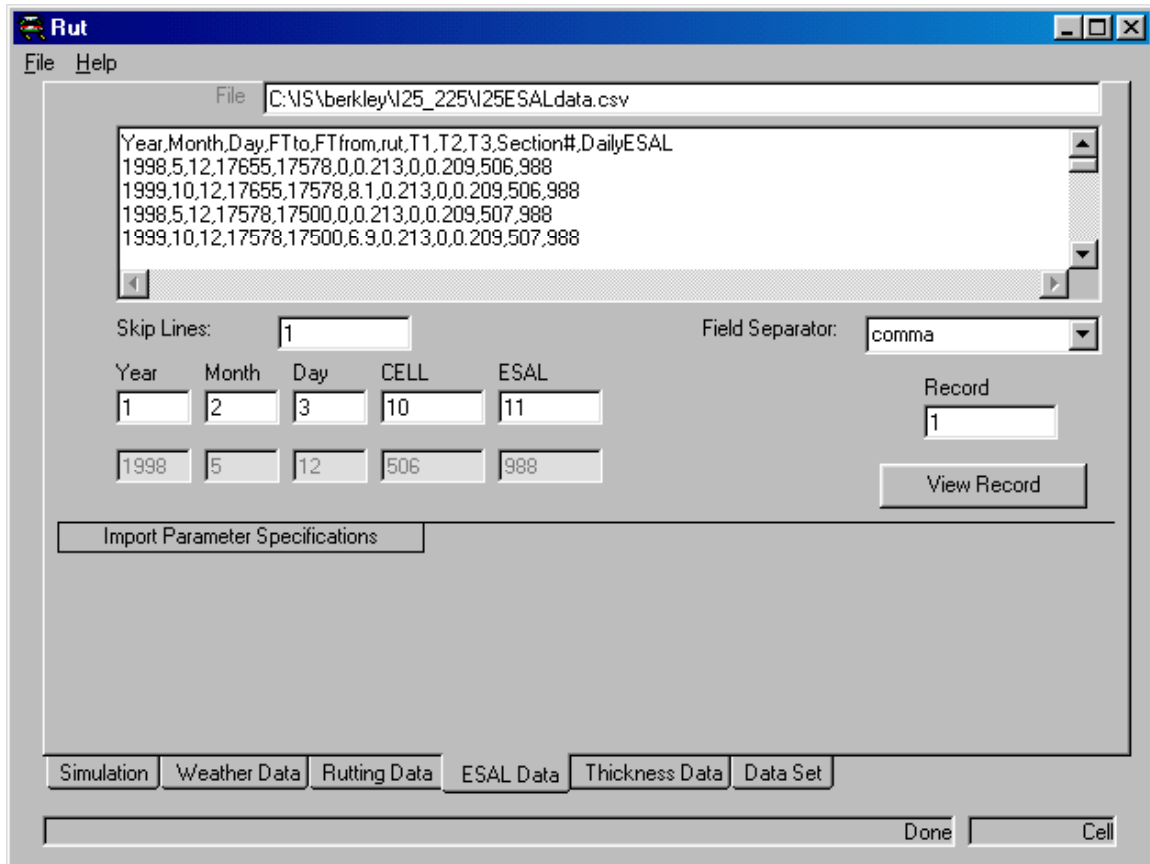
$$\text{RutDepth} = \alpha \times (N^{\beta})$$

Where N is the number of accumulated load applications. Beta is a fixed coefficient entered by the user, and the program estimates alpha by fitting the curve through the starting and ending rut values. Future versions of the program will allow additional (“intermediate”) rutting values to be entered. These values will be used to determine the value of the observed rut progression curve.

ESAL (Equivalent Single Axle Load) data is entered in the same manner as rutting data. ESAL values are *daily* equivalents and one value is entered for each cell value entered.



The current program accepts two input values for each cell. The first line of data is the daily ESALs for the initial time period. The second line is the date and the daily ESALs at the time of the last rut depth study performed on the cell. If the daily ESAL value for a cell at the initial time period is different from the ESAL value at the end period, the daily

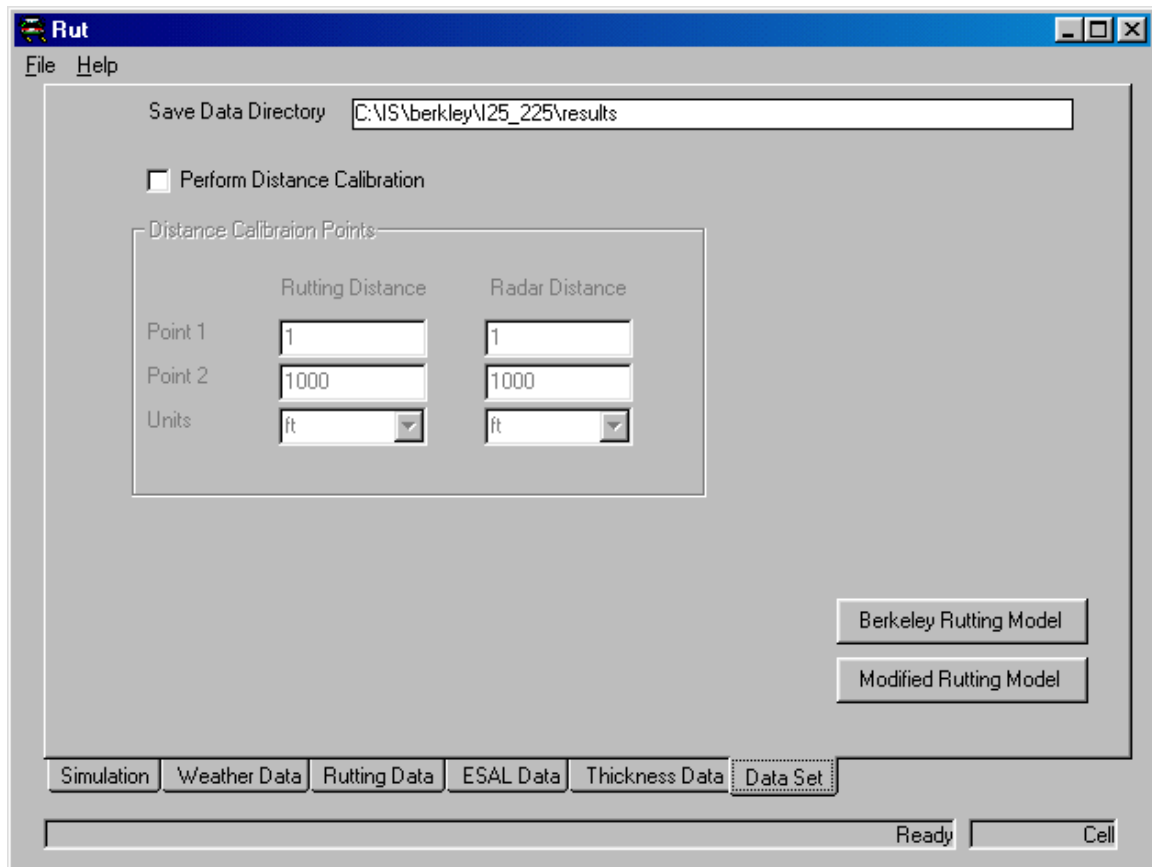


ESALs are linearly interpolated over the entire time period.

Future versions of the program will allow the input of multiple ESAL values at varying periods in the past and into the future so that future rutting can be modeled based upon both historical and future expected changes in traffic patterns.

Thickness data is entered as the measured thickness of each layer (T1-the asphalt concrete layer, T2-the granular base layer and T3-the subbase layer) at a given distance point.

Once the data files and their input specifications have been entered, the user can model



the rutting in each cell. First a data directory must be specified where the results will be stored. If the rutting distance values and the radar (thickness) distance values are in different scales or directions, the user can check the ‘Perform Distance Calibration’ box and enter the distance values of two corresponding points in each file in order to calibrate the thickness data to the rutting cell data locations.

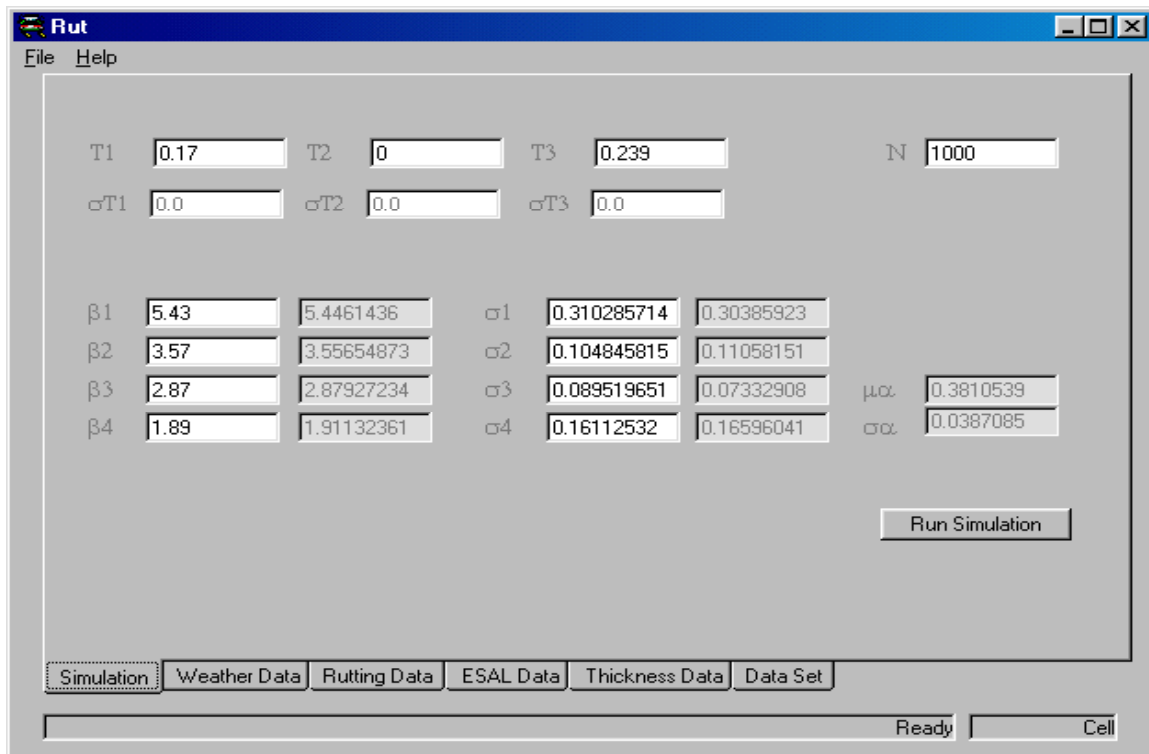
Two methods are available to model rutting. Both use the Pavement Rutting Model described by Archilla and Madanat with Bayesian updating added to incorporate the observed rutting behavior into the model. In the model,  $a$ , the rut depth caused by the first standard axle load, is defined as follows:

$$a = \beta_4 * \varepsilon^{-(\beta_1 * T_1 + \beta_2 * T_2 + \beta_3 * T_3)}$$

First method – was originally intended by Berkeley – assumed historic rutting data which yielded a standard deviation for the observed rutting – we had to extrapolate to time zero because we had no historic data. Second method – INFRA SENSE mod – introduce the concept of homogenous sections. Use variation of a over homo section to get stdev of a for Bayesian. Also introducing the variation of thickness in prior model

Selecting the ‘Berkeley Rutting Model’ button performs the first method. When the button is selected, the data files are read, and the Berkeley rutting model is implemented for each cell of rutting data entered. First the Thermal Index (TI) is calculated from the weather data, the daily ESAL values are interpolated and cumulative 2-week values obtained. Then a Monte Carlo simulation is run to obtain estimates of the mean and standard deviation of “a” using the experimental parameters obtained from the AASHO Road Test and the cell thickness values for T1, T2 and T3 read in from the file. If required, the user can change the materials parameters Beta1 through Beta4 and/or their standard deviations, by modifying them on the Simulation tab. On this tab, the user can also change the number of samples used to perform the simulation (N), although 1000 is the recommended value to use.

Next an estimate of a is obtained for each 2 week time interval as follows:

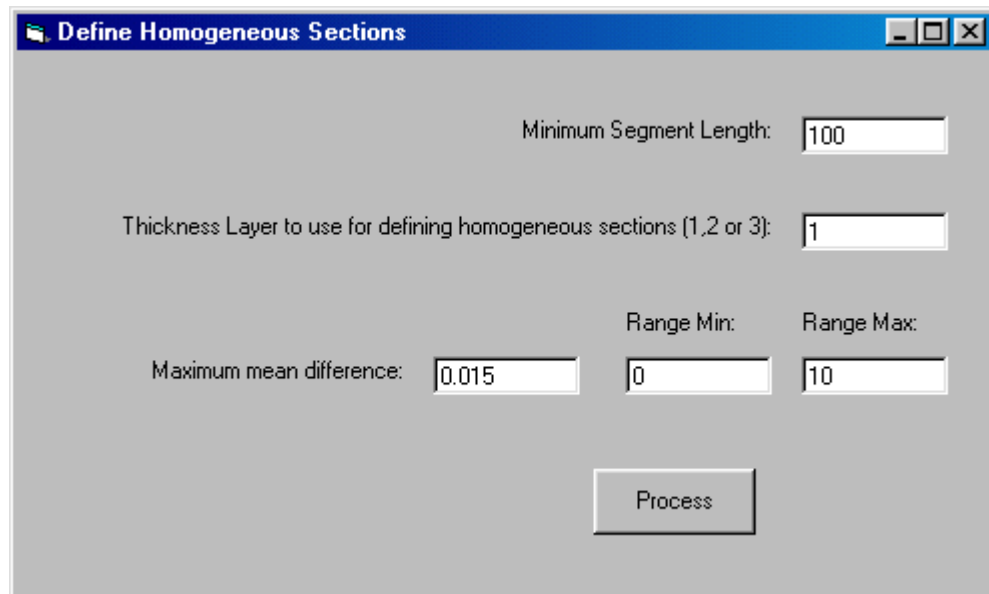


$$a_i = \frac{\Delta \text{RutDepth}_i}{\varepsilon^{\beta_8 * \left(\frac{\text{TI}_i}{N}\right)} * \beta_9 * \left(\frac{\Delta \text{ESAL}_i}{\text{ESAL}_i^{(1-\beta_9)}}\right)}$$

The mean and standard deviation of these estimates of a are then calculated and combined with the simulated values of a to provide a posterior a which is used to predict rutting:

$$\text{RutDepth} = a * \left[ \varepsilon^{\beta_8 * \left(\frac{\text{TI}_i}{N}\right)} * \beta_9 * \left(\frac{\Delta \text{ESAL}_i}{\left(\frac{\text{ESAL}_i}{N}\right)^{(1-\beta_9)}}\right) \right]$$

By selecting the second button, ‘Modified Rutting Model’, homogeneous sections of



pavement are defined based upon the user’s definition of a homogeneous section. The user must specify a minimum acceptable segment length, a maximum difference in thickness between segments, and a minimum and maximum range value to use when reading in the input data. Once the sections are created, the spacial variance in the measured thickness for each section is then used in the simulation process in the estimate of a. Hence, when rutting is estimated for each cell, a prior, which now contains an

estimate of the spacial variance in the thickness of the homogeneous section, is combined with the observed a values for the cell to create a new posterior a.

For each model, results for each cell are stored in the chosen results directory. Each cell is modeled in a two files named from the cellID. The rutting data is stored in a file called d<cellID>.csv and the corresponding model parameters are stored in the file called m<cellID>.csv. For example, for the cell 509, the results files will be named “d509.csv” and “m509.csv”. The data results file contained coma separated values of rutting depth for the entire range of time periods given. The data is in the format “year, month, day, rutting depth”.

Year,Month,Day,Rut
1998,5,12,3.71992338314279
1998,5,26,4.27306987093113
1998,6,9,4.63402365138021
1998,6,23,4.90846833152598
1998,7,7,5.13248863008526
1998,7,21,5.3230953453578
1998,8,4,5.48976309203014
1998,8,18,5.63834949797894
1998,9,1,5.77274663743439

The model parameter file stores the model input assumptions and the calculated model parameters.

Date of Analysis Run: 3/14/01  
Rutting Data Start Date: 5/12/1998 (3.72) (0.0)  
Rutting Data End: 10/12/1999 (7.7) (7.7)  
Rutting Data Interpolation: Alpha 0.552531444919107, Beta 0.2  
Beta: 5.43, 3.57, 2.87, 1.89, 2.98, 3.89, 1.81, 1.6, 0.452, 0.022  
Thickness: 0.301, 0, 0.222  
A(mean) - Simulation: 0.198871  
A(stdev) - Simulation: 0.041978  
A(mean) - Observed: 0.012448  
A(stdev) - Observed: 0.017052  
A(mean) - Posterior: 0.038851  
  
A(mean) - ASHO calc: 0.194954  
Rutting Number: 2.27157

From the file menu, the user may store all project settings. All values from the data input screens will be saved from the File, SaveProject menu and can later be reloaded from the File, LoadProject menu. This option saves considerable effort in reentering information if several runs on the same data need to be performed. A final selection from the File menu, MatrixReport allows the user to select a group of cells from the data files stored in the selected results directory to use in creating a matrix report. This report will take data at user selected time slices from the selected cells to create a report showing the change in rutting over time in entire asphalt interval.

## Systems Specifications

The specifications are divided into equipment specifications and software specifications. The equipment specifications govern the type of data that is generated by the sensor equipment for use in the pavement performance analysis. The software specifications govern the manner in which the cracking and rutting models are implemented on the sensor data

### Equipment specifications

The hardware specifications primarily address the frequency, resolution, accuracy, and format of the collected data.

#### Rutting:

Measurement unit: mm

Measurement Resolution: < 0.1 mm

Reporting Frequency: between 10 and 30 meters

Accuracy: +/-0.5mm

Positioning accuracy - chainage :  $\pm 0.05\%$

Width of coverage: one lane, both wheelpaths

Format of data: average rut depth for each reported cell

#### Cracking:

Measurement: fatigue (alligator) cracking

Definition of Fatigue Cracking: series of interconnected cracks, developing into many sided sharp-angled pieces, usually less than 0.3 m on the longest side

Measurement unit: percentage (% of affected area per total area observed)

Measurement Resolution: < 0.5%

Reporting Frequency: between 10 and 30 meters

Accuracy: +/-1.0%

Positioning accuracy - chainage :  $\pm 0.05\%$

Width of coverage: one lane

### Layer Thickness

Measurement: Measurement of surface (asphalt), base, and sub-base thicknesses, measured in meters

Measurement Resolution:  $\pm 0.01\text{m}$

Collection Frequency: one data point per meter

Reporting Frequency: average value over 10-30 meters

Accuracy:  $\pm 5\%$

Width of Coverage: Centerline of the lane

### Sample rutting and cracking data

Currently Available Equipment – Rut and Crack Surveys

Cell #	Beg Station	End Station	Fatigue Cracking	Rut Depth (in.)
1	0	75	0.00%	0.14
2	75	151	0.00%	0.15
3	151	226	0.00%	0.15
4	226	302	0.00%	0.14
5	302	377	0.00%	0.13
6	377	453	0.00%	0.14
7	453	528	0.00%	0.17
8	528	603	0.00%	0.17
9	603	679	0.00%	0.15
10	679	754	3.87%	0.17
11	754	830	4.53%	0.17
12	830	905	3.87%	0.22
13	905	981	3.87%	0.22
14	981	1056	4.20%	0.18
15	1056	1131	0.00%	0.20
16	1131	1207	2.76%	0.24
17	1207	1282	0.00%	0.25
18	1282	1358	1.77%	0.25
19	1358	1433	21.66%	0.27
20	1433	1509	12.71%	0.21
21	1509	1584	27.73%	0.28
22	1584	1659	26.41%	0.25
23	1659	1735	16.46%	0.19
24	1735	1810	19.23%	0.21
25	1810	1886	27.96%	0.20
26	1886	1961	17.79%	0.16
27	1961	2037	25.52%	0.18
28	2037	2112	22.32%	0.21
29	2112	2187	12.60%	0.20
30	2187	2263	11.82%	0.16
31	2263	2338	8.73%	0.19
32	2338	2414	3.54%	0.19
33	2414	2489	10.39%	0.23
34	2489	2565	8.29%	0.24
35	2565	2640	32.93%	0.23
36	2640	2715	17.90%	0.24
37	2715	2791	13.48%	0.22
38	2791	2866	11.38%	0.28
39	2866	2942	23.76%	0.19
40	2942	3017	11.82%	0.19
41	3017	3093	8.29%	0.19
42	3093	3168	11.93%	0.17



ARAN Equipment for Rut Depth (from Roadware, Canada)



ARAN Equipment for Rut Depth and Crack Detection (from Roadware, Canada)



Laser RST for Cracking and Rutting Measurements (from IMS/Terracon, USA)



PavVue Vehicle for Rut Depth and Cracking Measurement (from IMS, USA)



Survey Vehicle for Rut Depth and Crack Detection (from GIE, Canada)



Survey Vehicle for Rut Depth and Crack Detection (from Pavdex, USA)



Rutting/Cracking Survey Vehicles from WDM (UK)

**Currently Available Equipment – GPR Thickness Surveys**



Single Antenna (CPC, DK)    Dual Antenna (IMS/Terracon, USA)



Single Antenna, Rear (WaveTech, USA)      Dual Antenna, Rear (GSSI, USA)

## REFERENCES

1. AASHTO (1993), AASHTO Guide for Design of Pavement Structures, American Association of State Highway and Transportation Officials, Washington, D.C.
2. Ali, H., S. Tayabji, and F. La Torre (1998). Calibration of a Mechanistic-Empirical Rutting Model for In-Service Pavements. Presented for publication at the 77th Annual Meeting of the Transportation Research Board, Washington, D.C.
3. Archilla, A.R. (2000). Development of Rutting Progression Models by Combining Data from Multiple Sources. Ph.D. Dissertation, University of California, Berkeley, CA.
4. Behzadi G. and W.O. Yandell (1996). Determination of Elastic and Plastic Subgrade Soil Parameters for Asphalt Cracking and Rutting Prediction. Transportation Research Record 1540 TRB, National Research Council, Washington, D.C., 97-104.
5. Ben-Akiva, M. and T. Morikawa (1990). Estimation of switching models from revealed preferences and stated intentions, Transportation Research, A, Vol. 24A, No. 6, 485-495.
6. Butler B.C., Carmichael R.F. III, and Flanagan P.R., (1985), "Impact of Pavement Maintenance on Damage Rate, Volume 2", *Final Report*, ARE Inc., TX.
7. Button, J.W., D. Perdomo, and R.L. Lytton (1990). Influence of Aggregate on Rutting in Asphalt Concrete Pavements. Transportation Research Record 1259, TRB, National Academy of Sciences, Washington, D.C., 141-152.
8. Deacon J.A., J.T. Harvey, A. Tayebali, and C.L. Monismith (1997), "Influence of Binder Loss Modulus on the Fatigue Performance of Asphalt Concrete Pavements", Association of Asphalt Paving Technologists, Asphalt paving technology, Vol. 66.
9. Diylajee, V.A., and G.P. Raymond (1982). Repetitive Load deformation of Cohesionless Soil. Journal of Geotechnical Engineering Division, ASCE 108 (10), 1215-1229.
10. Finn F., C. Saraf, R.Kulkarni, K.Nair, W. Smith, and A.Abdullah (1997), "The Use of Distress Subsystem for the Design of Pavement Structures", International Conference on the Structural Design of Asphalt Pavements, Vol. I, University of Michigan, Ann Arbor, MI.

11. GEIPOT (1982), Research on the Interrelationships between Costs of Highway Construction, Maintenance and Utilization (PCIR), Final Report, 12 volumes, Empresa Brasileira de Planejamento de Transportes (GEIPOT), Ministry of Transport, Brasilia, Brazil.
12. Greene, W. H. (1997), *Econometric Analysis*, Third Edition, Prentice Hall, Upper Saddle River, New Jersey.
13. Haas, R., W. R. Hudson, J. Zaniewski (1994), *Modern Pavement Management*, Krieger Publishing Company, Florida.
14. Harvey, J.T., L. du Plessis, F. Long, J A. Deacon, I. Guada, D. Hung, C Scheffy (1997). CAL-APT Program: Test Results from Accelerated Pavement Test on Pavement Structure Containing Asphalt Treated Permeable Base (ATPB)- Section 500RF. Report prepared for California Department of Transportation, Pavement Research Center, Institute of Transportation Studies, University of California, Berkeley, CA.
15. Harvey J.T., J.A. Deacon, A.A. Tayebali, R.B. Leahy, and C.L. Monismith (1997), “A Reliability-Based Mix Design and Analysis System for Mitigating Fatigue Distress”, Eighth International Conference of Asphalt Pavements, Vol. I, Proceedings, University of Washington, Seattle, WA.
16. Heckman, J.J., (1981), “Statistical Models for Discrete Panel Data,” in *Structural Analysis of Discrete Data with Econometric Applications*, edited by C.F. Manski and D. McFadden, pp. 114-178, MIT Press, Cambridge, MA.
17. Hiltunen D.R. and R. Roque (1994), “A Mechanics-Based Prediction Model for Thermal Cracking of Asphalt Concrete Pavements”, *Asphalt Paving Technology, Journal of the Association of Asphalt Paving Technologists*, Vol. 63.
18. Hodges J.W., Rolt J., and Jones T.E., (1975), "The Kenya Road Transport Cost study: Research on Road Deterioration", *Laboratory Report 673*, Transport and Road Research Laboratory, Crowthorne, England.
19. HRB (1962), *The AASHO Road Test - Report 5 — Pavement Research*, Highway Research Board Special Report 61E, Publication No. 954, National Academy of Sciences - National Research Council, Washington, DC.

20. Kalbfleisch J. D., and Prentice R. L. (1980), *The Statistical Analysis of Failure Time Data*, John Wiley and Sons, New York, NY.
21. Kandhal, P.S., S.A. Cross, and E.R. Brown (1993), *Heavy-Duty Asphalt Pavements in Pennsylvania: Evaluation for Rutting*. Transportation Research Record 1384, TRB, National Academy of Sciences, Washington, D.C, 49-58.
22. Kenis, W.J. (1977), *Predictive Design Procedures: A Design Method for Flexible Pavements Using the VESYS Structural Subsystem*, Proceedings, 4th International Conference on the Structural Design of Asphalt Pavements, Ann Arbor, Michigan, 101-130.
23. Khedr, S.A. (1986). *Deformation Mechanism in Asphaltic Concrete*. Journal of Transportation Engineering, ASCE 112(1), 29-45.
24. Lister, N.W. (1981). *Heavy Wheel Loads and Road Pavements – Damage Relationships*. Symposium on Heavy Freight Vehicles and their Effects. Organization for Economic Cooperation and Development, Paris.
25. Long F., J. Harvey, C. Scheffy, and C.L. Monismith (1996), “Prediction of Pavement Fatigue for California Department of Transportation Accelerated Pavement Testing Program Drained and Undrained Test Sections”, Transportation Research Record 1540, TRB, National Research Council, Washington, D.C.
26. Madanat S., M. Karlaftis and P. McCarthy (1997). "Development of Probabilistic Infrastructure Deterioration Models with Panel Data", ASCE Journal of Infrastructure Systems, Vol.3, No.1.
27. Madanat S., S. Bulusu and A. Mahmoud (1995), "Estimation of Infrastructure Distress Initiation and Progression Models", ASCE Journal of Infrastructure Systems, Vol. 1, No 3.
28. Madanat S., H. C. Shin (1998), “Development of Distress Progression Models Using Panel Data Sets of In-Service Pavements”, Transportation Research Record 1643, TRB, National Research Council, Washington, D.C.
29. Maree, J.H., C.R. Freeme, N.J.W. van Zyl and P.F. Savage (1982). *The Permanent Deformation of Pavements with Untreated Crushed-stone Bases as Measured in Heavy Vehicle Simulators Tests*. Proceedings 11th Conference, Australian Road Research Board, Melbourne, Australia.

30. Markow M.J., and Brademeyer B., (1981), "Modification of the System EAROMAR", *Final Technical Report*, CTM Incorporated, Springfield, VA.
31. Meeker W. Q. and L. A. Escobar (1984), *Statistical methods for reliability data*, John Wiley and Sons, New York, NY.
32. Monismith, C. L. (1976), *Rutting Prediction in Asphalt Concrete Pavements*, Transportation Research Record 616, Transportation Research Board, National Academy of Sciences, Washington D.C, 2-8.
33. OECD (1988), *Heavy trucks, climate and pavement damage*, prepared by an OECD scientific experts group. Organisation for Economic Co-operation and Development, Paris, France ; OECD Publications and Information Center [distributor], Washington, D.C..
34. Paterson William D. O. (1987), *Road deterioration and maintenance effects: models for planning and management*, The Highway Design and Maintenance Standard Series, Published for The World Bank, The John Hopkins University Press, Baltimore, MD.
35. Peirsly L., and Robinson R., (1982), "The TRRL Road Investment Model for Developing Countries (RTIM2)", *Laboratory Report 1057*, Transport and Road Research Laboratory, Crowthorne, England.
36. Pindyck R.S., and Rubinfeld D.L., (1991), *Econometric Models and Economic Forecasts*, McGrawHill Inc., New York, NY.
37. Queiroz C.A.V. (1981), *Performance Prediction Models for Pavement Management in Brazil*, Ph.D. dissertation, University of Texas, Austin, TX.
38. Saraf, C.L. (1982). *Verification and Calibration of the PDMP and COLD Computer Programs*. Proceedings Fifth International Conference on Structural Design of Asphalt Pavements, University of Michigan and Delft University of Technology, Ann Arbor, Michigan, 321-332.
39. SHRP (1993), *Distress Identification Manual for the Long-Term Pavement Performance Project*, Report SHRP-P-338, Strategic Highway Research Program, National Research Council, Washington, D.C.
40. Tayebali A.A., J.A. Deacon, J.S. Coplantz, J.T. Harvey, and C.L. Monismith (1994), "Mix and Mode-of-Loading Effects on Fatigue Response of Asphalt-Aggregate

Mixes”, Asphalt Paving Technology, Journal of the Association of Asphalt Paving Technologists, Vol. 63.

41. Thompson, M.R. and D. Nauman (1993), Rutting Rate Analyses of the AASHO Road Test Flexible Pavements. Transportation Research Record 1384, 36-48, TRB, National Research Council, Washington, D.C.
42. Train K., (1986), *Qualitative Choice Analysis: Theory, Econometrics and An Application to Automobile Demand*, MIT Press, Cambridge, MA.
43. Vuong, B., and P. Amstrong (1991). Repeated Load Triaxial Testing on the Subgrades from Mulgrace ALF Site, Australian Road Research Board, Melbourne, Australia.
44. Yoder, E.J. and Witczak, M.W., (1975). Principles of Pavement Design, John Wiley & Sons, New York, NY.

# **Pavement Evaluation Using Integrated Data from High-Speed Sensors**

## **Recommendations**

The work carried out in the first Phase of this project demonstrated how newly formulated models for pavement rutting and cracking can be implemented using data from current high speed pavement survey technology. The demonstrated effort showed how data from conventional high speed rutting, cracking, and pavement thickness (GPR) sensors can be integrated into the models to predict future performance of pavement sections. The demonstration also showed how compensation could be made for the absence of historical condition data (as is often the case) by using spatial variability in structurally homogeneous sections, as identified through the GPR thickness data.

Software was developed for implementation of the portion of the rutting and simulations were conducted to predict future rutting using current condition data from an in-service pavement. Software was also developed for implementation of the cracking model.

The three areas for recommended future work are:

- 1) Complete the development and testing of the rutting and cracking models and conduct trial simulations using the software developed in Phase I
- 2) Apply the rutting and cracking models to pavement sections in California representing a range of structural, traffic, and environmental conditions
- 3) Correlate the model predictions with actual changes in surface conditions.

### Recommended Task 1. Model Simulations

#### 1.1 Rutting Model

The rutting simulations in Phase I utilized the portion of the model that represented rutting in the base layer. The portion of the model that represents rutting in the asphalt layer was combined with the base rutting model toward the end of the project. The combined model needs to be incorporated into simulation software and simulations need to be carried out using actual pavement data.

#### 1.2 Cracking Model

In Phase I the cracking model was programmed into the simulation software but there was not adequate time to run simulations. Such simulations will be carried out on one of the Phase I data sets to insure proper performance of the software and reasonableness of results.

### Recommended Task 2. Application of Models to California Pavement Sections

The objective of this task is to apply the cracking and rutting model software to pavement sections representing typical California conditions. This task will include selection of test

sections, collection of surface and GPR data on these sites, and application of prediction models to the data.

## 2.1 Selection of Test Sites

The plan is to selection approximately 30 pavement sections for detailed evaluation. These can include special test sites in California that are currently being intensely monitored. Sections can also be selected in conjunction with a current Caltrans program to assess pavement design procedures. Under this Caltrans program, Stantec, under contract with Caltrans, is collecting surface condition data on 1000 pavement sections throughout California. In addition to the condition data, information on traffic (ESALs), pavement structure, and construction history are being assembled into a database. We will utilize this database to provide a set of sites with representative set of pavement age, construction history, structure, traffic, and environmental exposure.

## 2.2. Collection of Data on Test Sites

Arrangements will be made to collect rutting, cracking, and GPR data on each test section. Data will be collected and processed for utilization in the cracking and rutting prediction software.

## 2.3 Data Processing

Data from the test sites will be processed to yield predictions of cracking and rut depth for future time horizons and future conditions (i.e., changes in traffic, climactic events, etc.). The processed data will be evaluated to insure that reasonable results are obtained.

## Recommended Task 3 – Correlation of Predictions to Actual Condition

The test sections will be re-surveyed for rutting and cracking after one year and again after two years. The results of these followup surveys will be correlated with the model predictions.